Australian Telecommunications Research Institute

Signal Formats for Code Division Multiple Access Wireless Networks

Beata Joanna Wysocki

This thesis is presented as part of the requirements for

the award of the Degree of Doctor of Philosophy

of the

Curtin University of Technology

August 1999

To my sons Tad and Mike,
and in memory of my late parents
Leonard Swiecki and Genowefa Swiecka.

Acknowledgements

I would like to thank here all who helped me during my PhD studies by inspiring discussions, assisting in my research as well as supporting morally and financially.

I wish to thank Curtin University of Technology and the Australian Telecommunications Research Institute for admitting me into the PhD program, and for the continuing institutional support throughout the duration of my studies. In particular, I am very grateful for all the assistance I received from the Office of Graduate Studies, and the Scholarship Office. I also want to acknowledge here the generous sponsorship of the successive directors of both Australian Telecommunications Research Institute and the Cooperative Research Centre for Broadband Telecommunications and Networking. Their financial support considerably reduced the strains I exposed my family to as a result of my PhD involvement.

As for the people associated with, first of all I want to thank to my supervisor, Dr Hans-Jürgen Zepernick. Without his tremendous support, guidance, understanding of sometimes-difficult problems, and a thorough supervision, this thesis would never see the daylight. I wish to acknowledge also the role of Dr Hashem Razavi of Curtin University of Technology who was my initial supervisor in my PhD studies and who convinced me that I can achieve success in telecommunications research. Through all my days at Curtin University of Technology, I could always count on his wisdom and rational advice.

Let me take here the opportunity to express my gratitude to my fellow postgraduate colleagues and the research staff involved in the CRC-BTN research project: "Wireless ATM LANs" for the inspiration, comments and assistance, which significantly helped me in concluding my research. This gratitude is also extended to the administrative staff of ATRI and CRC-BTN for the great sense of humour which often unexpectedly lightened researchers' daily life.

In addition, I wish to thank the examiners for their valuable comments, which considerably improved this thesis.

Finally, I want to thank my whole family for the patience, understanding and help in overcoming all sorts of problems during the course of my PhD research.

Abstract

One of the fundamental problems related to the development of direct sequence code division multiple access (DS CDMA) wireless data networks is design of spreading sequences possessing semi-optimal characteristics. In this thesis, we introduce three new methods to design spreading sequences, which can be optimised to achieve the desired characteristics.

We show that the level of MAI for the DS CDMA systems utilising the example sets of sequences designed by the use of these techniques can be relatively low, compare to the case when the well known Gold-like sequences [29] are used. In addition, we show that by using one of the methods introduced in the thesis, we can construct sets of orthogonal sequences possessing acceptable correlation properties, even for an asynchronous operation, while another of the introduced methods can be used if design of sequences of an arbitrary length is required.

Our new methods to design complex polyphase sequences are orientated towards the short length sequences, as a target application for them are high data rate wireless networks. Those methods are based on using discretised chirp pulses, pulses consisting of discretised multiple chirps, or linear combinations of them. In order to achieve orthogonality among the designed polyphase sequences, we combined the sequences based on superimposed chirps and double chirps with the sequences derived from the orthogonal Walsh functions.

Finally, we utilise the three most promising sequence sets designed by the use of the introduced methods to simulate the multiuser DS CDMA systems. We compare performance of those simulated systems with the performance of the simulated system utilising 15-chip Gold-like sequences. The comparison results indicate that by using our design methods, we can produce useful sequence sets for applications where short spreading sequences are required. The presented results also demonstrate that the performance of systems utilising those sequences can be significantly better in terms of the number of simultaneously active users or bit error rate (BER) that the performance of the system employing Gold or Gold-like sequences of the similar length.

Glossary of Terms and Abbreviations

A - constant amplitude

$ACCF_{max}$ - maximum value for the aperiodic CCFs over the whole set of sequences

ACF - autocorrelation function

AIP - Average Interference Parameter

BER - Bit Error Rate

BPSK - Binary Phase Shift Keying

$C = \{\hat{a}^{(1)}, \ldots, \hat{a}^{(r)}, \ldots, \hat{a}^{(N-1)}\}$ - Chu sequences

CCF - crosscorrelation function

CDMA - Code Division Multiple Access

DS - Direct Sequence

DS - BPSK - Direct Sequence Binary Phase Shift Keying

DS CDMA - Direct Sequence Code Division Multiple Access

DSP - Digital Signal Processing

DS - QPSK - Direct Sequence Quaternary Phase Shift Keying

DS SS - Direct Sequence Spread Spectrum

E_b - energy of a signal corresponding to a single data bit

EOE - Equal Odd and Even (sequence set with Equal Odd and Even CCFs)

F - merit factor, or figure of merit

$F = \{\hat{a}^{(1)}, \ldots, \hat{a}^{(r)}, \ldots, \hat{a}^{(q-1)}\}$ - Frank-Zadoff sequences

FFT - Fast Fourier Transform

FH - Frequency Hopping

T - data bit duration

T_c - chip time

T_h - hop time

T^i, $i = 0, 1, 2, \ldots$ - shift operator

TH - Time Hopping

$U_{m,p,s}(N)$ - set of Opperman and Vucetic sequences

W_d - baseband bandwidth required for data

W_{ss} - spread spectrum bandwidth

Wal(m, t) - Walsh functions; $m = 0, 1, 2, \ldots$

$\{a_n\}$ - complex sequence

$\{b_k\}$ - sequence of data symbols

$\{b_n\}$ - complex sequence

$b(t)$ - bipolar data signal

$b_+(t)$, $b_-(t)$ - baseband chirp pulses

c_{max} - maximum nontrivial value of aperiodic correlation for the set of sequences

$c(t)$ - carrier signal

$c_+(t)$ - positive chirp pulse

$c_-(t)$ - negative chirp pulse

$c_{i,k}(\tau)$ - discrete aperiodic correlation function

$d(t)$ - data modulated signal

f - frequency

f_c, f_0 - carrier frequency

$f_i(t)$ - instantaneous frequency

$\{g_n\}$ - spreading sequence of length N with elements $_k$; $k = 1, 2, \ldots, N$

G_p - processing gain

$G(a, b)$ - set of binary Gold codes

H_{2^m} - $2^m \times 2^m$; $m = 1, 2, \ldots$ Hadamard matrix

$H(a, b)$ - Gold-like sequences

ISI - inter-symbol interference

ISM - Industrial, Scientific, and Medical (frequency band)

$K_L(a, b, c)$ - large set of Kasami sequences

$K_S(a, b)$ - small set of Kasami sequences

M - number of sequences in the set (size of the set)

MAI - Multi-Access Interference

MLSE - Maximum-Likelihood Sequence Estimation

N - length of a spreading sequence

N_0 - one-sided Gaussian noise power spectral density

PN - pseudo-noise or pseudo-random sequences

PSD - Power Spectral Density

QPSK - Quaternary Phase Shift Keying

$R(t)$ - received signal

$R_a(\tau)$ - discrete autocorrelation function

$R_{a,b}(\tau)$ - discrete crosscorrelation function

R_{AC} - average mean-square value of autocorrelation for every sequence in the set

R_{CC} - average mean-square value of crosscorrelation for every sequence in the set

$\mathrm{Rad}_m(t)$ - Rademacher functions; $m = 1, 2, 3, \ldots$

SNR - Signal-to-Noise Ratio

SS - Spread Spectrum

$g(t)$ - physical realisation of the spreading sequence $\{g_n\}$

$gcd(i, j)$ - greatest common divisor of i and j

h - modulation index

$h(x)$ - linear generator polynomial

$n(t)$ - noise

$q_p(t)$ - elementary phase pulse

$r_a(\tau)$ - normalised discrete autocorrelation function

r_{am} - maximum off-peak (out-of-phase) autocorrelation value for the set of sequences

$r_i(\tau)$ - autocorrelation function of the sequence $\{a_n^{(i)}\}$

$r_{a,b}(\tau)$ - normalised discrete crosscorrelation function

r_{cm} - maximum crosscorrelation value for the set of sequences

$r_{i,j}(\tau)$ - crosscorrelation function between sequence $\{a_n^{(i)}\}$ and sequence $\{a_n^{(j)}\}$

r_{max} - maximum nontrivial correlational value for the set of sequences

$\hat{r}_{i,k}(\tau)$ - odd correlation between sequence $\{a_n^{(i)}\}$ and sequence $\{a_n^{(j)}\}$

$s(t)$ - transmitted, spread spectrum signal

sgn(.) - signum function

t - time

$w^{(i)}(t)$ - frequency distorting function

$\hat{w}_m$ - bipolar Walsh sequence; $m = 0, 1, 2, ...$

ϕ_0 - initial phase

$\phi(n)$ - Euler's totient function

$\phi^{(i)}(t)$ - information carrying phase component

$\mu_{k,i}(\tau)$ - crosscorrelation parameter

$v(t)$ - modulated BPSK signal

$\rho(t)$ - received signal

$\rho_{k,i}$ - average interference parameter

$\sigma(t)$ - complex envelope

τ - propagation delay

$\zeta(t)$ - triangular wave

ω_0 - angular frequency of the carrier signal

$\Pi_{T_c}(t)$ - unit - magnitude rectangular pulse of the duration T_c

$\otimes$ - Kronecker product

$\oplus$ - *modulo*-2 sum, 'exclusive OR' operator

Contents

List of Figures

List of Tables

1. Introduction

Over the last decade, mobile telephony services have been growing at an extremely rapid rate. On the other hand, the growth in wireless data applications has been rather marginal. Several technological issues have contributed to such a situation. Among those issues, an important one has been the poor performance of wireless data systems, due to low bit rates, high latencies and high error rates of existing wide-area wireless interfaces. However, there are several technology trends that are going to increase the rate of deployment and use of wireless data services. One of the major factors, which will prompt a more widespread application of wireless data services, is the introduction of the third-generation mobile telecommunication systems.

Current work plans at both the global and regional levels for developing third-generation systems envisage that the basic standardisation process should be completed by the year 2000. This is considered to be the target for both International Telecommunication Union (ITU) proposed IMT-2000 (Universal Mobile Telecommunications by the year 2000) [14], and the European UMTS (Universal Mobile Telecommunications System) [43], [103], standards. As a result of the research interactions the scope and aims of IMT-2000 and UMTS are harmonised, and the possible solutions for the UMTS radio interface are now proposed as members of the IMT-2000 radio interface 'family' [78].

One of the competing techniques proposed for providing multiple access to the common air interface in the next generation of wireless data networks is direct sequence code division multiple access (DS CDMA) [84]. The users of such systems are distinguished by the user specific spreading sequences employed in creation of users' signals, and errors encountered during transmission are either caused by impairments of the channel or by interference among simultaneous users. This multi-access interference (MAI) is a major source of the transmission errors in such schemes and is due to the non-ideal characteristics of the applied spreading sequences. It can be mitigated either by utilising very complicated and costly multi-user detection algorithms or simply by drastically reducing the number of simultaneously active users. However, neither of these approaches seems to be economically viable. In fact, we want to maximise the number of concurrent users sharing the same radio channel while maintaining the desired transmission reliability. Additionally, we want to minimise the costs of the

transceivers in order to broaden the scope of possible uses. Therefore, design of sequences possessing semi-optimal characteristics and systems utilising these sequences have become the fundamental problem, which needs to be addressed for low cost DS CDMA transceivers operating in a scenario of many simultaneously active users, at data rates attractive from the viewpoint of multimedia applications.

Moreover, it is expected that in the radio interface, there will coexist data services characterised by different data rate. In order to accommodate such services, and provide for the optimal bandwidth utilisation, the radio signal should in all cases occupy the same bandwidth. Therefore, the sequence design method should be able to produce sequences of any arbitrary length for wireless data applications.

It is also generally accepted that for the downlink (i.e. base station to mobile terminal transmission), the conditions of synchronous operation can be met. Hence, it would be beneficial if the designed codes were orthogonal or almost orthogonal for their perfect synchronisation. This would allow for cancellation of the MAI for the downlink, and for simpler receivers in mobile terminals.

In the thesis, we will introduce three new methods to design spreading sequences, which can be optimised to achieve the desired characteristics. We will show that the level of MAI for the DS CDMA systems utilising the example sets of sequences designed by the use of these techniques can be relatively low, compared to the case when the well known Gold-like sequences [29] are used. In addition, we will show that by using one of the methods introduced in the thesis, we can construct sets of orthogonal sequences possessing acceptable correlation properties, even for an asynchronous operation, while another of the introduced methods can be used if design of sequences of an arbitrary length is required.

The thesis is organised as follows. In Chapter 2, we discuss the basic principles of direct sequence spread spectrum (DS SS) communications positioned in the context of general spread spectrum signalling. We consider here two most prevailing pass-band DS SS schemes, i.e. DS SS combined with binary phase shift keying [84], DS BPSK, and DS SS combined with quaternary phase shift keying [58], DS QPSK. Later we introduce the concept of DS CDMA together with the issues of the MAI and the inter-symbol interference (ISI). We show the major causes of both the MAI and ISI and briefly describe the conventional techniques for combating these problems.

Chapter 3 deals with basic characteristics and measures proposed in literature (e.g. [29], [58], [79], [85]) to assess spreading sequences, and the whole sets of spreading sequences, from the viewpoint of their usefulness in DS CDMA communication systems. Firstly, we introduce the definitions of periodic and aperiodic correlation functions together with some well known theoretical bounds [95], [111]. Then, based on Pursley's work [85], we describe the relationship between values of mutual crosscorrelation functions and the error performance of the DS CDMA system for many simultaneously active users. After that, we present the measures used recently (e.g. [79]) to characterise performance of spreading sequence sets used for asynchronous DS CDMA systems. These measures, being the average mean square aperiodic crosscorrelation and the average mean square aperiodic autocorrelation, can be used to compare sequence sets, even for sequences of different lengths, and different set sizes. Chapter 3 contains also a practical example, where the introduced characteristics and measures are evaluated for the set of Gold sequences of length 31 [29].

In Chapter 4 we present some examples of spreading sequences proposed in the literature for DS CDMA applications. We start from looking into binary orthogonal sequences derived from Rademacher and Walsh functions [113]. Then, we consider the m-sequences [84], Gold and Gold-like sequences, Kasami sequences, and Barker sequences [29]. In most of the cases we present the correlation functions for the example sequence sets and the computed values of their average mean square aperiodic crosscorrelation and the average mean square aperiodic autocorrelation. Later, we investigate into the complex polyphase sequences, in particular, the families having 'good' aperiodic correlation properties, making them the potential candidates for use in the wireless DS CDMA data networks. Those considered sequences are: complex m-sequences [58], Frank-Zadoff-Chu sequences [17], [32], EOE sequences [29], [34], and Opperman-Vucetic sequences [79]. Finally, we present the table summarising the parameters of all sequence sets considered in this chapter.

Our new methods to design complex polyphase spreading sequences for wireless data applications are introduced in Chapter 5. The aim of the research reported in this chapter was to find the design method, which could produce spreading sequences exhibiting better correlation performance than the known sequences of the comparable length, and for the comparable set size. We were particularly interested in the sequences of short lengths, as a targeted application for them were high data rate wireless net-

works. For such networks, because of the spectral requirements, the spreading ratio is rather limited. All of the work described in this chapter is original, however, we have published some of the findings earlier in [114], [116], [117], [118], [119].

Continuing the work started in Chapter 5, in Chapter 6, the three most promising sequence sets, designed by the use of the introduced methods, have been utilised to simulate the multiuser DS CDMA system. The simulation results are presented and compared with the performance of a multiuser DS CDMA system employing Gold-like sequences of length 15. The outcomes of this comparison show that by using the methods introduced in Chapter 5 we can design sequence sets better suited for use in high rate multiuser DS CDMA wireless data networks. Again, as in Chapter 5, all work reported here is fully original, with the results partially reported in [115] and [118].

Chapter 7 concludes the thesis, and contains some topics for future research, which could complement investigations covered in this thesis.

2. Direct Sequence Spread Spectrum Communication Systems

2.1 Background

In general, a spread spectrum signal is generated by modulating a data signal onto a wideband carrier, so that the resultant transmitted signal has bandwidth being much larger than the data signal bandwidth, and which is relatively insensitive to the data signal [91]. A block diagram of a spread spectrum transmitter is shown in Figure 1, where $d(t)$ denotes the data modulated signal, $s(t)$ is the transmitted, spread spectrum signal, and $\{g_n\}$ denotes the spreading sequence of length N with elements g_n; n = 1, 2, ..., N.

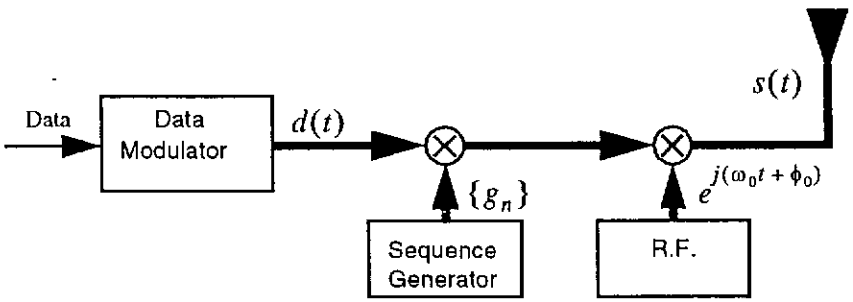

Figure 1: A spread spectrum transmitter.

Thick lines in that block diagram indicate in-phase and quadrature signals with the in-phase channel bearing the real part of complex signal, and the quadrature channel bearing the imaginary part. Hence, the transmitted signal $s(t)$ is represented by:

$$s(t) = d(t)g(t)e^{j(\omega_0 t + \phi_0)}, \tag{1}$$

where $g(t)$ is the physical realisation of the spreading sequence $\{g_n\}$, usually repeated cyclically. The actual implementation of the transmitter may be significantly different from that indicated in Figure 1.

The spreading signal $g(t)$, often referred to as the spread spectrum code signal [91], determines the type of spread spectrum signalling. The most widely applied code signals are as follows:

- Direct Sequence (DS) Signal with chip time T_c:

$$g(t) = \sum_n g_n \Pi_{T_c}(t - nT_c) \tag{2}$$

where $|g_n| = 1$ for all n, and $\Pi_{T_c}(t)$ is a unit - magnitude rectangular pulse of the duration T_c given, generally, by:

$$\Pi_{T_c}(t) = \begin{cases} 1, & 0 \le t < T_c \\ 0, & \text{otherwise} \end{cases} \tag{3}$$

- Frequency Hopping (FH) Signal with hop - time T_h:

$$g(t) = \sum_n e^{j(\omega_n t + \phi_n)} \Pi_{T_h}(t - nT_h) \tag{4}$$

where ϕ_n is an element of a sequence of independent random variables, uniform on $(-\pi, \pi)$.

Other types of SS signals include:

- time - hopping (TH) [21],
- chirp signals (CS) [10], [91].

Hereafter, we will limit our considerations to DS signals only.

The main advantages of SS signal are [58]:

i. resists intentional and non-intentional interference, an important feature for indoor communications;

ii. has the ability to eliminate or alleviate the effect of multipath propagation, which can be a big obstacle in urban communication;

iii. can share the same frequency band (as an "overlay") with other users; because of its noise-like signal characteristics;

iv. it is permitted to operate unlicensed SS systems with RF-power up to 1W in three ISM (Industrial, Scientific, and Medical) fre-

quency bands: 902-928MHz, 2.4-2.4835GHz, and 5.725-5.85 GHz;

v. can be used for licensed satellite communication in CDMA mode;

vi. offers a certain degree of privacy, due to the use of pseudo-random spreading codes, which make it difficult to intercept the signal;

One of the most important parameters of the SS systems is the processing gain G_p, defined as a ratio of the spread spectrum bandwidth W_{ss} to the baseband bandwidth required for data W_d [58]:

$$G_p = \frac{W_{ss}}{W_d} \tag{5}$$

In this chapter, we will discuss the basic principles of DS SS on the basis of DS-BPSK and DS-QPSK, and later, we consider application of DS SS technique to code division multiple access (CDMA) systems.

2.2 General Principles of DS Spread Spectrum.

2.2.1 DS-BPSK

DS SS combined with BPSK as a data modulation, is one of the most commonly considered SS schemes. A block diagram of a DS-BPSK transmitter is presented in Figure 2.

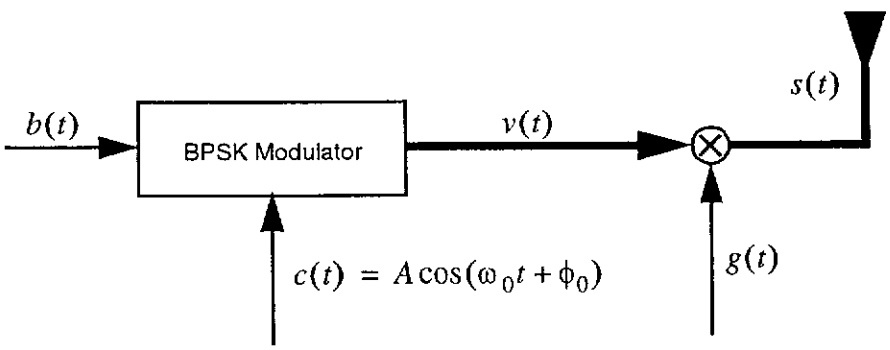

Figure 2: Block diagram of DS BPSK transmitter.

The bipolar data signal $b(t)$, corresponding to a sequence of data symbols $\{b_k\}$, $b_k = \pm 1$, can be represented as:

$$b(t) = \sum_{k=-\infty}^{\infty} b_k \Pi_T(t - kT), \tag{6}$$

where $\Pi_T(t)$ is given by the equation (3), and T is the data bit duration. The carrier signal, $c(t)$ is a cosinusoidal waveform of a constant amplitude A:

$$c(t) = A\cos(\omega_0 t + \phi_0). \tag{7}$$

In the case of BPSK modulation, where $b(t)$ is a modulating signal, the modulated signal $v(t)$ can be expressed as:

$$v(t) = Ab(t)\cos(\omega_0 t + \phi_0), \tag{8}$$

since multiplication by "-1" is equivalent to the phase shift of "π", and multiplication by "1" is equivalent to the phase shift of "0".

According to (1), the transmitted DS BPSK signal is given by:

$$s(t) = Ag(t)b(t)\cos(\omega_0 t + \phi_0) \tag{9}$$

Because the final formula describing DS BPSK signal is a product of $b(t)$, $g(t)$ and the carrier waveform, we can reverse the order of operations, and perform spreading in the base-band without changing the transmitted signal $s(t)$. A block diagram for such an alternative DS BPSK transmitter is shown in Figure 3.

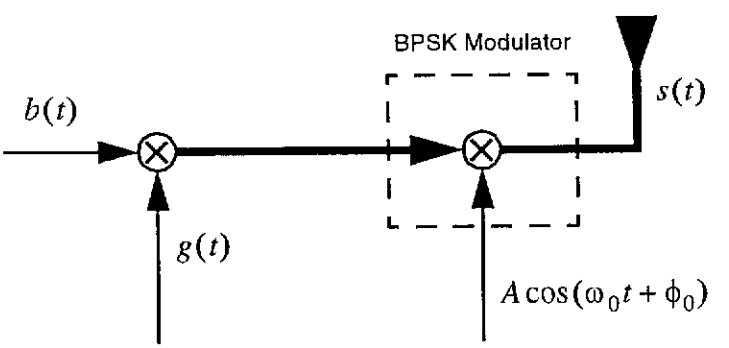

Figure 3: Base-band spreading DS BPSK transmitter.

Example signals for the transmitter of Figure 3 are plotted in Figure 4. In many applications of DS BPSK, as well as in the given example, one data bit is equal to one period of spreading signal i.e., $T = NT_c$, where N is the period (length) of the pseudo noise (PN) spreading sequence. In the case of Figure 4, we have used $N = 7$, and the spreading sequence $\{g_n^{(j)}\}$ is the so called m-sequence [29], [58] given by:

$$\{g_n^{(j)}\} = (0, 0, 1, 1, 1, 0, 1). \tag{10}$$

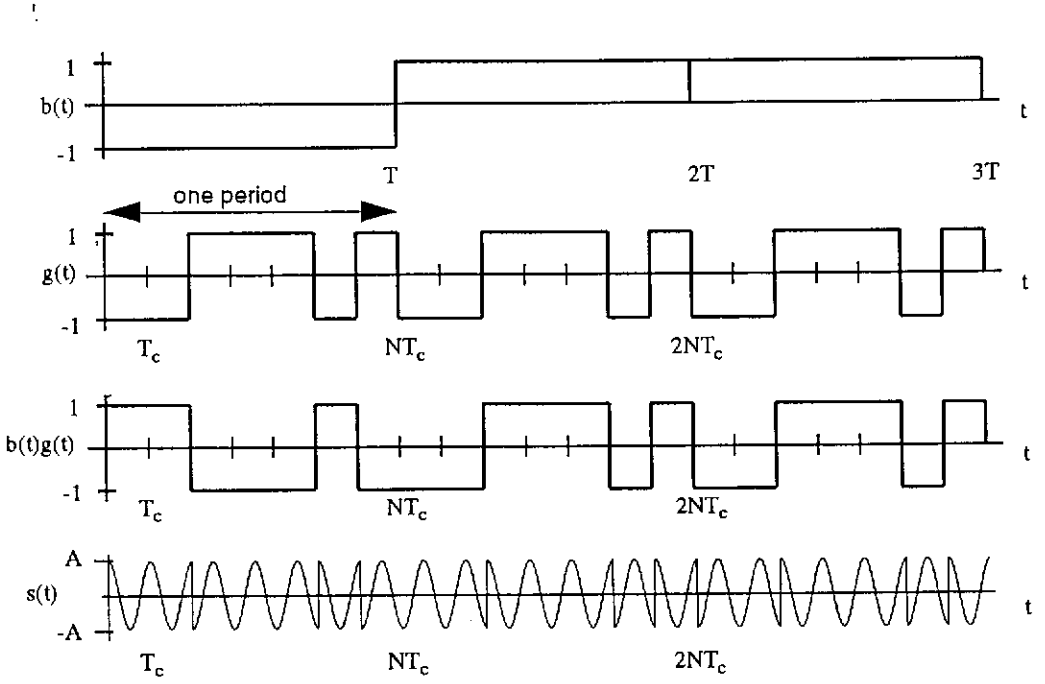

Figure 4: Example signals for the DS BPSK transmitter;
$N = 7, \phi_0 = 0, \omega_0 = 2\pi/T_c$.

At the receiver end, the DS BPSK demodulator is expected to recover the data signal $b(t)$, and finally, the sequence of data symbols $\{b_k\}$ from the received signal $\rho(t)$. Because of the propagation delay τ, the received signal $\rho(t)$ can be expressed as:

$$\begin{aligned} \rho(t) &= s(t-\tau) + n(t) \\ &= Ab(t-\tau)g(t-\tau)\cos[\omega_0(t-\tau) + \phi_0] + n(t) \end{aligned}, \tag{11}$$

where $n(t)$ is the noise from the channel and the front-end of the receiver.

The block diagram of the one of possible DS BPSK demodulator structures is pre-

sented in Figure 5. More possible structures can be found in [84]. To analyse its operation, let us assume that there is no noise, i.e.

$$n(t) = 0. \tag{12}$$

The received signal is first despread to reduce the wide bandwidth back to narrowband, then it is mixed with the locally generated carrier waveform to obtain a baseband signal, and finally it is demodulated using a conventional BPSK demodulator.

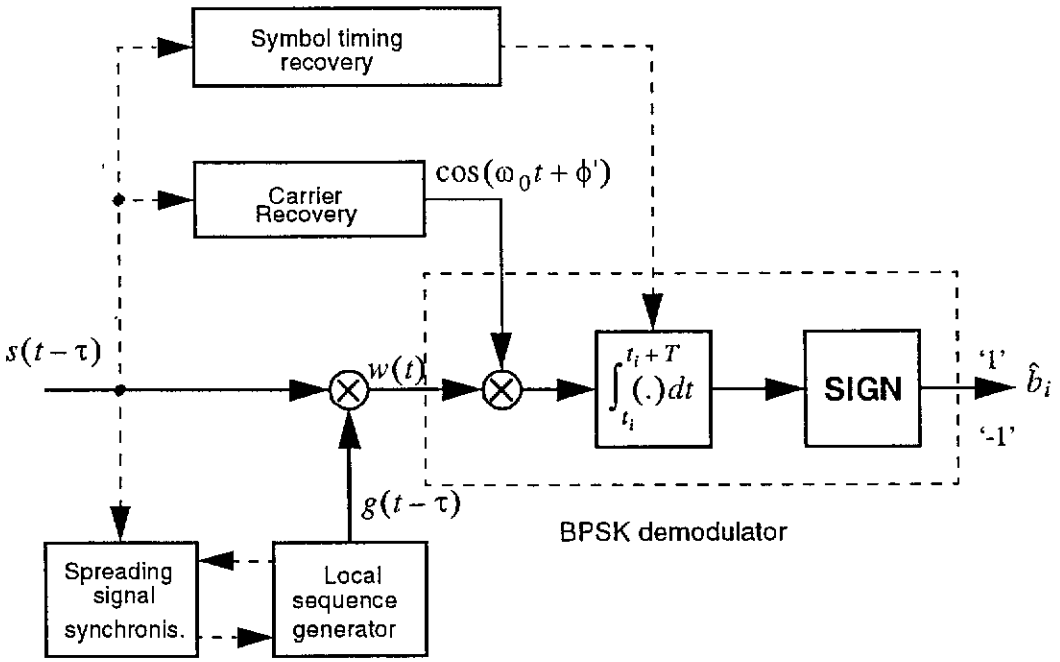

Figure 5: Block diagram of a conventional DS BPSK receiver.

To despread, the received signal is multiplied by the synchronised spreading signal $g(t-\tau)$, generated at the receiver, which yields:

$$w(t) = Ab(t-\tau)g^2(t-\tau)\cos(\omega_0 t + \phi'), \tag{13}$$

where:

$$\phi' = \phi_0 - \omega_0 \tau. \tag{14}$$

Since we have:

$$|g_n| = 1 \tag{15}$$

for every possible value of n, then

$$g^2(t-\tau) \equiv 1, \tag{16}$$

and we obtain:

$$w(t) = Ab(t-\tau)\cos(\omega_0 t + \phi'). \tag{17}$$

This resulting signal is a bandpass signal with the bandwidth $2/T$. To demodulate it, we assume here that the receiver knows the phase ϕ', the carrier frequency $f_0 = \omega_0/2\pi$, as well as the beginning of each bit. The example plots of some of the DS BPSK demodulator signals are plotted in Figure 6.

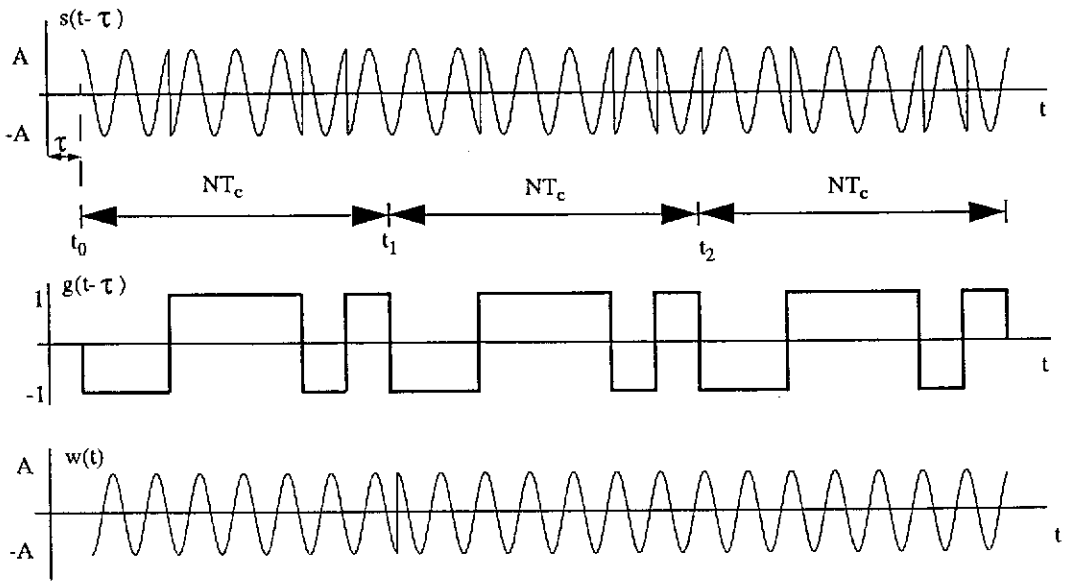

Figure 6: Example signals for the DS BPSK receiver; $N = 7, \phi_0 = 0, \omega_0 = 2\pi/T_c$.

To demodulate ith data symbol, the signal $w(t)$ is multiplied by the locally generated carrier waveform, and the correlator computes:

$$
\begin{aligned}
z_i &= \int_{t_i}^{t_i+T} w(t)\cos(\omega_0 t + \phi')dt \\
&= \int_{t_i}^{t_i+T} Ab(t-\tau)\cos^2(\omega_0 t + \phi')dt \\
&= \frac{A}{2}\int_{t_i}^{t_i+T} b(t-\tau)[1-\cos(2\omega_0 t + 2\phi')]dt
\end{aligned}
\quad , \tag{18}
$$

where $t_i = iT + \tau$ is the beginning of the ith bit. Since the data signal $b(t-\tau)$ is always equal to +1 or -1 during each bit, the first term in the integration gives T or $-T$. The second term is a double-frequency component which is approximately zero after the integration due to the low-pass characteristic of the integrator. Hence, the result is:

$$
z_i = \begin{cases} AT/2, & b_i = 1 \\ -AT/2, & b_i = -1 \end{cases} . \tag{19}
$$

Passing this through a threshold device with treshold of 0 yields a *sign* function, binary output of '1' or '-1'. Additionally, in the presence of noise, i.e. when the condition (12) is not satisfied, the output of the integrator also has a noise component, which can be a source of errors.

It should be noted here, that the order of despreading and shifting the received signal to the baseband can be reversed without altering the result.

The analysis of the imperfect synchronisation, i.e. wrong carrier phase and wrong spreading sequence phase in the receiver can be found in literature, e.g. [58].

2.2.2 DS QPSK

Even though there is no restrictions on the modulation type which can be used in DS SS systems (e.g. [84], [96]) not many modulation schemes have been considered for such applications. Apart from BPSK which we considered in the previous section, and its differential form DBPSK [84], only Quadrature Phase-Shift Keying (QPSK) [84] is a modulation scheme commonly discussed in conjunction with DS SS systems [58].

Let us consider a DS QPSK transmitter having a functional block diagram presented in Figure 7. It consists of two branches: the in-phase and the quadrature branches.

The input data signal $b(t)$ is split into two channels $b_I(t)$ and $b_Q(t)$ using a serial to parallel converter, as it is shown in Figure 7, and spread separately using two spreading sequences $g_I(t)$ and $g_Q(t)$. Hence, the DS QPSK signal is:

$$\begin{aligned} s(t) &= s_I(t) + s_Q(t) \\ &= Ab_I(t)g_I(t)\cos(\omega_0 t + \phi_0) + Ab_Q(t)g_Q(t)\sin(\omega_0 t + \phi_0) \\ &= \sqrt{2}A\sin[\omega_0 t + \phi_0 + \gamma(t)] \end{aligned} \quad , \qquad (20)$$

where:

$$\gamma(t) = \text{atan}\left[\frac{b_I(t)g_I(t)}{b_Q(t)g_Q(t)}\right] \quad . \qquad (21)$$

$$= \begin{cases} \pi/4\,, & \text{if } b_Q(t)g_Q(t) = 1 \text{ and } b_I(t)g_I(t) = 1 \\ 3\pi/4\,, & \text{if } b_Q(t)g_Q(t) = -1 \text{ and } b_I(t)g_I(t) = 1 \\ 5\pi/4\,, & \text{if } b_Q(t)g_Q(t) = -1 \text{ and } b_I(t)g_I(t) = -1 \\ 7\pi/4\,, & \text{if } b_Q(t)g_Q(t) = 1 \text{ and } b_I(t)g_I(t) = -1 \end{cases}$$

Therefore, the signal $s(t)$ can take on four different phases $\phi_0 + \pi/4$, $\phi_0 + 3\pi/4$, $\phi_0 + 5\pi/4$, and $\phi_0 + 7\pi/4$. The example signal plots for DS QPSK transmitter are presented in Figure 8, under the assumption that $\phi_0 = 0$.

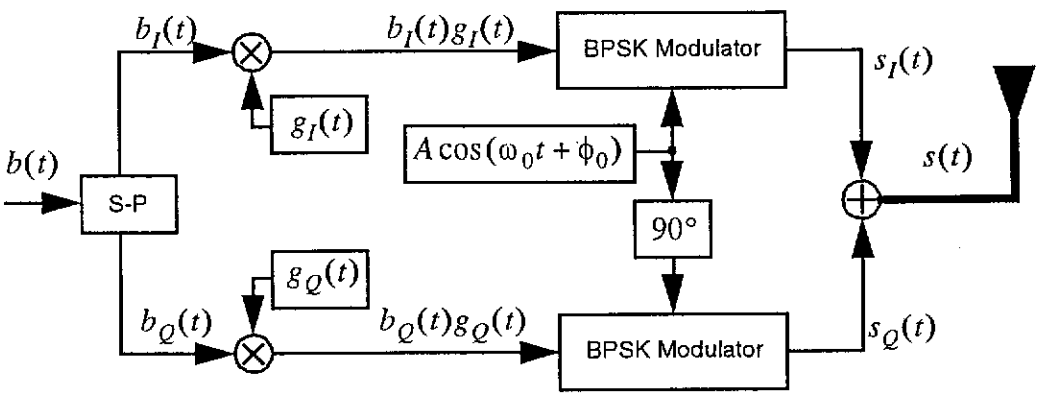

Figure 7: Functional block diagram of DS QPSK transmitter.

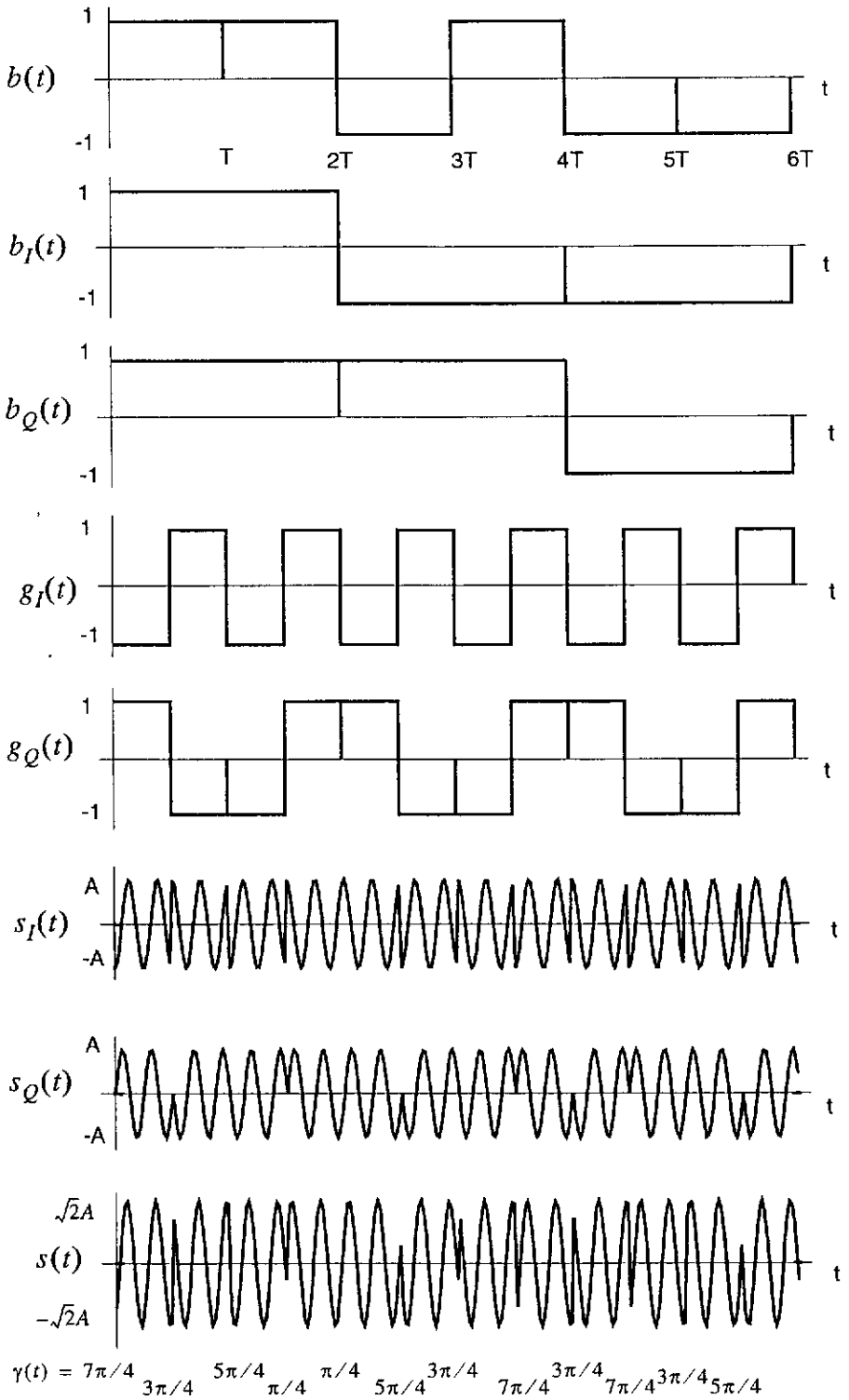

Figure 8: Example signals for the DS QPSK transmitter;
$N = 4, \phi_0 = 0, \omega_0 = 4\pi/T_c$.

At the receiver, we need to despread the in-phase and the quadrature components of the incoming signal separately using the sequences $g_I(t)$ and $g_Q(t)$, as it is shown in Figure 9.

Ignoring noise, and denoting the propagation delay as τ, the incoming signal $s(t-\tau)$ is given by:

$$s(t-\tau) = Ab_I(t-\tau)g_I(t-\tau)\cos(\omega_0 t + \phi') + Ab_Q(t-\tau)g_Q(t-\tau)\sin(\omega_0 t + \phi'), \quad (22)$$

where ϕ' is given by equation (14).

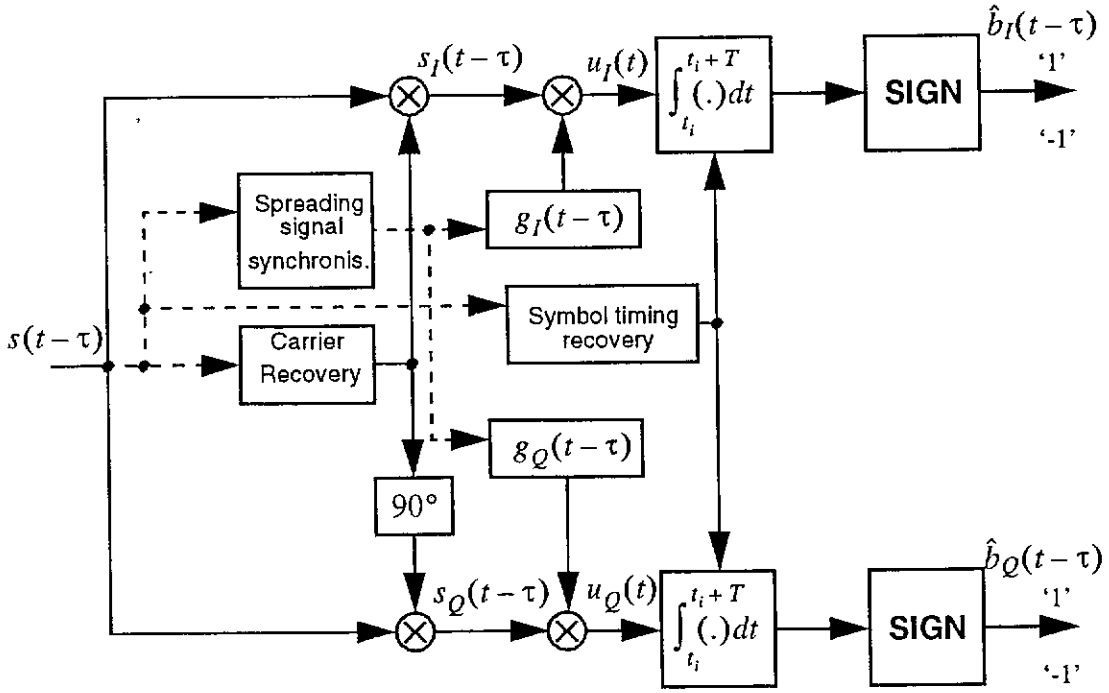

Figure 9: Functional block diagram of DS QPSK receiver.

The signals before integrators are:

$$\begin{aligned} u_I(t) &= Ab_I(t-\tau)\cos^2(\omega_0 t + \phi') \\ &\quad + Ab_Q(t-\tau)g_I(t-\tau)g_Q(t-\tau)\sin(\omega_0 t + \phi')\cos(\omega_0 t + \phi') \\ &= Ab_I(t-\tau)\frac{1}{2}[1 + \cos(2\omega_0 t + 2\phi')] \\ &\quad + Ab_Q(t-\tau)g_I(t-\tau)g_Q(t-\tau)\frac{1}{2}\sin(2\omega_0 t + 2\phi') \end{aligned} \quad (23)$$

$$
\begin{aligned}
u_Q(t) &= Ab_Q(t-\tau)\sin^2(\omega_0 t+\phi') \\
&\quad + Ab_I(t-\tau)g_I(t-\tau)g_Q(t-\tau)\sin(\omega_0 t+\phi')\cos(\omega_0 t+\phi') \\
&= Ab_Q(t-\tau)\frac{1}{2}[1-\cos(2\omega_0 t+2\phi')] \\
&\quad + Ab_I(t-\tau)g_I(t-\tau)g_Q(t-\tau)\frac{1}{2}\sin(2\omega_0 t+2\phi')
\end{aligned}
\tag{24}
$$

The sum of these signals is integrated over one bit interval, which gives AT at the output of the integrator if the corresponding message bit is '+1' or $-AT$ if it is '-1'. This is due to the fact that all terms with the doubled frequency are averaged to zero. After passing this through devices performing a *sign* operation, we obtain binary outputs of '1' or '-1' for both channels, and finally, one can multiplex the in-phase and quadrature channels back.

The two spreading signals $g_I(t)$ and $g_Q(t)$ do not need to be orthogonal [84], because of the orthogonality of the carrier waveforms used in the in-phase and quadrature channels. Therefore, they can be chosen independently, or they may be obtained from one single spreading signal $g(t)$. For example, $g_I(t) = g(t)$, and $g_Q(t)$ may be a delayed replica of $g(t)$.

The bandwidth of modulated signals $s_I(t)$ and $s_Q(t)$ are the same, and therefore equal to the bandwidth of the aggregate signal $s(t)$. Because, the data rates of $b_I(t)$ and $b_Q(t)$ are equal to half the rate of $b(t)$, the bandwidth occupied by a DS QPSK signal equals to the half of the bandwidth occupied by an equivalent DS BPSK signal. Alternatively, a DS QPSK system can transmit twice as much data as a DS BPSK system that uses the same bandwidth and has the same processing gain [58], [84] and signal to noise ratio [84].

A disadvantage of a DS QPSK system lays in a higher complexity than that of a DS BPSK system. In addition, if the two carriers used for demodulation at the receiver are not truly orthogonal, then there will be a cross talk between the in-phase and quadrature channels, which can significantly impair the system performance.

2.3 Direct Sequence Code Division Multiple Access

2.3.1 General Principles

A block diagram of a conventional DS CDMA system [58], [84] is shown in Figure 10. The first block represents the data modulation of a carrier $c(t)$. Usually, this is of the form $c(t) = A\cos(\omega_0 t)$ and the modulation is either BPSK or QPSK, however, there is no restriction placed neither on the waveform nor the modulation type [96].

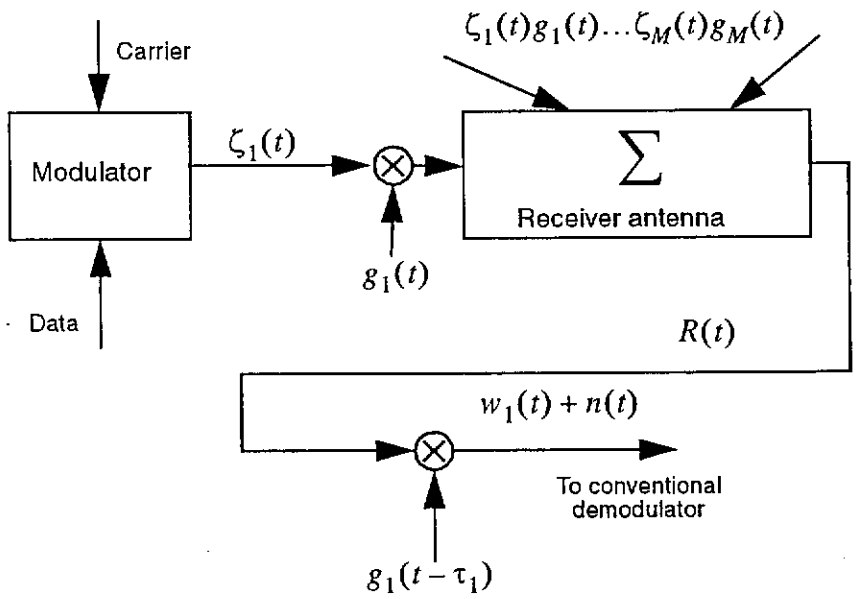

Figure 10: Block diagram of a conventional DS-CDMA system.

In the case of an angular modulation, the modulated signal, $\zeta_1(t)$, is expressed as:

$$\zeta_1(t) = A\cos[\omega_0 t + \phi_1(t) + \phi_0] \tag{25}$$

where: A is the amplitude of modulated signal, $\omega_0 = 2\pi/T_0$ denotes angular carrier frequency, T_0 is a period of the carrier, $\phi_1(t)$ represents the information carrying phase function, ϕ_0 is an initial value of the phase.

Next, the signal $\zeta_1(t)$ is multiplied by the spreading signal $g_1(t)$ belonging to user 1, and the resulting signal $g_1(t)\zeta_1(t)$ is transmitted over the radio channel. Simultaneously, all other users 2 through M multiply their signals by their own spreading signatures. The signal $R(t)$ intercepted in the receiver antenna, neglecting the differ-

ent path losses and channel noise, is given by:

$$R(t) = g_1(t-\tau_1)\zeta_1(t-\tau_1) + g_2(t-\tau_2)\zeta_2(t-\tau_2) + \ldots \quad , \\ + g_M(t-\tau_M)\zeta_M(t-\tau_M) \tag{26}$$

where τ_i; i =1, 2, ... , M denotes delay corresponding to different transmission paths associated with the user i.

Assuming the receiver configured to receive messages from user 1, the despread signal $w_1(t)$ is given by:

$$w_1(t) = g_1^{\,2}(t-\tau_1)\zeta_1(t-\tau_1) + \ldots + g_1(t-\tau_1)g_M(t-\tau_M)\zeta_M(t-\tau_M) \tag{27}$$

where the term $g_1^{\,2}(t-\tau_1)\zeta_1(t-\tau_1)$ is the desired signal and the other terms $g_1(t-\tau_1)g_i(t-\tau_i)\zeta_i(t-\tau_i)$; $(i \neq 1)$ are the interfering signals responsible for the multiaccess interference (MAI). Because the signal is finally demodulated using the correlation detector, with stronger crosscorrelation between the user spreading signal $g_1(t-\tau_1)$ and spreading signals of the other users $g_i(t-\tau_i)$; $i = 2, \ldots, M$ the MAI becomes more severe. For example, in the case of BPSK, to obtain the received data bit $\hat{b}_1$ the received signal $R(t)$ is correlated with $g_1(t-\tau_1)$:

$$\hat{b}_1 = \begin{cases} 1, & \int_T R(t)g_1(t-\tau_1)dt > 0 \\ -1, & \int_T R(t)g_1(t-\tau_1)dt < 0 \end{cases} . \tag{28}$$

2.3.2 Multipath Propagation

One of the features of mobile or indoor microwave systems is multipath propagation [50], [87] where the receiver antenna, even with only a single transmitter, intercepts signals coming through different paths and thus exhibiting different delays. Therefore the received signal $R(t)$ is in such a case equal to:

$$R(t) = A_1 g_1(t-\tau_1)\zeta_1(t-\tau_1) + A_2 g_1(t-\tau_2)\zeta_1(t-\tau_2) + \ldots \\ \ldots + A_L g_1(t-\tau_L)\zeta_1(t-\tau_L) \tag{29}$$

where the coefficients $A_1 > A_2 > \ldots > A_L$ represent amplitudes of signals having different propagation paths. Usually receiver is synchronized with the strongest signal component $A_1 g_1(t-\tau_1)\zeta_1(t-\tau_1)$ corresponding, in most of the cases, to the direct line of sight path, if such a one exists. Hence, the other terms, are sources of the inter-symbol interference [87] (ISI), since their delays $\tau_i;\ (i \neq 1)$, are not equal to τ_1.

In order to minimise the ISI, the codes $g_1(t), \ldots, g_M(t)$ are optimized to have low autocorrelation for delays greater than a single chip. An example of such optimized codes is a set of Gold codes [29], [84]. For the short length codes, however, even Gold codes exhibit quite significant auto-correlation which for some values of the delay can reach very substantial magnitudes of 0.71 [84].

The best known method of resolving problems associated with the multipath propagation is, however, use of the RAKE receiver [58], [87]. To analyse its operation for the user 1, let us suppose that the multipath delay spread [87] is T_m seconds. Thus, there are:

$$L = \frac{T_m}{T_c} + 1 \tag{30}$$

resolvable multipath fading signals at the receiver. Each of these L resolvable paths has an independent attenuation α_{1i}, and introduces a random phase shift $\Delta\phi_{1i}$, where $i = 1, 2, \ldots, L$. If the values of these parameters change slowly enough, they can be estimated by using the information from the previous bit intervals, and the optimum receiver is the tapped delay line receiver shown in Figure 11.

The amplitudes of the locally generated carriers $A_{11}, A_{12}, \ldots, A_{1L}$ are inversely proportional to the attenuations of the resolvable paths $\alpha_{11}, \alpha_{12}, \ldots, \alpha_{1L}$, respectively, while their initial phases $\phi_{11}, \phi_{12}, \ldots, \phi_{1L}$ are calculated using the formula:

$$\phi_{1i} = \phi_0 + \Delta\phi_{1i}; \qquad i = 1, 2, \ldots, L \tag{31}$$

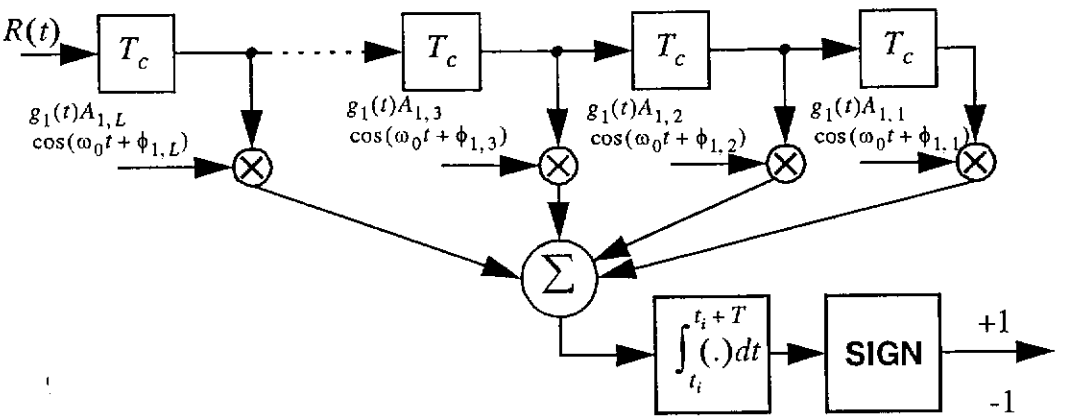

Figure 11: RAKE matched filter receiver with BPSK demodulation.

where ϕ_0 is the initial phase of the emitted signal, and the values for $\Delta\phi_{1i}$ are estimated at the receiver. Such a receiver coherently collects the signal energy from all the resolvable multipath signals that carry the same data and fall within the span of the delay time. Because it acts like a garden rake and correlation functions are matched to multipath signals, the tapped delay line receiver of Figure 11 is referred to as the RAKE matched filter receiver.

Analysis of the RAKE receiver performance in the case of Rician fading channel [87] is very complicated, and even for a simpler case of Rayleigh channel [50], [87], the derivation of the closed formula for the probability of error is not a simple task. A closed formula for the probability of error in the worst-case Rayleigh fading in a system using DS BPSK and the RAKE receiver is given by [58]:

$$P_{e,BPSK} = \left(\frac{1-\sqrt{\frac{SNR}{1+SNR}}}{2}\right)^L \sum_{k=0}^{L-1}\binom{L-1+k}{k}\left(\frac{1+\sqrt{\frac{SNR}{1+SNR}}}{2}\right)^k \qquad (32)$$

$$\approx \left(\frac{1}{4SNR}\right)^L \binom{2L-1}{L}$$

where the signal-to-noise ratio (SNR), $SNR = \frac{1}{L}(E_b/N_0)$, is assumed here to be

equal for all L path, E_b is the energy of a signal corresponding to a single data bit, $N_0/2$ is the two-sided noise power spectral density of a zero-mean additive Gaussian noise. The approximation given by equation (32) is good for large values of *SNR*.

A numerical example given in [58] shows that for a diversity of order $L = 4$, the RAKE-BPSK receiver reduces the required E_b/N_0 by 14 dB at $P_e = 10^{-3}$. Higher order diversity yields a better diversity gain, and diversity combining is more effective in Rayleigh fading channel than in Rician fading channel.

The full performance analysis of the RAKE receivers is quite complicated and significantly exceeds the framework of this thesis. Interested readers can, however, find more details in several references, e.g. [3],[16], [37], [104].

2.3.3 Multiuser Detection

In Section 2.3.1, we considered a conventional DS CDMA system treating each user separately. Hence, we regarded signals corresponding to other users as interference, i.e. MAI. The detection of the desired signal in the presence of MAI is possible because of the inherent interference suppression capability of DS SS scheme measured by the processing gain. That capability is, however, limited, and as the number of interfering users increases, the level of MAI increases as well, resulting in a serious degradation of performance, i.e. increasing bit error rate or frame error rate. This is particularly severe, if the ratio of spreading sequence length to the number of simultaneously active users is less than about 2 [2].

Even if the number of users is not too large, some users may be received at such high levels that a lower power users may be swamped out [26]. This is the near/far effect, where users near the receiver are received at higher powers than those far away, which affects the transmission performance for the users further away from the receiver. The near/far effect is not limited to the near/far scenario, but can also take place in the case of some users experiencing deep fades during transmission.

According to [26], there are two major limits to present DS CDMA systems:

- All users interfere with all other users, and these interferences add to cause performance degradation.
- The near/far problem is serious and tight power control is needed to combat it.

Theoretically, system performance and capacity can be improved by considering all users jointly [108]. Such a joint detection, where each user is detected with some additional information about other users' transmissions is usually referred to as multi-user detection [2], [26], [108]. A canonical structure of of a multiuser CDMA receiver is given in Figure 12 [2].

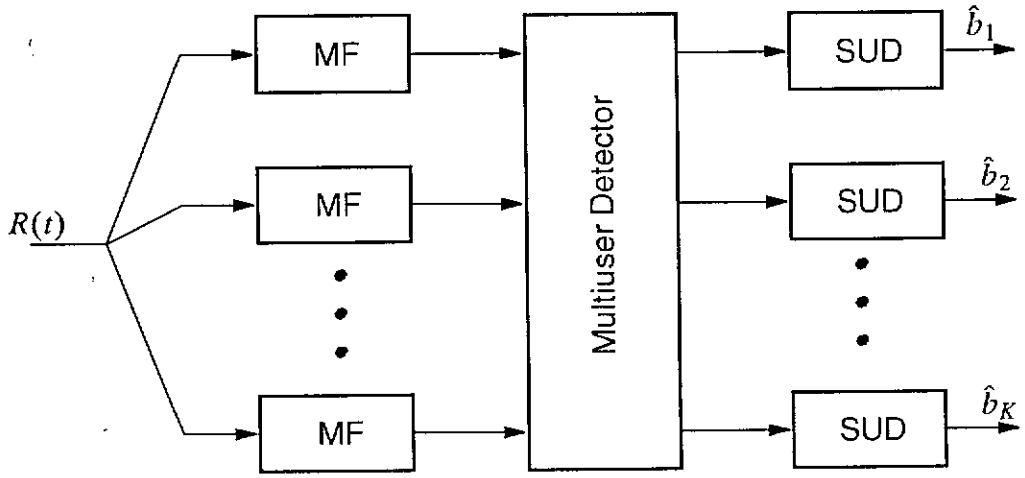

Figure 12: Canonical structure of a multiuser CDMA receiver; MF - matched filter, SUD - single user decoder.

In a multiuser detector, instead of users being considered as interferers for each other, they are being used for their mutual benefit by joint detection. The optimal detector for the synchronous system performs an exhaustive search among all possible combinations of transmitted symbols of the users for each time interval [108]. The optimal detector selects the hypothesis about the input sequence, which maximises the conditional probability or likelihood of the given output sequence [26]. This strategy is of course the maximum-likelihood sequence estimation (MLSE) [84]. The problem with such a detector is that the complexity grows exponentially with the number of users. For K users system, the detector must search through a tree with 2^{K-1} nodes and 2^K branches for each symbol interval [2], [108].

For asynchronous CDMA, the MLSE detector can be implemented using the Viterbi algorithm [107]. However, the resulting Viterbi algorithm has 2^{K-1} states and requires K storage updates per transmission.

Although the optimal detection provides an excellent performance, it is too complicated for practical implementation. Therefore, suboptimal approaches are being sought. There is a wide range of possible performance/complexity combinations possible, e.g.:

i. the decorrelating detector [62], [63],

ii. multistage detectors [35], [105], [106],

iii. decision-feedback detectors [23], [24], [25],

iv. successive interference cancellers [46], [81],

to mention only some major categories of them. The analysis of the multiuser detectors exceeds significantly the scope of this thesis. However, an interesting reader can find a comprehensive tutorial and a good bibliography in [26].

Albeit the suboptimum multiuser detectors can significantly improve the system performance compared to the case where conventional single-user detectors are used, they are still too complex to be, at present time, successfully implemented at high data rates as required for the wireless data networks.

3. Sequence Comparison Criteria

In order to compare different sets of spreading sequences, we need a standard, or quantitative measure for the judgment. We will introduce here some useful criteria which can be used for such a purpose. They are based on the correlation functions of the set of sequences, since both the level of multiaccess interference and synchronisation amiability depend on the crosscorrelations between the sequences and the autocorrelation functions of the sequences, respectively. There are, however, several specific correlation functions which can be used to characterise a given set of the spreading sequences [29], [79], [85]. In this chapter, we will briefly introduce some of the most commonly used criteria, and consider an example of their use.

3.1 Periodic Correlation Functions and Their Properties

Let us consider two complex sequences $\{a_n\}$, and $\{b_n\}$, both having a period N. Their discrete crosscorrelation function $R_{a,b}(\tau)$ is defined as [29]:

$$R_{a,b}(\tau) = \sum_{n=0}^{N-1} a_n b_{n+\tau}^{*}, \tag{33}$$

where b_n^{*} denotes the complex conjugate of b_n. The discrete autocorrelation function $R_a(\tau)$ of the sequence $\{a_n\}$ is defined as [29]:

$$R_a(\tau) = \sum_{n=0}^{N-1} a_n a_{n+\tau}^{*}. \tag{34}$$

Very often, instead of the above unnormalised correlation functions, their normalised equivalents are used:

$$r_{a,b}(\tau) = \frac{1}{N}\sum_{n=0}^{N-1} a_n b_{n+\tau}^{*} \qquad r_a(\tau) = \frac{1}{N}\sum_{n=0}^{N-1} a_n a_{n+\tau}^{*}. \tag{35}$$

The defined above discrete periodic correlation functions have got several useful

properties. Below is the short summary of some of the most useful of them:

v. The autocorrelation is an even function of τ

$$R_a(-\tau) = R_a(\tau). \tag{36}$$

vi. The peak autocorrelation occurs at zero delay:

$$R_a(0) \geq R_a(\tau), \qquad \tau \neq 0. \tag{37}$$

vii. The crosscorrelation functions have the following symmetry:

$$R_{a,b}(\tau) = R_{b,a}(-\tau). \tag{38}$$

viii. Crosscorrelation functions are not, in general, even functions, and their peak values can be at different delays for different pairs of the sequences.

The more comprehensive list of the properties of discrete periodic correlation functions can be found in [29].

For the set $\{a_n^{(i)}\}, i = 0, 1, \ldots, M-1, n = 0, 1, \ldots, N-1$ of M periodic spreading sequences of the period N, we can define:

i. Autocorrelation function $r_i(\tau)$ of the sequence $\{a_n^{(i)}\}$:

$$r_i(\tau) = \frac{1}{N} \sum_{n=0}^{N-1} a_n^{(i)} [a_{n+\tau}^{(i)}]^* \tag{39}$$

ii. Crosscorrelation function $r_{i,j}(\tau)$ between sequence $\{a_n^{(i)}\}$ and sequence $\{a_n^{(j)}\}$:

$$r_{i,j}(\tau) = \frac{1}{N} \sum_{n=0}^{N-1} a_n^{(i)} [a_{n+\tau}^{(j)}]^* \tag{40}$$

iii. Maximum nontrivial correlational value [29] r_{max}:

$$r_{max} = \max\{r_{am}, r_{cm}\}\ , \tag{41}$$

where r_{am} is the maximum off-peak (out-of-phase) autocorrelation value, and r_{cm} is the maximum crosscorrelation value, i.e.

$$r_{am} = \max_{\substack{0 \le i < M \\ 1 \le \tau < N}} \{|r_i(\tau)|\} \tag{42}$$

$$r_{cm} = \max_{\substack{0 \le i,j < M,\, i \ne j \\ 0 \le \tau < N}} \{|r_{i,j}(\tau)|\} \tag{43}$$

Depending on the application, the requirements for the set of spreading sequences are different. For those sequences which are used for DS CDMA the maximum nontrivial correlational value r_{max} should be kept as low as possible in order to facilate synchronisation and to minimise multiaccess interference.

The lower bounds on the minimum possible value of the parameter r_{max} are given by Sidelnikov bound [29], Sarwate bound [89] and Welch bound [111]. Sarwate has proven that:

$$r_{cm}^2 + \frac{N-1}{N(M-1)} r_{am}^2 \ge 1 \ , \tag{44}$$

from which we can derive the Welch [111] bound:

$$r_{max} = \max\{r_{am}, r_{cm}\} \ge \sqrt{\frac{M-1}{NM-1}} . \tag{45}$$

The Welch bound can be used to complex-valued sequences in general. For those sequences, whose symbols are complex qth roots of unity, we can apply the Sidelnikov bound which is, in most cases, tighter than the bound obtained by restricting the Welch bound to sequences of symbols being complex roots of unity.

When $M = N^u$, $N \gg u$ and $u \ge 1$ is an integer, the Sidelnikov bounds can be well approximated by [29]:

$$r_{max}^2 \geq \begin{cases} \frac{1}{N}\left[2u+1-\frac{1}{1\cdot 3\cdot 5\cdot \ldots \cdot (2u-1)}\right], & \text{for binary sequences} \\ \frac{1}{N}\left[u+1-\frac{1}{1\cdot 2\cdot 3\cdot \ldots \cdot u}\right] & \text{for nonbinary sequences} \end{cases} . \quad (46)$$

If $M \approx N$, then $u \approx 1$ and:

$$r_{max} \geq \begin{cases} \sqrt{\frac{2}{N}}, & \text{for binary sequences} \\ \sqrt{\frac{1}{N}}, & \text{for nonbinary sequences} \end{cases} . \quad (47)$$

The periodic correlation functions albeit useful in estimating performance of a set of spreading sequences for some applications, are not helpful in evaluating performance of such a set in the case of asynchronous DS CDMA system. This is due to the fact that consecutive bits of data transmitted in the interfering channels can be of different signs [58].

3.2 Discrete Aperiodic Correlation Functions and Their Properties

One of the first detailed investigations of the asynchronous DS CDMA system performance which dealt with aperiodic cross-correlation effects was published in 1969 by Anderson and Wintz [5]. They obtained a bound on the signal-to-noise ratio at the output of the correlation receiver for a CDMA system with a hard-limiter in the channel. They also clearly demonstrated in their paper the need for considering the aperiodic crosscorrelation properties of the spreading sequences. Since that time, many additional results have been obtained (e.g. [67] and [85]) which helped to clarify the role of aperiodic correlation in asynchronous DS CDMA systems.

For general complex-valued sequences $\{a_n^{(i)}\}$ and $\{a_n^{(k)}\}$ of length N, the discrete aperiodic correlation function is defined as [29]:

$$c_{i,k}(\tau) = \begin{cases} \frac{1}{N}\sum_{n=0}^{N-1-\tau} a_n^{(i)}[a_{n+\tau}^{(k)}]^*, & 0 \le \tau \le N-1 \\ \frac{1}{N}\sum_{n=0}^{N-1+\tau} a_{n-\tau}^{(i)}[a_n^{(k)}]^*, & 1-N \le \tau < 0 \\ 0, & |\tau| \ge N \end{cases} \quad (48)$$

The sequences $\{a_n^{(i)}\}$ and $\{a_n^{(k)}\}$ in (48) are of the finite length N and are not necessarily single periodic sequences of period N. When $\{a_n^{(i)}\} = \{a_n^{(k)}\}$, Eqn. (48) defines the discrete aperiodic autocorrelation function. In similar way, as with the periodic correlation functions, we can define the maximum nontrivial value of aperiodic correlation c_{max}:

$$c_{max} = \max\{c_{am}, c_{cm}\}, \quad (49)$$

where c_{am} is the maximum out-of phase autocorrelation value, and c_{cm} is the maximum crosscorelation value, defined analogically as for the periodic correlation values (see Eqs. (42), and (43)).

Another important parameter used to assess the synchronisation amiability of spreading sequences is a merit factor, or a figure of merit [10], [38], which specifies the ratio of the energy of autocorrelation function mainlobes to the energy of the autocorrelation function sidelobes in the form:

$$F = \frac{c_i(0)}{2\sum_{\tau=1}^{N-1} |c_i(\tau)|^2}. \quad (50)$$

In CDMA systems we want to have the maximum nontrivial value of aperiodic correlation as small as possible, and the merit factor as great as possible for all of the sequences.

Some of the important properties of aperiodic auto- and crosscorrelation functions are as follows:

i. In-phase value:

$$c_{i,k}(0) = r_{i,k}(0) \quad \text{and} \quad c_i(0) = r_i(0) \ . \tag{51}$$

ii. Symmetry:

$$c_{i,k}(-\tau) = [c_{k,i}(\tau)]^* \quad \text{and} \quad c_i(-\tau) = [c_i(\tau)]^* \ . \tag{52}$$

iii. Correlation bound; Sarwate has proven [88], [89] that for the maximum out-of-phase autocorrelation value c_{am}, and the maximum crosscorrelation value c_{cm} the following relationship holds:

$$(2N-1)c_{cm}^2 + \frac{2(N-1)}{M-1}c_{am}^2 \geq 1 \ , \tag{53}$$

which leads to the following result due to Welch [3]:

$$c_{max}^2 = \max\{c_{am}^2, c_{cm}^2\} = \frac{M-1}{2NM-M-1} \ . \tag{54}$$

where N is the length of the sequences and M is the size of the sequence set.

iv. Even correlation $r_{i,k}(\tau)$ (i.e. periodic correlation) and odd correlation $\hat{r}_{i,k}(\tau)$ which are defined as follows:

$$r_{i,k}(\tau) = c_{i,k}(\tau) + c_{i,k}(\tau - N) \quad , \tag{55}$$
$$\text{and} \quad r_{i,k}(N-\tau) = [r_{i,k}(\tau)]^*$$

$$\hat{r}_{i,k}(\tau) = c_{i,k}(\tau) - c_{i,k}(\tau - N) \quad , \tag{56}$$
$$\text{and} \quad \hat{r}_{i,k}(N-\tau) = -[\hat{r}_{i,k}(\tau)]^*$$

$$r_i(\tau) = c_i(\tau) + c_i(\tau - N) \quad \text{and} \quad r_i(N-\tau) = [r_i(\tau)]^* \ , \tag{57}$$

$$\hat{r}_i(\tau) = c_i(\tau) - c_i(\tau - N) \quad \text{and} \quad \hat{r}_i(N-\tau) = -[\hat{r}_i(\tau)]^* \ , \tag{58}$$

In asynchronous CDMA systems, since the even and odd correlation functions appear with equal probability, both functions are of equal importance.

Knowledge of the maximum nontrivial value of aperiodic correlation or maximum values of odd and even correlation values is useful in the analysis of the worst case interference scenario in asynchronous CDMA systems. It is, however, inadequate in estimating the most meaningful performance parameter of the CDMA system, the average bit error rate (BER).

3.3 Error Performance of CDMA System Due to Multiaccess Interference

The BER in a multiple access environment depends on the modulation technique used, demodulation algorithm, and the signal-to-noise ratio (SNR) available at the receiver. Pursley [85] showed that in the case of a BPSK, asynchronous, DS-CDMA system, it is possible to express the average SNR at the receiver output of a correlator receiver of the ith user as a function of the average interference parameter (AIP) for the other K users of the system and the power of white Gaussian noise present in the channel. The SNR for the ith user, denoted as SNR_i, can be expressed in the form:

$$\mathrm{SNR}_i = \left(\frac{N_0}{2E_b} + \frac{1}{6N^3} \sum_{k=1, k \neq i}^{K} \rho_{k,i} \right)^{-0.5}, \tag{59}$$

where E_b is the bit energy, N_0 is the one-sided Gaussian noise power spectral density, and $\rho_{k,i}$ is the AIP, defined for a pair of sequences as [7]:

$$\rho_{k,i} = 2\mu_{k,i}(0) + \mathrm{Re}\{\mu_{k,i}(1)\}. \tag{60}$$

The crosscorrelation parameters $\mu_{k,i}(\tau)$ are defined by:

$$\mu_{k,i}(\tau) = N^2 \sum_{n=1-N}^{N-1} c_{k,i}(n) c^*_{k,i}(n+\tau). \tag{61}$$

However, following the derivation in [52], $\rho_{k,i}$ for complex valued sequences may be well approximated as:

$$\rho_{k,i} \approx 2N^2 \sum_{n=1-N}^{N-1} |c_{k,i}(n)|^2. \tag{62}$$

The formula (59), has been derived by Pursley in [85] under the assumption that relative phase shifts $\theta_{i,k}$ between carrier waves of the ith user and the interfering users are random, and uniformly distributed in the interval $(0, 2\pi]$, and that the relative time delays $\tau_{i,k}$ between the ith user and the interfering users are random, and uniformly distributed in the interval $[0, T)$, where T is the duration of a single data bit.

3.4 Performance Comparison of Different Sets of Spreading Sequences

Recently, the definition of "good" signatures for CDMA systems has been moving away from the measure of the maximum nontrivial value of correlation (either aperiodic or periodic) to the mean-square value of the aperiodic crosscorrelation [52]. This measure, is far more reasonable in the context of CDMA systems, because the average BER for such systems is dependent on the SNR described by the formulae (59)-(62) rather than the worst case error associated with the peak crosscorrelation values between individual users.

In order to evaluate the performance of a set of M sequences as a whole, the average mean-square value of crosscorrelation for every sequence in the set, denoted by R_{CC}, was introduced by Oppermann and Vucetic [79], [80] as a measure of the set crosscorrelation performance:

$$R_{CC} = \frac{1}{M(M-1)} \sum_{i=1}^{M} \sum_{k=1,(k\neq i)}^{M} \sum_{\tau=1-N}^{N-1} |c_{i,k}(\tau)|^2. \tag{63}$$

A similar measure, denoted by R_{AC}, was introduced in [79] for comparing the autocorrelation performance:

$$R_{AC} = \frac{1}{M}\sum_{i=1}^{M} \sum_{\tau=1-N,(\tau\neq 0)}^{N-1} |c_i(\tau)|^2 \quad . \tag{64}$$

This value allows for comparison of the autocorrelation properties of the set on the same basis as the crosscorrelation properties. These two measures have been used in [79] as the basis for comparing the sequence sets. They can also be used as the optimisation criteria in design of the new sequence sets, as it is later used in this thesis.

3.5 Numerical Example

To illustrate significance of the concepts presented in the chapter, let us consider the set of bipolar Gold sequences of period $N = 31$. The bipolar Gold sequences of a given period N can be obtained from the set of binary Gold codes $G(a, b)$ which elements are described [29] by the formula:

$$\begin{aligned} G(a,b) &= \{g_n^{(j)}, j = 1, \ldots, N+2\} \\ &= \{a, b, a \oplus Tb, a \oplus T^2 b, \ldots, a \oplus T^{N-1} b, a \oplus T^N b\} \end{aligned} \tag{65}$$

where a and b are two preferred m-sequences [29] of the period N, and T is a shift operator. For a given sequence $a = \{a_n\} = (a_1, a_2, a_3, \ldots, a_{N-1}, a_N)$ the shift operator T shifts a cyclically to the right by one place, that is:

$$\begin{aligned} a &= (a_1, a_2, a_3, \ldots, a_{N-1}, a_N) \\ Ta &= (a_N, a_1, a_2, \ldots, a_{N-2}, a_{N-1}) \\ T^2 a &= (a_{N-1}, a_N, a_1, \ldots, a_{N-3}, a_{N-2}) \\ &\ldots \qquad\qquad \ldots \\ T^N a &= a \end{aligned} \quad . \tag{66}$$

The bipolar sequences are then obtained from the set $G(a, b)$, using the following formula:

$$G_{\pm}(a,b) = \left\{(-1)^{g_n^j}, j = 1, \ldots, N+2, n = 1, \ldots, N\right\}, \tag{67}$$

which translates 'ones' of the original Gold code into 'negative ones' and 'zeros' of the original Gold code into 'positive ones'. The full list of the bipolar Gold spreading sequences of length 31 obtained from the pair of m-sequences:

$$a = (0000100101100111110001101110101),$$

$$b = (0001010110100001100100011110111),$$

is given in Table 1.

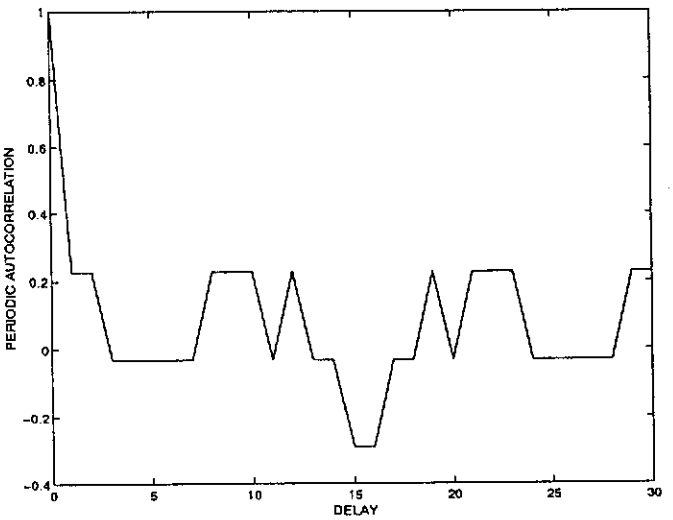

Figure 13 Periodic autocorrelation for the Gold sequence:
(+ - - - - + + + + + - - - - + - - - + - - - - - - - + - + - +).

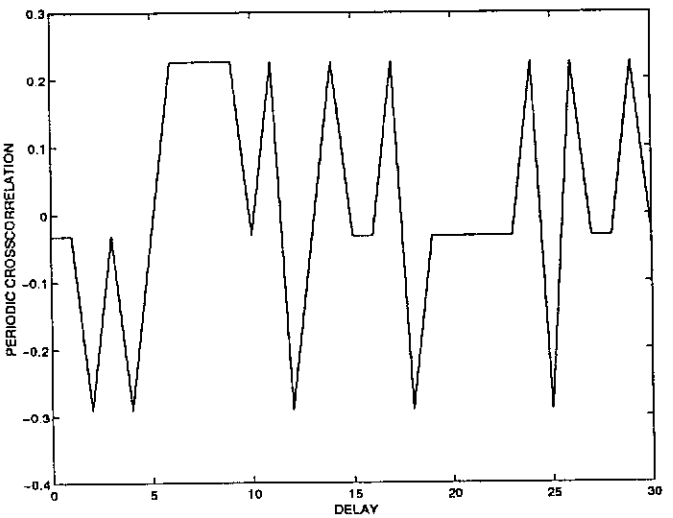

Figure 14: Periodic crosscorrelation between the sequences:
(+ + + + - + + - + - - + + - - - - - + + + - - + - - - + - + -) and
(- - - + - + - - - - + - + + - - - - - - + - + + - + + - + - + - -) .

Table 1: Bipolar Gold spreading sequences of length 31.

l	Spreading Sequence
1	+ + + + − + + − + − − + + − − − − − + + + − − + − − − + − + −
2	+ + + − + − + − − + − + + + + − − + + − + + − − − − − + − − −
3	− + + + + + − − − + − − + − − − + + + + − − − − + + + − − − +
4	− − + + − − + + + + + + − − − − − + − + + + − + + + + − + + +
5	− − − + − + − − − − + − + + − − − − − − + − + + − + + − + − −
6	+ − − − − + + + + + − − − − + − − − + − − − − − − − − + − + − +
7	− + − − + + + − − − + + − + − + − − + + − + − + + + − − − + − +
8	− − + − + − + − + + − − + + + − + − + + + + + + − + − + + − +
9	− − − + + − − − + − + + − − + + − + + + + − + − − − + + − − +
10	− − − − − − − + + − − − + + − + + − − + + − − − + − − − − + +
11	− − − − + + − + − − − + − − + − + + + − + − − + + + − + + + −
12	+ − − − + − + + − + − + + + − + − + − + − − − + − + + + − − −
13	+ + − − + − − − − + + + + − + − + − − − + + − + − − + − − + +
14	− + + − + − − + + + + − + − − + − + + − − − + + − − − − + + −
15	+ − + + + − − + − − + − − − − − + − − + − + − − − − − + + − −
16	+ + − + − − − + − + − − − + − − − + + − + + + + + − − + − − +
17	− + + − − + − + − + + + − + + − − − − + − − + − − + − + − + +
18	− − + + + + + + − + + − + + + + − − + − + + − − + − + + − + −
19	+ − − + − − + − − + + − − − + + + − + + − − + + + + − − − + −
20	+ + − − − + − − + + + − − + − + + + + + + + − − − + + + + + −
21	+ + + − + + + + + − + − − + + − + + − + + − + + + − + − − − −
22	+ + + + + − + − − − − − − + + + − + − − + − − − − + − − + + +
23	− + + + − − − − + + − + − + + + + − − − − − − + + − + + + − −
24	+ − + + − + − + + − + + + + + + + + + − − + − + − + − − − − +
25	− + − + − + + + − − − − + − + + + + − + − + + + − − + + + + +
26	− − + − − + + − − + − + − − − + + + − − + + + − − − − − − − −
27	+ − − + + + + − + + + + + + − − + + − − − − + − + − − + + + +
28	− + − − − − + − + − + − + − + − − + − − − + − − + + − + − − −
29	+ − + − + + − − + − − − − − − + − − − − − + + + + + + + − + +
30	− + − + + − + + + − − + − + − − + − + − − + + − − + + − − + −
31	+ − + − − − − − − − − + + + + − − + + + − + + − + − + − + + −
32	+ + − + + + − + + + − + + − + + − − − + + + + − + + − − + − −
33	+ + + − − − + + − − + + + − − + + − + − + − + − + − + + + + + − +

To calculate the periodic correlations we use the formulae (39) and (40), and the

example plots are given in Figure 13 and Figure 14 for the periodic correlation values, and in Figure 15 and Figure 16 for the aperiodic correlations. It is visible from the plot in Figure 14 that, even for the perfect synchronisation, the sequences are not orthogonal

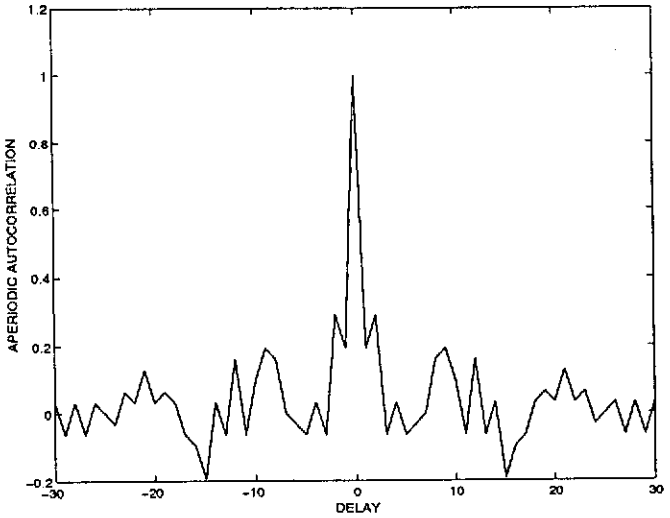

Figure 15: Aperiodic autocorrelation for the Gold sequence:
(+ - - - + + + + + - - - - + - - - + - - - - - - - + - + - +) .

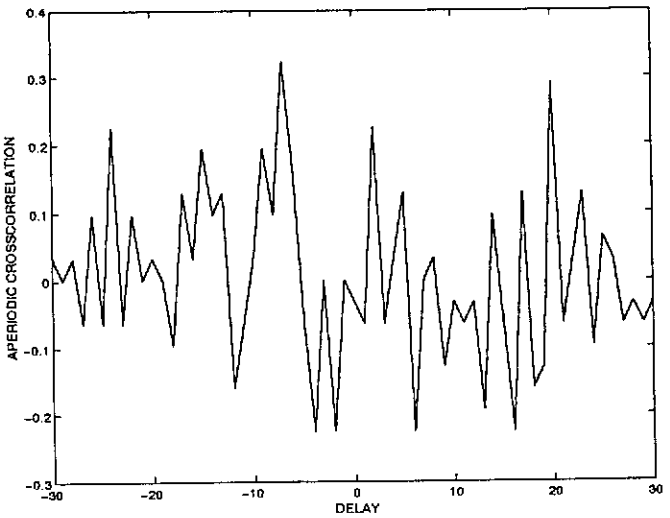

Figure 16: Aperiodic crosscorrelation between the sequences:
(+ + + + - + + - + - - + + - - - - - + + + - - + - - - + - + -) and
(- - - + - + - - - - + - + + - - - - - - + - + + - + + - + - -) .

The maximum nontrivial periodic correlations and the maximum nontrivial aperi-

odic correlations are equal to 0.2903 and 0.4194, respectively.

As far as the correlation measures given by formulae (63) and (64) are concerned, we have calculated their values, and the results are listed in Table 2 for the whole set of 33 spreading sequences, and for some smaller subsets of sequences. It is interesting to notice here that the values of R_{CC} have very small variations among the different subsets of sequences, while the values of R_{AC} depend strongly on the number of sequences in the set.

Table 2: Calculated values of the parameters R_{CC} and R_{AC} for the selected subsets of bipolar Gold spreading sequences.

M	Sequences	R_{CC}	R_{AC}
33	all	0.9707	1.0064
26	1-13, 14-16,19, 22, 25, 27-33	0.9693	0.7802
26	1-26	0.9714	0.7735
13	1-13	0.9725	0.3469
13	5-13, 29-32	0.9640	0.3724
13	3-8, 12-17	0.9686	0.3738
10	1-10	0.9794	0.2593
10	3-8, 21-24	0.9959	0.3178
10	10-14, 28-33	0.9478	0.3680

4. Spreading Sequences

In DS SS systems, a spreading waveform is a time function of a spreading sequence. Ideally, all spreading sequences used in a DS CDMA system should be pseudo-noise (PN) or pseudo-random sequences. The PN sequences, however, are deterministically generated in order to ensure the possibility of despreading at the receiver. In this chapter, we will briefly introduce some typical sets of spreading sequences proposed for use in DS CDMA systems. First, we will consider binary sequences, looking into the possible sets of orthogonal sequences, and then discuss some typical families of binary PN sequences. Later, we will consider nonbinary spreading sequences, concentrating on complex polyphase sequences with good aperiodic correlation properties.

4.1 Binary Sequences

In order to consider how far a binary sequence $\{a_n\}$ of period N resembles a PN sequence, Fan and Darnell [29] have defined the following randomness criteria:

i. The out-of-phase periodic ACF should be a small constant c, that is:

$$R(\tau) = \sum_{n=0}^{N-1} \hat{a}_n \hat{a}_{n+\tau} = \begin{cases} N, & \tau \equiv 0 \\ c, & \tau \not\equiv 0 \end{cases}, \tag{68}$$

where

$$\hat{a}_n = (-1)^{a_n} \in \{+1, -1\}, \; a_n \in \{1, 0\}. \tag{69}$$

ii. In every period, the number of 1s is nearly equal to the number of 0s. The disparity is preferred not to exceed 1; thus

$$\left| \sum_{n=0}^{N-1} \hat{a}_n \right| \le 1. \tag{70}$$

iii. Defining a run as a string of consecutive identical symbols, in every period, half the runs have length one, one-quarter have

length two, one-eight length three, etc., as long as the number of runs of a given length exceeds 1. In addition, for each of these lengths, there are equally many runs of 1s and of 0s.

Binary sequences having the above three randomness characteristics are referred to as optimal binary sequences, pseudo-random sequences or PN sequences. The three randomness properties are so strict that only a few classes of sequences (e.g. m-sequences discussed in Section 4.1.2) can satisfy all of them. Therefore, in the following sections we present also some other classes of sequences which can be considered in DS CDMA wireless data systems.

4.1.1 Orthogonal Binary Sequences

Orthogonal binary sequences are usually defined on the base of known sets of orthogonal two-valued functions. The two functions $\gamma_i(t)$ and $\gamma_j(t)$ are said to be orthogonal in the interval $[t_1, t_2)$, if [84]:

$$\int_{t_1}^{t_2} \gamma_i(t)\gamma_j(t)dt = \begin{cases} 0, \text{ if } & \gamma_i(t) \not\equiv \gamma_j(t) \\ K, \text{ if } & \gamma_i(t) \equiv \gamma_j(t) \end{cases} . \tag{71}$$

If the constant K is equal to 1, for every function in the set, the set is referred to as a set of orthonormal functions.

a) Rademacher functions

One of the simplest sets of orthonormal two-valued functions is a set of odd Rademacher functions, defined on the interval $\left[-\frac{1}{2}, \frac{1}{2}\right)$ as [113]:

$$\mathrm{Rad}_m(t) = \begin{cases} 1, & m = 0 \\ \mathrm{sgn}[\sin(2^m \pi t)], & m = 1, 2, 3, \ldots \end{cases} . \tag{72}$$

The plots of the first five Rademacher functions are given in Figure 17, and in Table 3,

the list of the corresponding binary sequences is presented.

It is easy to notice that the Rademacher sequences have very poor autocorrelation properties, and that the number of sequences of a given length N is very low.

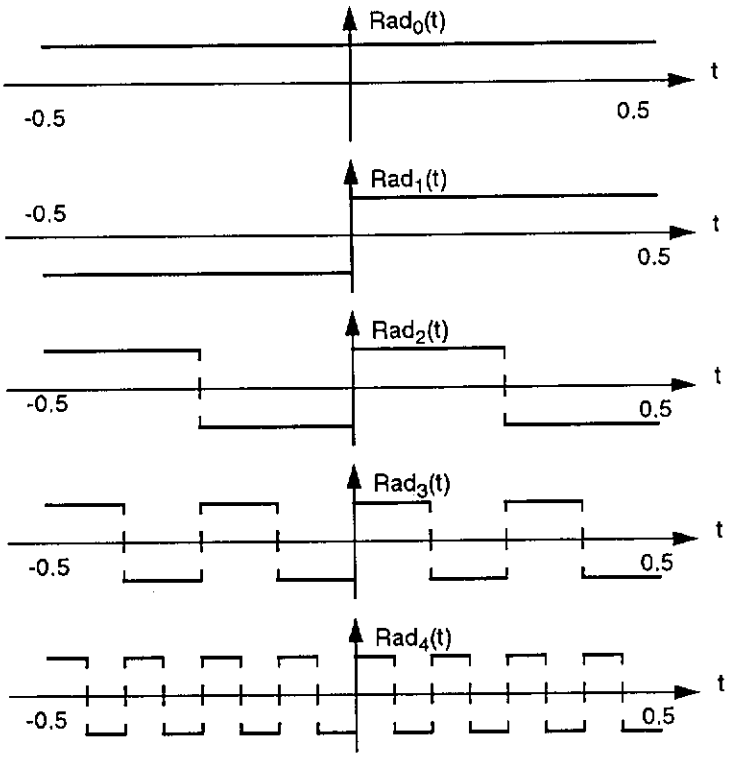

Figure 17: Odd Rademacher functions of orders 0 to 4.

Table 3: Rademacher sequences of length 16.

No.	Sequence
0	(0000000000000000)
1	(1111111100000000)
2	(0000111100001111)
3	(0011001100110011)
4	(0101010101010101)

Note: Bipolar sequences are obtained using equation (69).

b) Walsh functions

A larger set of orthogonal sequences of length $N = 2^m$; $m = 0, 1, 2, \ldots$, can be constructed on the basis of Walsh functions. There are couple of formal definitions of Walsh functions introduced in the literature [9], [44]. Here, we will use their definition on the interval [0, 1) [100]:

$$\mathrm{Wal}(0, t) = x_0(t) = 1; \quad 0 \le t < 1 \tag{73}$$

$$\mathrm{Wal}(1, t) = x_1(t) = \begin{cases} 1, & 0 \le t < 0.5 \\ -1, & 0.5 \le t < 1 \end{cases}$$

$$\mathrm{Wal}(2, t) = x_2^1(t) = \begin{cases} 1, & 0 \le t < 0.25 \text{ and } 0.75 \le t < 1 \\ -1, & 0.25 \le t < 0.75 \end{cases}$$

$$\mathrm{Wal}(3, t) = x_2^2(t) = \begin{cases} 1, & 0 \le t < 0.25 \text{ and } 0.5 \le t < 0.75 \\ -1, & 0.25 \le t < 0.5 \text{ and } 0.75 \le t < 1 \end{cases}$$

and recursively for $m = 1, 2, \ldots$ and $k = 1, \ldots, 2^{m-1}$ we have:

$$\mathrm{Wal}(2^{m-1} + k - 1, t) = x_m^k(t), \tag{74}$$

where

$$x_{m+1}^{2k-1}(t) = \begin{cases} x_m^k(2t), & 0 \le t < 0.5 \\ (-1)^{k+1} x_m^k(2t-1), & 0.5 \le t < 1 \end{cases} \tag{75}$$

$$x_{m+1}^{k}(t) = \begin{cases} x_m^k(2t), & 0 \le t < 0.5 \\ (-1)^{k} x_m^k(2t-1), & 0.5 \le t < 1 \end{cases}$$

The first eight Walsh functions are plotted in Figure 18. In the same way, as with Rademacher sequences, we can derive Walsh sequences from the Walsh functions. The list of all 16 such sequences of length 16 is given in Table 4.

A simple method to generate bipolar Walsh sequences is by use of Hadamard matrix [82], [93]. A Hadamard matrix is an orthogonal $2^m \times 2^m$; $m = 1, 2, \ldots$ matrix whose elements are the real numbers +1 and -1. An orthogonal matrix is a matrix

whose rows are orthogonal n-tuples (over the field of real numbers in this case).

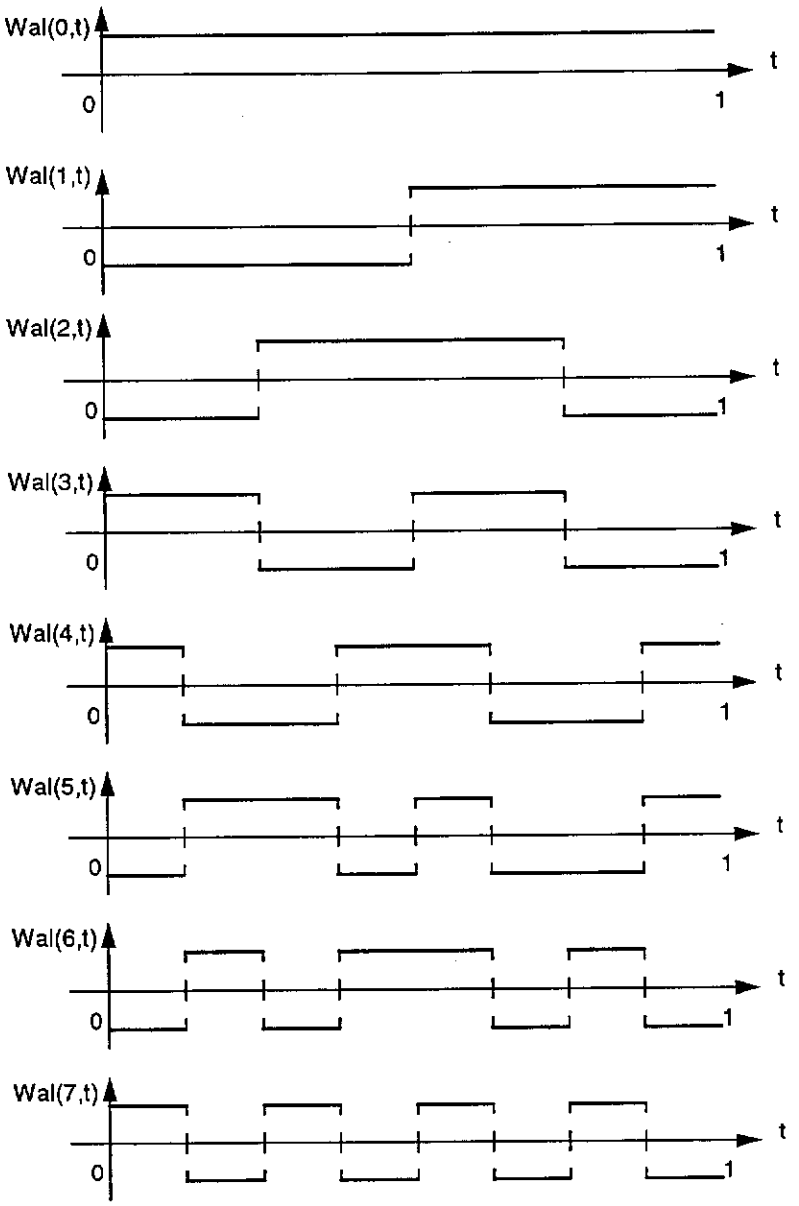

Figure 18: First eight Walsh functions.

There is a theorem associated with Hadamard matrices, which states:

If H_{2^m} is a $2^m \times 2^m$; $m = 1, 2, \ldots$ Hadamard matrix, then the matrix:

$$H_{2^{m+1}} = H_2 \otimes H_{2^m} = \begin{bmatrix} H_{2^m} & H_{2^m} \\ H_{2^m} & -H_{2^m} \end{bmatrix} \tag{76}$$

is a $2^{m+1} \times 2^{m+1}$ Hadamard matrix.

Table 4: List of Walsh sequences of length 16.

No.	Sequence
0	(0000000000000000)
1	(1111111100000000)
2	(1111000000001111)
3	(0000111100001111)
4	(0011110000111100)
5	(0011110011000011)
6	(0011001111001100)
7	(0011001100110011)
8	(0110011001100110)
9	(0110011010011001)
10	(0110100110010110)
11	(0110100101101001)
12	(0101101001011010)
13	(0101101010100101)
14	(0101010110101010)
15	(0101010101010101)

Note: Bipolar sequences are obtained using equation (69).

It is clear that the matrix:

$$H_2 = \begin{bmatrix} 1 & 1 \\ 1 & -1 \end{bmatrix} \tag{77}$$

is a Hadamard matrix, and that its rows correspond to bipolar Walsh sequences of length $N = 2^1 = 2$. It can also be shown [58] that, in general, rows of the Hadamard matrix of an order 2^m; $m = 1, 2, 3, \ldots$, obtained from the matrix H_2 given by (77),

are bipolar Walsh sequences of length $N = 2^m$; $m = 1, 2, 3, \ldots$.

Example: It easy to notice that starting from H_2 given by (77) we obtain:

$$H_{16} = \left[\begin{array}{cccccccc|cccccccc|l}
1 & 1 & 1 & 1 & 1 & 1 & 1 & 1 & 1 & 1 & 1 & 1 & 1 & 1 & 1 & 1 & \hat{w}_0 \\
1 & -1 & 1 & -1 & 1 & -1 & 1 & -1 & 1 & -1 & 1 & -1 & 1 & -1 & 1 & -1 & \hat{w}_{15} \\
1 & 1 & -1 & -1 & 1 & 1 & -1 & -1 & 1 & 1 & -1 & -1 & 1 & 1 & -1 & -1 & \hat{w}_7 \\
1 & -1 & -1 & 1 & 1 & -1 & -1 & 1 & 1 & -1 & -1 & 1 & 1 & -1 & -1 & 1 & \hat{w}_8 \\
1 & 1 & 1 & 1 & -1 & -1 & -1 & -1 & 1 & 1 & 1 & 1 & -1 & -1 & -1 & -1 & \hat{w}_3 \\
1 & -1 & 1 & -1 & -1 & 1 & -1 & 1 & 1 & -1 & 1 & -1 & -1 & 1 & -1 & 1 & \hat{w}_{12} \\
1 & 1 & -1 & -1 & -1 & -1 & 1 & 1 & 1 & 1 & -1 & -1 & -1 & -1 & 1 & 1 & \hat{w}_4 \\
1 & -1 & -1 & 1 & -1 & 1 & 1 & -1 & 1 & -1 & -1 & 1 & -1 & 1 & 1 & -1 & \hat{w}_{11} \\
\hline
1 & 1 & 1 & 1 & 1 & 1 & 1 & 1 & -1 & -1 & -1 & -1 & -1 & -1 & -1 & -1 & \hat{w}_1 \\
1 & -1 & 1 & -1 & 1 & -1 & 1 & -1 & -1 & 1 & -1 & 1 & -1 & 1 & -1 & 1 & \hat{w}_{14} \\
1 & 1 & -1 & -1 & 1 & 1 & -1 & -1 & -1 & -1 & 1 & 1 & -1 & -1 & 1 & 1 & \hat{w}_6 \\
1 & -1 & -1 & 1 & 1 & -1 & -1 & 1 & -1 & 1 & 1 & -1 & -1 & 1 & 1 & -1 & \hat{w}_9 \\
1 & 1 & 1 & 1 & -1 & -1 & -1 & -1 & -1 & -1 & -1 & -1 & 1 & 1 & 1 & 1 & \hat{w}_2 \\
1 & -1 & 1 & -1 & -1 & 1 & -1 & 1 & -1 & 1 & -1 & 1 & 1 & -1 & 1 & -1 & \hat{w}_{13} \\
1 & 1 & -1 & -1 & -1 & -1 & 1 & 1 & -1 & -1 & 1 & 1 & 1 & 1 & -1 & -1 & \hat{w}_5 \\
1 & -1 & -1 & 1 & -1 & 1 & 1 & -1 & -1 & 1 & 1 & -1 & 1 & -1 & -1 & 1 & \hat{w}_{10}
\end{array}\right] . \quad (78)$$

As indicated on the right hand side of (78), each row of the matrix H_{16} corresponds to one bipolar Walsh sequence.

By examining Walsh sequences listed in Table 4, it is clear that they do not fulfil the randomness criteria. In order to assess their usefulness in DS CDMA systems, let us examin their correlation properties using the methods described in the previous chapter. Because the bipolar Walsh sequences are orthogonal, their crosscorrelation functions take zero if the functions are perfectly synchronised ($\tau = 0$). However, for other values of τ, they can take quite significant values, with the normalised periodic CCFs reaching 1. Also their autocorrelation properties are far from acceptable, with some of them, e.g. $\hat{w}_5$ or $\hat{w}_{16}$, corresponding to the rectangular functions having their periods of 2 and 1 chips, respectively. The example plots of periodic ACF and CCF for Walsh sequences are given in Figure 19 and Figure 20, with delay expressed in chips.

The aperiodic crosscorrelation functions are not as bad as the periodic ones, with the average mean-square value of crosscorrelation, R_{CC}, equal to 0.7292.

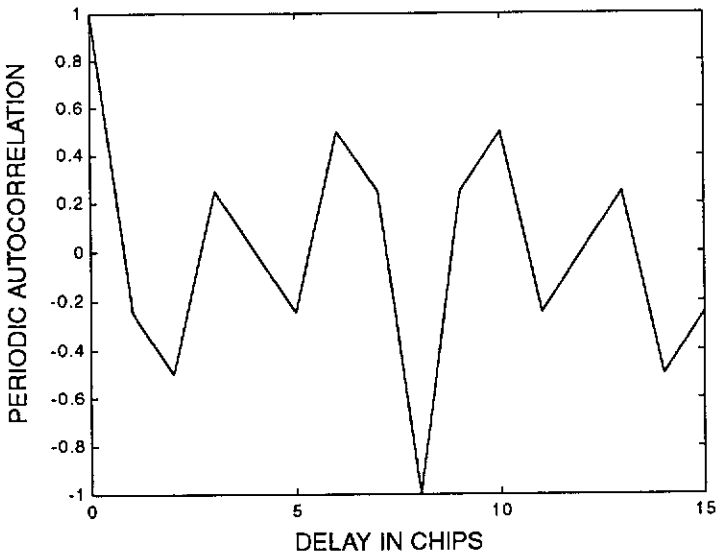

Figure 19: Normalised periodic autocorrelation function for $\hat{w}_5$.

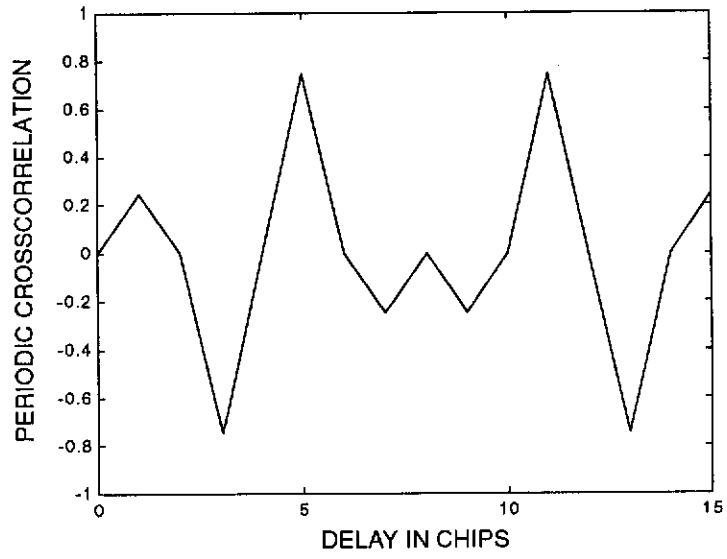

Figure 20: Normalised periodic crosscorrelation between sequences $\hat{w}_5$ and $\hat{w}_{10}$.

On the other hand, the aperiodic autocorrelation functions are very poor, with the coefficient R_{AC} (see Section 3.4) equal to 4.0625. The example plots of normalised aperiodic autocorrelation and crosscorrelation functions are given in Figure 21 and

Figure 22.

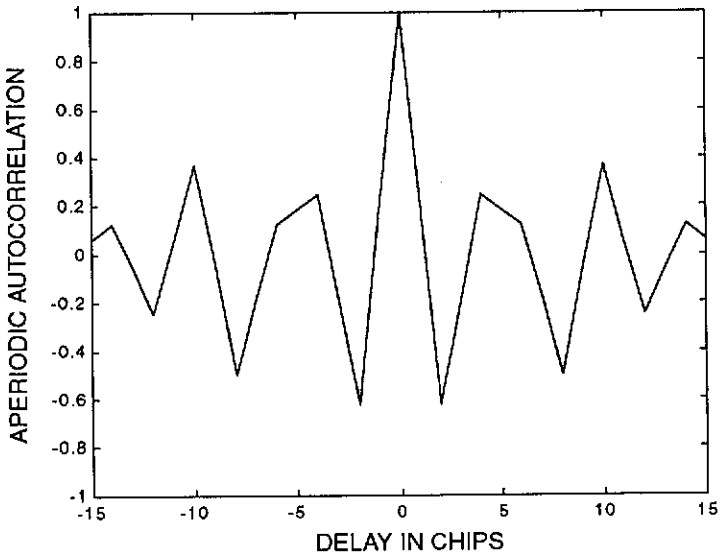

Figure 21: Normalised aperiodic autocorrelation function for $\hat{w}_5$.

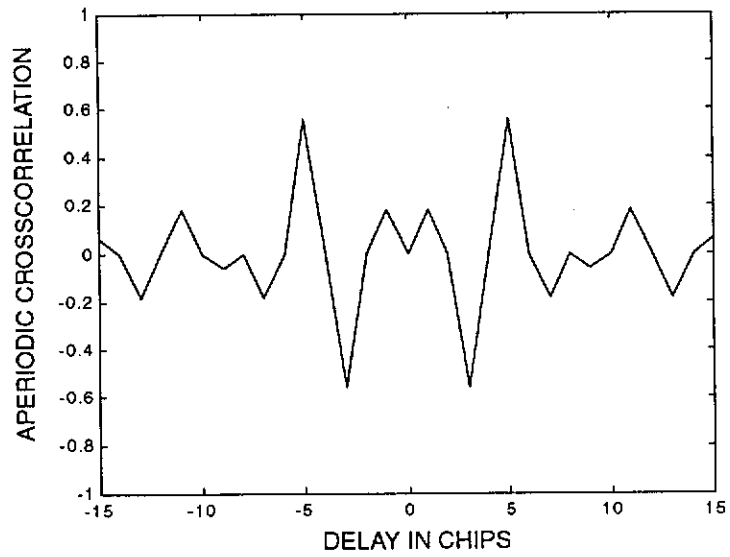

Figure 22: Normalised aperiodic crosscorrelation between sequences $\hat{w}_5$ and $\hat{w}_{10}$.

4.1.2 Maximal Length Sequences

One of the very few classes of PN sequences which can satisfy all three randomness criteria is the class of binary maximal length shift-register sequences, or m-sequences,

e.g. [29], [84]. The binary m-sequences are generated using linear feedback shift-register and exclusive OR-gates. A linear shift-register sequence is defined by a linear generator polynomial $h(x)$ of degree $m > 0$, where:

$$h(x) = h_0 x^m + h_1 x^{m-1} + \ldots + h_{m-1} x + h_m = \sum_{i=0}^{m} h_i x^{m-i}. \qquad (79)$$

To construct an m-sequence of length $2^m - 1$, the polynomial $h(x)$ needs to be a primitive polynomial [29], [58], [84] in which $h_0 = h_m = 1$. A mathematical definition of a primitive polynomial is that $h(x)$ is a primitive polynomial of degree m if the smallest integer n for which $h(x)$ divides $x^n + 1$ is $n = 2^m - 1$ [58]. A primitive polynomial is irreducible, which means that it cannot be factored into a product of polynomials with lower degrees; but the converse is not true. Extensive tables of primitive polynomials have been published in literature, e.g. [97], [122].

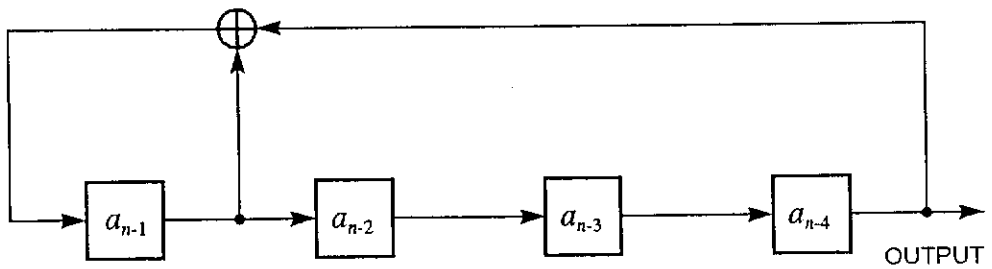

Figure 23: Feedback shift register corresponding to $h(x) = x^4 + x^3 + 1$.

Example: Let us consider the shift register, as shown in Figure 23, corresponding to the primitive polynomial:

$$h(x) = x^4 + x^3 + 1. \qquad (80)$$

Assuming the initial state 1000, we can easily obtain the output sequence utilising the *mod* 2 arithmetic. The first 18 states of the register are listed in Table 5. It is clearly visible that the output sequence 000111101011001 000... has a period of $2^4 - 1 = 15$.

Table 5: Consecutive states of the shift register of Figure 23.

No.	State
0	1000
1	1100
2	1110
3	1111
4	0111
5	1011
6	0101
7	1010
8	1101
9	0110
10	0011
11	1001
12	0100
13	0010
14	0001
15	1000
16	1100
17	1110

As we mentioned at the beginning of this section, m-sequences satisfy all three randomnes criteria. Apart from that, they have several other useful properties. A very comprehensive list of those properties can be found in [65]. Here, we give only some of those, which are most important from the viewpoint of DS CDMA systems.

i. The Shift Property: A cyclic shift (left- or right-cyclic) shift of an m-sequence is also an m-sequence. There are exactly $N = 2^m - 1$ nonzero m-sequences generated by $h(x)$.

ii. Characteristic Phase: Among N m-sequences generated by

$h(x)$, there is exactly one $\{a_n\}$ which has the property:

$$\forall_{n=0,1,2,\ldots} \{a_n\} = \{a_{2n}\}, \tag{81}$$

where $\{a_{kn}\}$ denotes the sequence obtained by taking every kth element of cyclicaly repeated sequence $\{a_n\}$.

iii. One more 1s than 0s: Any m-sequence contains 2^{m-1} 1s and $2^{m-1}-1$ 0s.

iv. The Shift-and-Add Property: The *mod* 2, term by term sum of an m-sequence and a cyclic shift of itself is another m-sequence generated by the same polynomial $h(x)$.

v. Runs: One-half of the runs have length 1, one-quarter have length 2, one-eighth have length 3, and so on, as long as these fractions give integral numbers of runs. In each case the number of runs of 0s is equal to the number of runs of 1s.

vi. Two Valued Autocorrelation: The normalised periodic autocorrelation function of an m-sequence is a two valued function:

$$r(\tau) = \frac{1}{N}\sum_{n=0}^{N-1}(-1)^{a_n \oplus a_{n+\tau}} = \begin{cases} 1, & \tau \equiv 0 \ (mod\ N) \\ -\frac{1}{N}, & \tau \not\equiv 0 \ (mod\ N) \end{cases}. \tag{82}$$

vii. Sampling: Sampling a binary m-sequence with each f such that f and N are relatively prime numbers and $1 \le f \le N-1$, $N = 2^m - 1$, will produce all $\frac{\phi(2^m-1)}{m}$ binary m-sequences of period $2^m - 1$ (each exactly m times), with $\phi(n)$ denoting the Euler's totient function [109], [110]. No other sequence will be produced.

viii. Sampling with $f = 2^l$, $l = 0, 1, 2, \ldots$: If a binary m-sequence is sampled with f equal to a power of 2, then the same sequence results.

Proof of those properties can be found in [58].

As far as m-sequences are concerned, usually for a given m, only a small subset of the m-sequences can be regarded as having good (low) CCFs among any pair of the sequences. According to the sampling property of m-sequences, any m-sequence of the length $2^m - 1$ can be generated from a given m-sequence $\{a_n\}$ of the same length $2^m - 1$ by sampling with an appropriate sampler f. Therefore, the problem of choosing m-sequences having low CCFs can be viewed as a problem of choosing appropriate values for the sampler f.

The methods of selecting the sampler f were presented by various authors, e.g. [40], [55], [64], [77], [90]. For m not being a power of 2, we can obtain from an m-sequence $\{a_n\}$ another m-sequence $\{b_n\}$ such that their periodic crosscorrelation function is a three-valued function, if the sampler $f = 2^k + 1$ or $f = 2^{2k} - 2^k - 1$, and k is an nonnegative integer. If in addition[1], $e = gcd(m, k)$ is such that m/e is odd, then the normalised aperiodic crosscorrelation $r_{a,b}(t)$ is three valued and [29]:

$$r_{a,b}(\tau) = \frac{1}{N}\begin{cases} -1 + 2^{(m+e)/2} & \text{occurs } 2^{m-e-1} + 2^{(m-e-2)/2} \text{ times} \\ -1 & \text{occurs } 2^m - 2^{m-e} - 1 \text{ times} \\ -1 - 2^{(m+e)/2} & \text{occurs } 2^{m-e-1} - 2^{(m-e-2)/2} \text{ times} \end{cases} . \qquad (83)$$

It is visible, that for low values of e, $r_{a,b}(t)$ takes smaller values more frequently.

By analysing equation (83), it can be noticed that, if $m \not\equiv 0 \pmod 4$, there always exist pairs of m-sequences with three-valued normalised periodic CCF, taking its value from the set $(1/N)\{-1 - 2^{\lfloor (m+2)/2 \rfloor}, -1, 1 + 2^{\lfloor (m+2)/2 \rfloor}\}$. A CCF taking on these three values is referred to as a preferred three-valued CCF and the corresponding pair of m-sequences is referred to as a preferred pair of m-sequences.

Preferred pairs of m-sequences do not exist if $m \equiv 0 \pmod 4$, however, there exist decimations which give four-valued periodic CCFs which are better than the three-valued periodic CCF.

Example: For $m = 5$, we have $N = 2^5 - 1 = 31$, and there are $\phi(31)/5 = 6$ cycli-

1. $gcd(i, j)$ denotes the greatest common divisor of i and j.

cally different[1] m-sequences of this period. They are all listed below:

$$
\begin{aligned}
a_1 &= (0000100101100111110001101110101)\\
a_2 &= (0001010110100001100100111110111)\\
a_3 &= (0011011111010001001010110000111)\\
a_4 &= (0111110010011000010110101000111)\\
a_5 &= (0010111110110011100001101010010)\\
a_6 &= (0111011000111110011010010000101)
\end{aligned}
$$

Since m is odd, the peak periodic crosscorrelation $r_{cm} = \frac{1}{31}(1 + 2^{\lfloor 3.5 \rfloor}) = \frac{9}{31}$ for pairs of the preferred sequences. However, for other pairs of m-sequences, r_{cm} can be higher. The list of r_{cm} for any pair of the m-sequences of the length 31 is given in Table 6, and the example plots of $r_{ij}(\tau)$ for the pair of preferred sequences $(\hat{a}^{(1)}, \hat{a}^{(3)})$, and the pair of nonpreferred sequences $(\hat{a}^{(1)}, \hat{a}^{(6)})$ are given in Figure 24 and Figure 25, respectively.

Table 6: List of r_{cm} for all pairs of m-sequences of length 31.

	$\hat{a}^{(1)}$	$\hat{a}^{(2)}$	$\hat{a}^{(3)}$	$\hat{a}^{(4)}$	$\hat{a}^{(5)}$	$\hat{a}^{(6)}$
$\hat{a}^{(1)}$	--	0.2903	0.2903	0.2903	0.2903	0.3548
$\hat{a}^{(2)}$	0.2903	--	0.2903	0.3548	0.2903	0.2903
$\hat{a}^{(3)}$	0.2903	0.2903	--	0.2903	0.3548	0.2903
$\hat{a}^{(4)}$	0.2903	0.3548	0.2903	--	0.2903	0.2903
$\hat{a}^{(5)}$	0.2903	0.2903	0.3548	0.2903	--	0.2903
$\hat{a}^{(6)}$	0.3548	0.2903	0.2903	0.2903	0.2903	--

1. Two sequences are cyclically different if one of them cannot be obtained from another one by a cyclic shift.

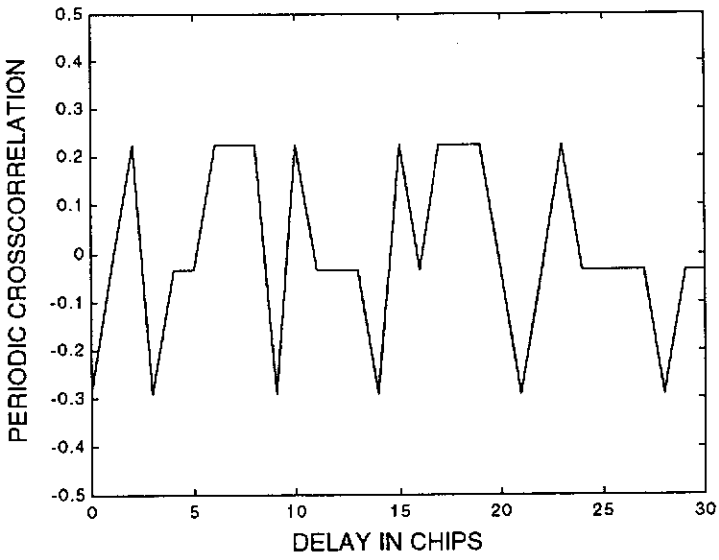

Figure 24: Periodic crosscorrelation function between the sequences $\hat{a}^{(1)}$ and $\hat{a}^{(3)}$.

A set of m-sequences which has the property that each pair in the set is a preferred pair is often referred to as a connected set of m-sequences. A largest possible connected set for a given N, is called a maximal connected set. [29].

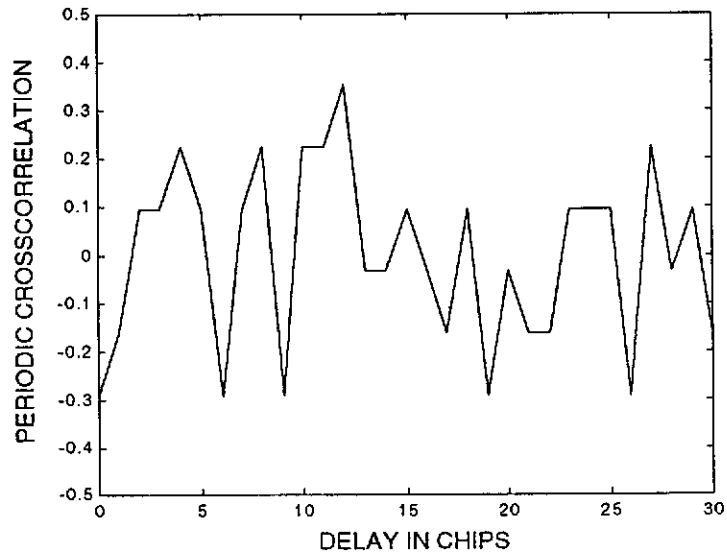

Figure 25: Periodic crosscorrelation function between the sequences $\hat{a}^{(1)}$ and $\hat{a}^{(6)}$.

4.1.3 *Gold and Gold-like Sequences*

For DS CDMA applications the number of sequences required is usually much larger than the size of the maximal connected set for a given N. Therefore, we need to obtain larger sets of sequences of length N, having good correlation functions. Certainly, such sets must contain some non-m-sequences, and their normalised out-of-phase ACF is usually not constant and exceeding $1/N$.

Gold [39] and Kasami [53] have proven that using the preferred m-sequences of length N, one can construct larger sets of sequences of length N, having better periodic crosscorrelation functions than the sets of all m-sequences of length N. However, this is obtained by increasing the value of out-of-phase ACFs compared to that of m-sequences of the same length.

In section 3.5, we have introduced the method of obtaining Gold sequences from a pair of preferred m-sequences of length N. We construct a set of Gold sequences by taking the element by element modulo-2 sum of one of the preferred m-sequences with each of the N cyclicly shifted versions of another preferred m-sequence. Including the two original preferred sequences in the set, we obtain a total of $N+2 = 2^m + 1$ sequences.

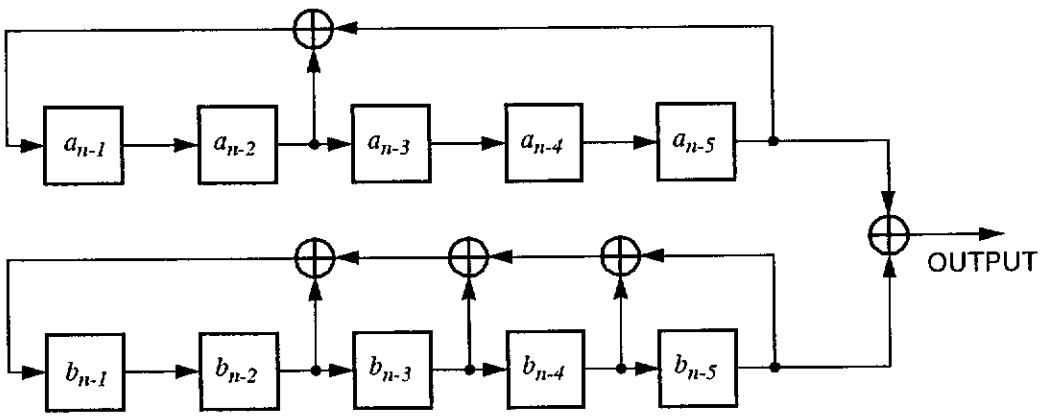

Figure 26: Two independent linear feedback shift registers used to generate Gold sequences.

There are two equivalent methods of implementing Gold sequences of period $N = 2^m - 1$ by using feedback shift registers. The first, definition based, method generates Gold sequences $G(a, b)$ utilising two independent feedback shift registers one generating the preferred m-sequence a and another one generating the preferred m-se-

quence b with two sequences being modulo-2 added chip-by-chip. The block diagram example of such a generator is presented in Figure 26, with the primitive polynomials $h_1(x) = x^5 \oplus x^3 \oplus 1$ and $h_2(x) = x^5 \oplus x^3 \oplus x^2 \oplus x \oplus 1$ corresponding to the sequences a and b, respectively. This generator generates Gold sequences of length 31. The exact generated sequence depends on the initial state of the registers.

The second method follows from the fact that the set of all sequences of the form $a \oplus b$, where a and b are two cyclically different m-sequences (a pair of preferred m-sequences is always cyclically different), is just the set of all sequences generated by the polynomial [29]:

$$h(x) = h_1(x)h_2(x) = x^{10} \oplus x^7 \oplus x^5 \oplus x^4 \oplus x^2 \oplus x \oplus 1. \tag{84}$$

Thus a feedback shift register implementing a polynomial $h(x)$ can be used to generate any of Gold sequences $G(a, b)$. It is possible to prove [29] that the maximum nontrivial periodic correlation value r_{max}, defined in Section 3.1, is given by:

$$r_{max} = \frac{1}{2^m - 1} \begin{cases} 1 + 2^{\frac{m+1}{2}}, & m \text{ odd} \\ 1 + 2^{\frac{m+2}{2}}, & m \equiv 2 \pmod 4 \end{cases}. \tag{85}$$

On the other hand, we have $N = 2^m - 1$ and $M = 2^m + 1$. Therefore, for large m, we have $N \approx M$, and according to Sidelnikov bound

$$r_{max} \geq \sqrt{\frac{2}{N}} = \frac{1}{2^m - 1}\sqrt{2^{m+1} - 2} \approx \frac{2^{\frac{m+1}{2}}}{2^m - 1}. \tag{86}$$

Utilising (85), for large odd m we have:

$$r_{max} = \frac{2^{\frac{m+1}{2}} + 1}{2^m - 1} \approx \frac{2^{\frac{m+1}{2}}}{2^m - 1}. \tag{87}$$

Thus, comparing (86) and (87), we can conlude that in such cases r_{max} for Gold

sequences approaches the Sidelnikov bound.

As we mentioned in the previous section, there is no preferred pair of m-sequences for $m \equiv 0 \ (mod\ 4)$, and therefore there are no Gold sequences of length $N = 2^m - 1, m \equiv 0 \ (mod\ 4)$. However, in literature [22], [29], [39], we can find description of the so called Gold-like sequences, having their properties similar to Gold sequences. There are two main classes of such sequences, denoted [29] as $H(a, b)$ and $I(a, b)$.

Construction of the set $H(a, b)$ of sequences follows from the fact that for $m \equiv 0 \ (mod\ 4)$ and $f = 1 + 2^{(m+2)/2}$ it can be proven that:

$$gcd(f, 2^m - 3) = 3. \tag{88}$$

Therefore, if a is an m-sequence of length $N = 2^m - 1$ generated by $h_1(x)$, and $b^{(k)}, k = 0, 1, 2$, is the result of decimating of k-positions cyclically shifted sequence a by a sampler f, then, according to the Sampling property of m-sequences, the $b^{(k)}$ are sequences of period $N' = N/gcd(f, N) = N/3$. They can be generated by the polynomial $h_2(x)$ whose roots are the fth powers of the roots of $h_1(x)$.Therefore set $H(a, b)$ being generated by the polynomial $h(x) = h_1(x)h_2(x)$, is defined as:

$$\begin{aligned} H(a, b) = \{ & a, a \oplus b^{(0)}, a \oplus Tb^{(0)}, a \oplus T^2 b^{(0)}, \ldots, a \oplus T^{N'-1} b^{(0)}; \\ & a \oplus b^{(1)}, a \oplus Tb^{(1)}, a \oplus T^2 b^{(1)}, \ldots, a \oplus T^{N'-1} b^{(1)}; \\ & a \oplus b^{(2)}, a \oplus Tb^{(2)}, a \oplus T^2 b^{(2)}, \ldots, a \oplus T^{N'-1} b^{(2)} \} \end{aligned} \tag{89}$$

where $T^i, i = 0, 1, 2, \ldots$ is the shift operator defined in Section 3.5. The sequences $b^{(k)}$ are repeated three times in order to perform the operation $a \oplus T^i b^{(k)}$ on a bit by bit basis. The number of sequences in the set $H(a, b)$ is equal to $M = N + 1 = 2^m$.

Example: For $m = 4$, we have $f = 1 + 2^{(4+2)/2} = 9$, and $gcd(f, 2^m - 1) = gcd(9, 15) = 3$. One of the m-sequences of the length 15 is given

by:

$$a = \{a_n\} = (011110101100100)$$

Table 7: Gold-like sequences of period $N = 15$.

No.	Gold-like Sequences
1	(011110101100100)
2	(000000010001011)
3	(110001110010011)
4	(101001000011111)
5	(100101011011001)
6	(100011010111010)
7	(000110011101000)
8	(010010110100010)
9	(011000100000111)
10	(111101101010101)
11	(101111001111100)
12	(010100111000001)
13	(111011100110110)
14	(001100001001101)
15	(110111111110000)
16	(001010000101110)

Decimating the sequence $T^k a$ with sampler $f = 9$ for $k = 0, 1, 2$, yields:

$$b^{(0)} = (011110111101111)$$

$$b^{(1)} = (011000110001100)$$

$$b^{(2)} = (001010010100101),$$

and all Gold-like sequences of the set $H(a, b)$, of size $M = 16$ and the period $N = 15$, can be synthesised using the formula (89). They are all listed in Table 7.

To illustrate correlational properties of the Gold-like sequences, the example plots

of normalised periodic ACF and CCF as well as the aperiodic ACF and CCF are given in Figure 27, Figure 28, Figure 29, and Figure 30, respectively. The average mean square measure of the aperiodic autocorrelation for the set $R_{AC} = 0.7490$, and aperiodic crosscorrelation measure $R_{CC} = 0.9627$.

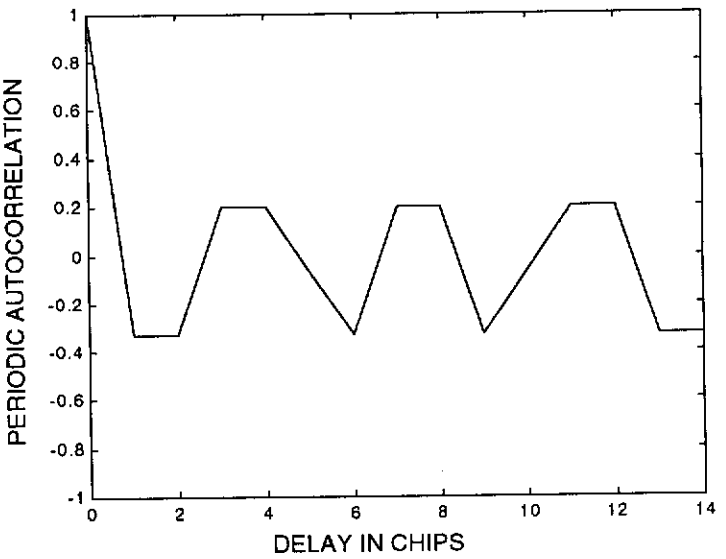

Figure 27: Periodic autocorrelation function for Gold-like sequence $a \oplus T^3 b^{(0)}$.

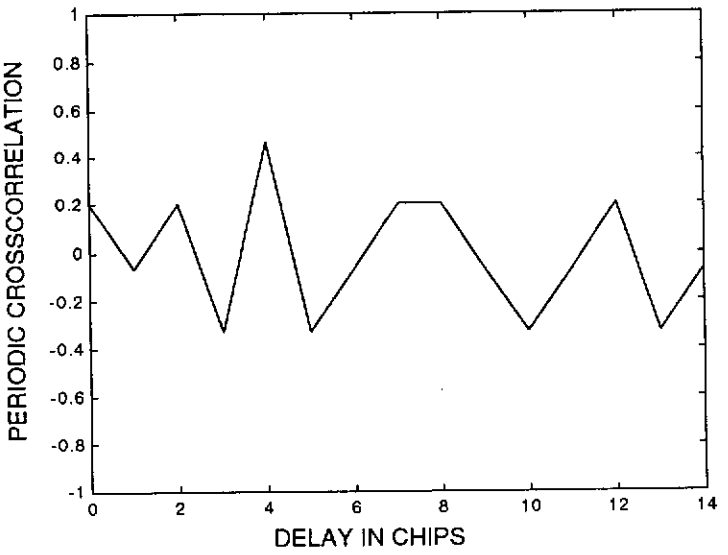

Figure 28: Periodic crosscorrelation between Gold-like sequences $a \oplus T^3 b^{(0)}$ and $a \oplus T^0 b^{(2)}$.

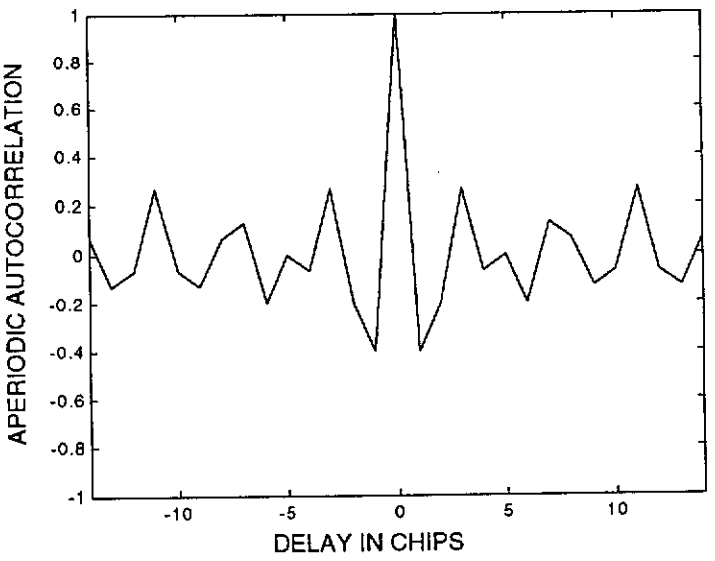

Figure 29: Aperiodic autocorrelation function for Gold-like sequence $a \oplus T^3 b^{(0)}$.

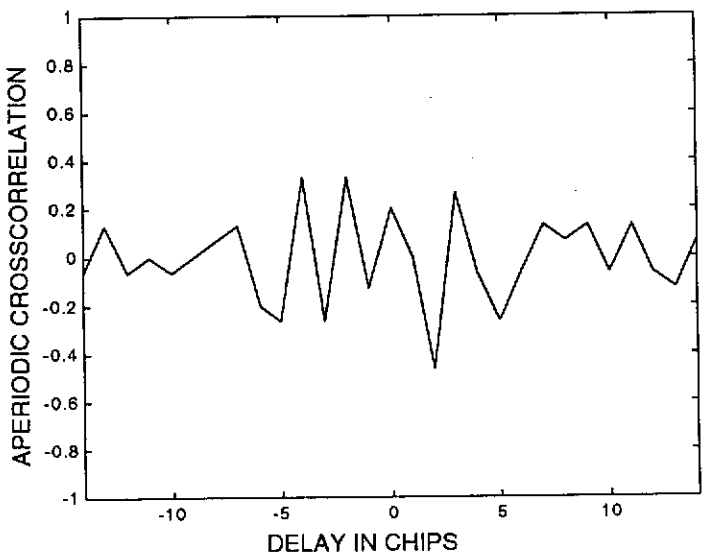

Figure 30: Aperiodic crosscorrelation between Gold-like sequences $a \oplus T^3 b^{(0)}$ and $a \oplus T^0 b^{(2)}$.

Another group of Gold-like sequences are those sequences which are obtained for $N = 2^m - 1$, $m \equiv 0 \ (mod \ 4)$ in the same way as Gold sequences if instead of preferred pair of m-sequences one uses pair of four-valued CCFs or reciprocal m-sequences [29] are used.

4.1.4 *Kasami Sequences*

There are two classes of Kasami sequences, the so called small sets of Kasami sequences denoted by $K_S(a, b)$, and the large sets of Kasami sequences denoted by $K_L(a, b, c)$. Both are constructed in a very simillar way to Gold or Gold-like sequences [29].

The small set of Kasami sequences is of the form:

$$K_S(a, b) = \left\{a, a \oplus b, a \oplus Tb, a \oplus T^2 b, \ldots, a \oplus T^{2^{m/2}-2} b\right\}, \tag{90}$$

where a is an m-sequence of period $N = 2^m - 1$, m is an even integer, and b is a sequence obtained from a by sampling it with a sampler $f = 1 + 2^{m/2}$. It is easy to notice (see Sampling property of m-sequences) that period N' of the sequence b is given by

$$N' = \frac{N}{gcd(N,f)} = 2^{m/2} - 1, \tag{91}$$

and that, in order to perform bit-by-bit operations prescribed by equation (91), the sequence b must be cyclically repeated.

Kasami has proven that the periodic crosscorrelation functions of small sets of Kasami sequences $a_i, a_j \in K_S(a, b)$, $i \neq j$, take only three values:

$$r_{a_i, a_j}(\tau) = \frac{-1}{2^m - 1} \text{ or } \frac{-1 - 2^{m/2}}{2^m - 1} \text{ or } \frac{-1 + 2^{m/2}}{2^m - 1}. \tag{92}$$

Clearly the value of r_{max} for small sets of Kasami sequences is much lower than the value of r_{max} for the set of Gold or Gold-like sequences of the same length. However, small sets of Kasami sequences contain only:

$$M = 2^{m/2} = \sqrt{N+1}, \tag{93}$$

compared to Gold or Gold-like sequences containing $M = N+2$ or $M = N+1$

sequences, respectively.

Much larger set of sequences $K_L(a, b, c)$, referred to as large set of Kasami sequences can be constructed on the basis of known set of Gold or Gold-like sequences for even values of m. There are two separate cases:

i. If $m \equiv 2 \pmod 4$, then

$$K_L(a, b, c) = \{G(a, b), G(a, b) \oplus c, G(a, b) \oplus Tc, \ldots, G(a, b) \oplus T^{2^{m/2}-2}c\}, \quad (94)$$

where $G(a, b)$ is the set of Gold sequences, c is obtained from a by sampling with the sampler $f = 1 + 2^{m/2}$ and

$$G(a, b) \oplus T^i c, \; i = 0, 1, \ldots, 2^{m/2} - 2$$

denotes the set $\{d \oplus T^i c: \; d \in G(a, b)\}$.

ii. If $m \equiv 0 \pmod 4$, then

$$\begin{aligned} K_L(a, b, c) = \{&H(a, b), H(a, b) \oplus c, \ldots, H(a, b) \oplus T^{2^{m/2}-2}c; \\ &b^{(0)} \oplus c, b^{(0)} \oplus Tc, \ldots, b^{(0)} \oplus T^{(2^{m/2}-1)/3-1}c; \\ &b^{(1)} \oplus c, b^{(1)} \oplus Tc, \ldots, b^{(1)} \oplus T^{(2^{m/2}-1)/3-1}c; \\ &b^{(2)} \oplus c, b^{(2)} \oplus Tc, \ldots, b^{(2)} \oplus T^{(2^{m/2}-1)/3-1}c\} \end{aligned} \quad (95)$$

where where $H(a, b)$ is the set of Gold-like sequences, c is obtained from a by sampling with the sampler $f = 1 + 2^{m/2}$,

$$H(a, b) \oplus T^i c, \; i = 0, 1, \ldots, 2^{m/2} - 2$$

denotes the set $\{d \oplus T^i c: \; d \in H(a, b)\}$, and the sequences $b^{(k)}$, $k = 0, 1, 2$ are obtained from the sequence $T^k a$ using a sampler $f = 1 + 2^{(m+2)/2}$.

Even though a large Kasami set contains both a small set of Kasami sequences and a set of Gold or Gold-like sequences as subsets, its maximum nontrivial periodic correlational value is the same as for Gold or Gold-like set.

4.1.5 *Barker Sequences*

The m-sequences have the best periodic autocorrelation functions as far as the minimum of the out-of-phase periodic autocorrelation is concerned. Barker [7] optimised sequences from the viewpoint of minimising sidelobes of the aperiodic autocorrelation function. Binary bipolar sequences a satisfying the condition:

$$|c_a(\tau)| \leq \frac{1}{N}, \quad \tau \neq 0 \tag{96}$$

are referred to as Barker sequences. Such sequences are known for length $N = 2, 3, 4, 5, 7, 11, 13$ and are listed below.

```
++
++-
+++-; ++-+
+++-+
+++--+-
+++---+--+-
+++++--++-+-+
```

No other binary Barker sequence of longer length is known. There are even proofs that they do not exist for odd values of N greater than 13 [102]. There is no general proof for even lengths, however, it is generaly believed that also no other even-length binary Barker sequence exists. To illustrate the aperiodic autocorrelation performance of Barker sequences, the plot of aperiodic autocorrelation function for the Barker sequence of length 13 is presented in .

Golomb and Scholtz [41], and Golomb and Win [42] investigated sequences whose elements are complex numbers of the absolute value 1, which sidelobes satisfy the original Barker constraint given by equation (96). Such sequences are referred to as generalised Barker sequences, and it is conjectured that 6-phase Barker sequences exist for all N [58].

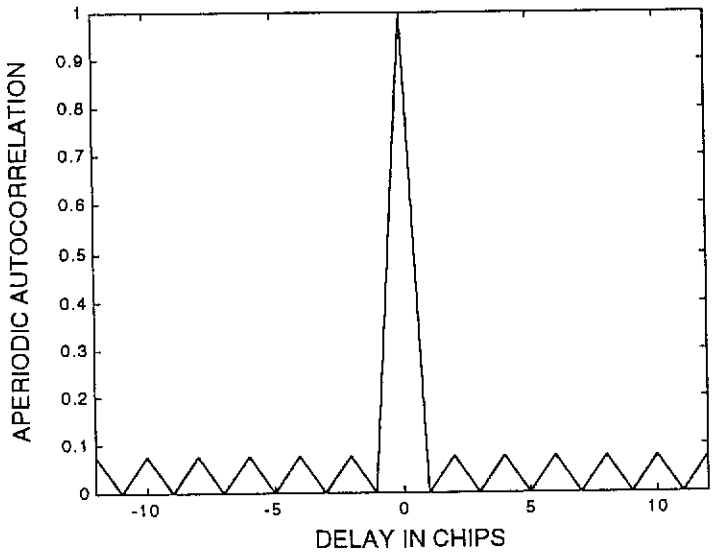

Figure 31: Autocorrelation function of Barker sequence, $N = 13$.

4.2 Nonbinary Sequences

In the previous section, while considering the generalised Barker sequences, we have already mentioned that a possible alternative to binary sequences lies in sequences which elements are complex numbers . Most of the complex sequences contemplated for DS CDMA applications are those which elements can be thought of as roots-of-unity, where the sequence values vary from symbol to symbol on the unit circle in the complex plane. This additional level of freedom increases the number of the sequences that have good correlation properties. In general, however, complex sequences may have also non-unity magnitudes. Another class of non-binary sequences are those where sequence elements are real but non-binary numbers, e.g. [15], [36], [48], [49], [72], [94]. In this section, we will introduce some examples of complex polyphase sequences with good correlation properties, e.g. [4], [6], [11], [27], [31], [57], [59], [60], [61], [70], [71], [73], [74], [75], [79], [99], which can be used for DS CDMA applications.

4.2.1 Complex m-sequences

The very natural extension of binary m-sequences discussed previously, are complex m-sequences [58]. For prime numbers p, the pth roots of unity are the complex num-

bers of the form:

$$e^{jk2\pi/p},\ 0 \le k \le p-1. \tag{97}$$

If $p = 2$, we have two roots equal to 1 and -1. The complex m-sequences are generated in the same way as their binary counterparts, i.e. they are generated by the use of primitive polynomial:

$$g(x) = g_0 x^m + g_1 x^{m-1} + \ldots + g_{m-1} x + g_m, \tag{98}$$

of degree m. The coefficients g_i, $i = 0, 1, \ldots, m$ of $g(x)$ take values from the set $\{0, 1, 2, \ldots, p-1\}$, and we have $g_m \neq 0$ and $g_0 \neq 0$. As with the binary m-sequences, we set $g(x) = 0$ and solving for x^m can find the shift-register circuit to generate sequences which is given in Figure 32 [58].

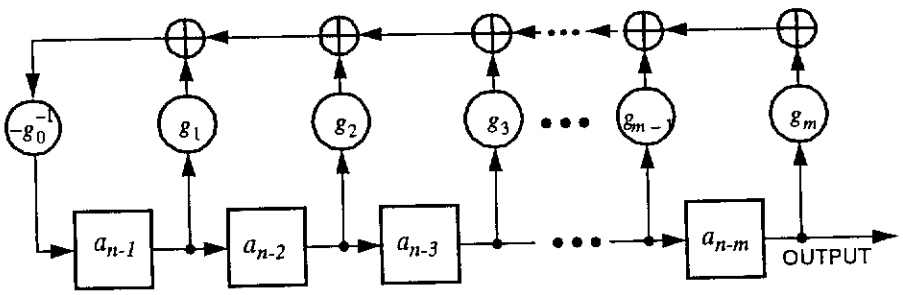

Figure 32: Shift-register circuit for generation of complex m-sequences.

The arithmetic in Figure 32 is computed *mod p*, and the period of complex m-sequences is $N = p^m - 1$.

As an example, the plot of magnitudes of periodic and aperiodic normalised ACFs are given in Figure 33 and Figure 34, respectively, for the complex m-sequence [29]:

$$\{a_n\} = (00101211201110020212210222). \tag{99}$$

The above sequence is generated for $m = 3$ and $p = 3$ by use of the primitive (*mod* 3) polynomial:

$$g(x) = x^3 + 2x + 1. \tag{100}$$

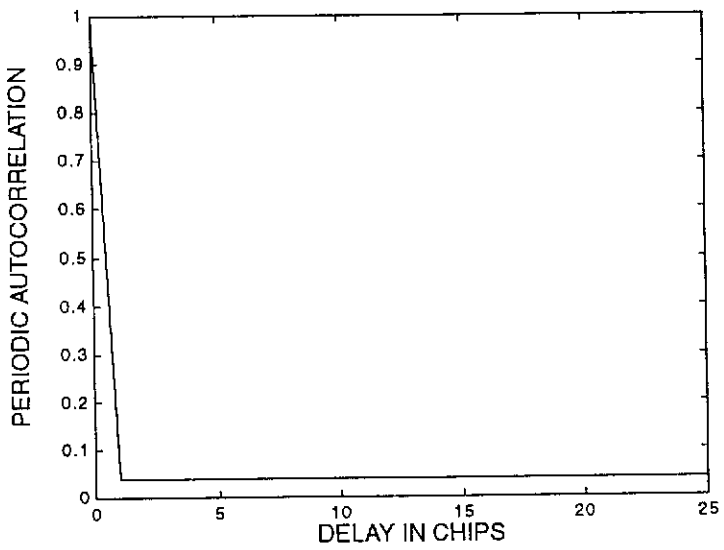

Figure 33: Magnitude of the normalised periodic ACF for the complex m-sequence $\{a_n\}$.

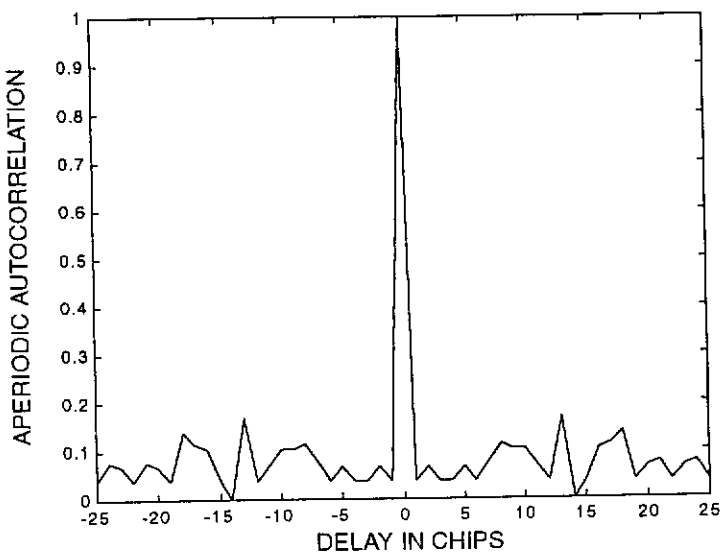

Figure 34: Magnitude of the normalised aperiodic ACF for the complex m-sequence $\{a_n\}$.

The elements of the complex sequence $\{\hat{a}_n\}$ are calculated using the formula:

$$\hat{a}_n = e^{j2\pi a_n/p}. \tag{101}$$

4.2.2 *Frank-Zadoff-Chu Sequences*

Frank-Zadoff sequences [32], denoted here by $F = \{\hat{a}^{(1)}, \ldots, \hat{a}^{(r)}, \ldots, \hat{a}^{(q-1)}\}$ are another class of polyphase sequences which can be used for DS CDMA application. They are defined for length $N = q^2$, where qth roots of unity are the elements of the sequences $\hat{a}^{(r)} = (\hat{a}_0^{(r)}, \hat{a}_1^{(r)}, \ldots, \hat{a}_{N-1}^{(r)})$, in which:

$$\hat{a}_n^{(r)} = \hat{a}_{lq+k}^{(r)} = e^{\frac{j2\pi}{q}rkl} = \alpha^{rkl}, \quad 0 \le k,l \le q, \tag{102}$$

$\alpha = e^{j2\pi/q}$, r and q are relatively prime numbers, q is any integer and $0 \le n \le q^2 - 1$.

The elements $\hat{a}_n^{(r)}$ of Chu sequences [17], denoted here by $C = \{\hat{a}^{(1)}, \ldots, \hat{a}^{(r)}, \ldots, \hat{a}^{(N-1)}\}$, $\hat{a}^{(r)} = (\hat{a}_0^{(r)}, \hat{a}_1^{(r)}, \ldots, \hat{a}_{N-1}^{(r)})$ of length N, are given by:

$$\hat{a}_n^{(r)} = \begin{cases} \exp\left[\frac{j\pi}{N}r(n+1)n\right], & N \text{ odd} \\ \exp\left(\frac{j\pi}{N}rn^2\right), & N \text{ even} \end{cases}, \tag{103}$$

where r and N are relatively prime numbers, and $0 \le n < N$.

It can be shown [29] that Frank-Zadoff sequences and Chu sequences belong to the class of the so called perfect sequences. It means that their periodic ACFs are given by:

$$r_r(\tau) = \begin{cases} 1, & \tau = 0 \ (mod\ N) \\ 0, & \tau \neq 0 \ (mod\ N) \end{cases}, \tag{104}$$

and their periodic CCFs are expressed as:

i. For Frank-Zadoff sequences:

$$r_{r,s}(\tau) = \sqrt{1/N}, \quad \forall \tau, r \neq s, \quad gcd(r-s, q) = 1, \ q \text{ is odd}. \tag{105}$$

ii. For Chu sequences:

$$r_{r,s}(\tau) = \sqrt{1/N}, \quad \forall \tau, r \neq s, \qquad (106)$$
$$gcd(r-s, N) = 1, \; gcd(r, N) = 1, \; gcd(s, N) = 1$$

Usually, the number of Frank-Zadoff sequences of a given length is very low, and the number of Chu sequences satisfying the conditions for optimal CCFs is very low, too. Therefore, very often it is convenient to use a combined set of Frank-Zadoff-Chu (FZD) sequences being the union of Frank sequences $F = \{\hat{f}_n^{(r)}\}$ and Chu sequences $C = \{\hat{c}_n^{(s)}\}$ of the same length, $N = q^2$ should be odd, and all conditions required for optimal CCFs in both types of sequences need to be satisfied. Certainly, ACFs of all sequences in the set are exactly the same as those of the Frank-Zadoff and Chu sequences. The CCF is equal to $\sqrt{1/N}$ for a pair of sequences being either a pair of Frank-Zadoff or a pair of Chu sequences. This is somehow more complicated if one of the sequences is a Frank-Zadoff sequence and the other is Chu sequence. According to [29] it is given by:

$$\left| r_{\hat{c}^{(s)}, \hat{f}^{(r)}} \right| = \sqrt{1/N}, \quad r \neq s \; (mod \; q) \qquad (107)$$

$$\left| r_{\hat{c}^{(s+hq)}, \hat{f}^{(r)}} \right| = \begin{cases} 0, & v \neq v_0 = \dfrac{q+1}{2} \\ |g(h,s)|, & v = v_0 = \dfrac{q+1}{2} \end{cases}, \quad r = s \; (mod \; q), \qquad (108)$$

where $0 \leq h < q$, $\tau = uq + v$, and

$$g(h,s) = \frac{q}{N} \sum_{k=0}^{\frac{q-1}{2}-1} \alpha^{(s+hq)k(k+1)/2q - su(k+v_0)} + \qquad (109)$$

$$\frac{q}{N} \sum_{k=\frac{q-1}{2}}^{q-1} \alpha^{(s+hq)k(k+1)/2q - s(u+1)(k+v_0)}$$

Example: For $q = 3$, $N = 9$, there are $M = q - 1 = 2$ Frank-Zadoff sequences. This corresponds to $gcd(r, q) = 1$, $r = 1, 2$. Also these two sequences have the

optimal periodic CCF:

$$\left|r_{\hat{f}_n^{(1)},\hat{f}_n^{(2)}}(\tau)\right| = \frac{1}{3}. \tag{110}$$

The sequences are given by:

$$\{\hat{f}_n^{(1)}\} = \left(1, 1, 1, 1, e^{j2\frac{\pi}{3}}, e^{j4\frac{\pi}{3}}, 1, e^{j4\frac{\pi}{3}}, e^{j2\frac{\pi}{3}}\right), \tag{111}$$

$$\{\hat{f}_n^{(2)}\} = \left(1, 1, 1, 1, e^{j4\frac{\pi}{3}}, e^{j2\frac{\pi}{3}}, 1, e^{j2\frac{\pi}{3}}, e^{j4\frac{\pi}{3}}\right)$$

There are $M = 6$ Chu sequences of length $N = 9$ for $r = 1, 2, 4, 5, 7, 8$. Out of this 6 sequences, we can chose only one pair which satisfy the condition:

$$gcd(r_1 - r_2, N) = 1, \tag{112}$$

where r_1, r_2 are sequence numbers.

Let us chose $r_1 = 4, r_2 = 5$. The corresponding Chu sequences can be obtained using equation (103), and are given by:

$$\{\hat{c}_n^{(4)}\} = \left\{1, e^{j8\frac{\pi}{9}}, e^{j6\frac{\pi}{9}}, e^{j12\frac{\pi}{9}}, e^{j8\frac{\pi}{9}}, e^{j12\frac{\pi}{9}}, e^{j6\frac{\pi}{9}}, e^{j8\frac{\pi}{9}}, 1\right\}, \tag{113}$$

$$\{\hat{c}_n^{(5)}\} = \left\{1, e^{j10\frac{\pi}{9}}, e^{j12\frac{\pi}{9}}, e^{j6\frac{\pi}{9}}, e^{j10\frac{\pi}{9}}, e^{j6\frac{\pi}{9}}, e^{j12\frac{\pi}{9}}, e^{j10\frac{\pi}{9}}, 1\right\}$$

Therefore, the FZC sequence set for $N = 9$ can consist of 4 sequences, e.g.[1]:

$$FZC = \{\hat{f}_n^{(1)}, \hat{f}_n^{(2)}, \hat{c}_n^{(4)}, \hat{c}_n^{(5)}\}. \tag{114}$$

To illustrate the correlation properties of the FZC sequences, the example plots of magnitudes of periodic ACF, and periodic CCFs are given in Figure 35 and Figure 36, while the magnitudes of their aperiodic ACFs and CCFs are given in Figure 37 and

1. Combinations of two Frank-Zadoff sequences of length 9 with other pairs of Chu sequences of length 9 are also possible.

Figure 38, respectively. The superiority of FZC sequences as far as their autocorrelation properties are concerned is fully reflected in the value of the R_{AC} coefficient which is equal to 0.0858.

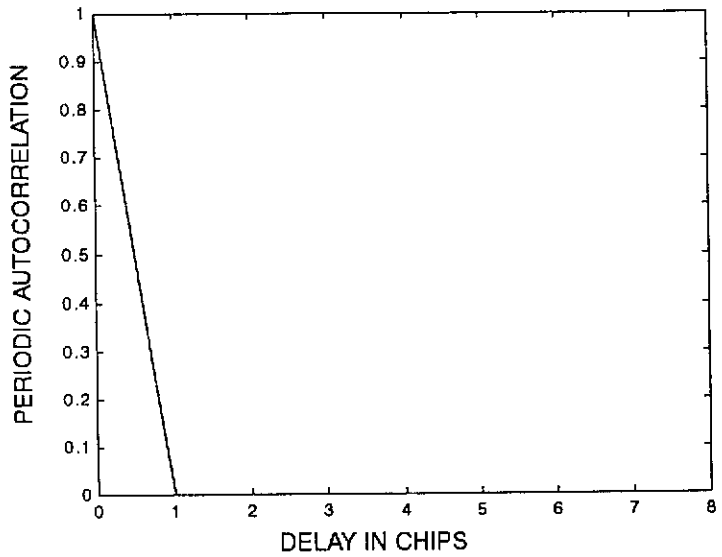

Figure 35: Magnitude of the normalised periodic autocorrelation function for FZC sequences.

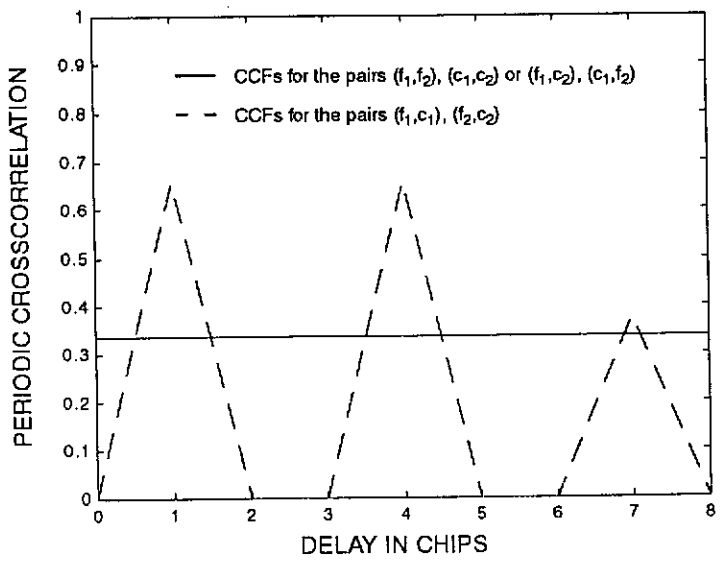

Figure 36: Magnitude of the normalised periodic crosscorrelation function for FZC sequences.

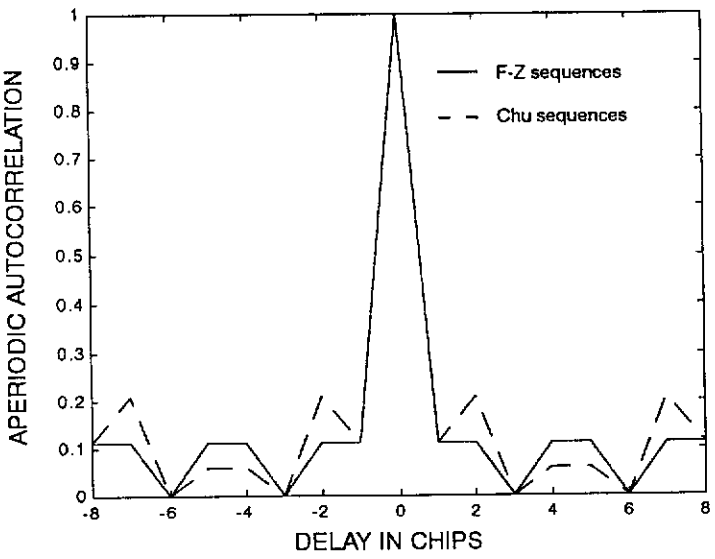

Figure 37: Magnitude of the normalised aperiodic autocorrelation function for FZC sequences.

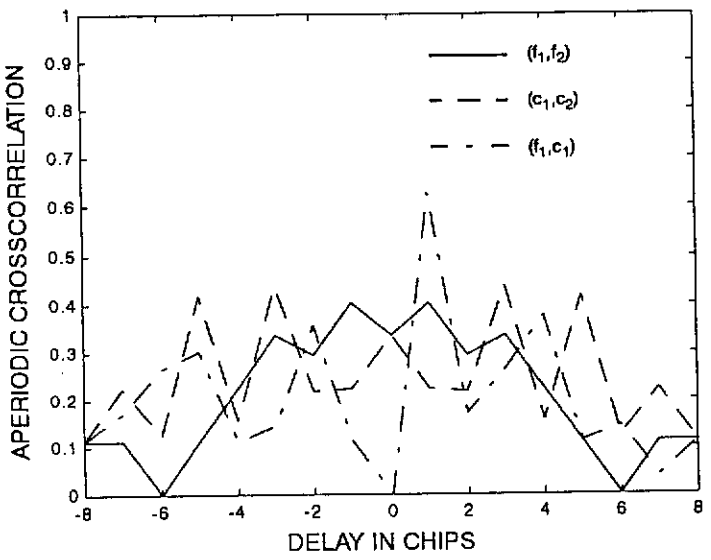

Figure 38: Magnitude of the normalised aperiodic crosscorrelation function for FZC sequences.

The aperiodic correlation properties are also good with the coefficient $R_{CC} = 1.0763$. The main disadvantage of FZC sequences is the size of a sequence set, which is usually much lower than the length of the sequence $M < N$.

4.2.3 *EOE Sequences*

A set of complex polyphase sequences $\{a_n^{(r)}\}$ of period N and size M is referred to as EOE sequence set, if and only if, they have *Equal Odd and Even* correlation functions at each time [29] [34], i.e.:

$$|R_{r,s}(\tau)| = |\hat{R}_{r,s}(\tau)|, \qquad \forall r, s, \tau, \quad 0 \le r, s \le M-1. \tag{115}$$

Recalling the definitions of odd and even correlation functions, we can write an equivalent condition using the aperiodic correlation function:

$$|C_{r,s}(\tau) + C_{r,s}(\tau - N)|^2 = |C_{r,s}(\tau) - C_{r,s}(\tau - N)|^2. \tag{116}$$

Therefore, we have:

$$Re\{|C_{r,s}(\tau)C_{r,s}^*(\tau - N)|\} = 0, \tag{117}$$

which yields:

$$\begin{aligned} |C_{r,s}(\tau)||C_{r,s}(\tau - N)| &= 0 \\ Arg[C_{r,s}(\tau)] - Arg[C_{r,s}(\tau - N)] &= \frac{\pi k}{2} \end{aligned} \tag{118}$$

where k is an arbitrary odd integer. The equation (118) constitutes a necessary and sufficient condition for constructing EOE sequences.

The best way of constructing EOE sequences is to first find a set $\{\hat{b}_n^{(r)}\}$ of arbitrary real-valued sequences of period N and size M, having good even correlation, for example Gold sequences or Kasami sequences. Then, we design complex-valued EOE sequences $\hat{a}_n^{(r)}$ having their elements described by:

$$\hat{a}_n^{(r)} = \hat{b}_n^{(r)} e^{\frac{j\pi k}{2N} n + \beta}, \quad 0 \le n \le N-1, \ 0 \le r \le M-1, \tag{119}$$

where k is an arbitrary constant and β is an arbitrary real constant such that $0 \le \beta \le 2\pi$. The sets of EOE sequences usually contain the name of the set of real-valued sequences in their name, for example EOE-Gold means the set of EOE

sequences obtained on the basis of a set of Gold sequences.

It is important to notice here a very important feature of EOE sequences [29]. It can be proven that the maximum nontrivial even and odd correlations of the complex valued EOE sequences are not higher than those of the original real-valued sequences.

Example: Let us consider the set of Gold sequences of length $N = 31$, as discussed in Section 3.5. On the basis of this set, we can construct a set of EOF sequences, assuming $k = 31, \beta = 0$. The sequences are listed in Table 8. The most important characteristics of the sequence set from the view point of their application in DS CDMA system are the aperiodic correlation functions, and the characteristic parameters R_{CC}, R_{AC}. Their values are as follows: $R_{CC} = 0.9707$ and $R_{AC} = 1.0064$, which are exactly the same as for the binary Gold sequences.

Table 8: EOE-Gold sequences of length 31.

No.	Sequence
1	(-1 0j)(0 -1j)(1 0j)(0 1j)(1 0j)(0 -1j)(1 0j)(0 -1j)(-1 0j)(0 1j)(-1 0j)(0 1j)(-1 0j)(0 1j) (-1 0j)(0 -1j)(1 0j)(0 1j)(1 0j)(0 1j)(-1 0j)(0 1j)(-1 0j)(0 1j)(1 0j)(0 1j)(-1 0j)(0 1j) (1 0j)(0 -1j)(-1 0j)
2	(-1 0j)(0 -1j)(1 0j)(0 -1j)(-1 0j)(0 1j)(1 0j)(0 -1j)(1 0j)(0 -1j)(-1 0j)(0 1j)(-1 0j)(0 -1j) (1 0j)(0 -1j)(1 0j)(0 -1j)(1 0j)(0 -1j)(-1 0j)(0 -1j)(-1 0j)(0 -1j)(1 0j)(0 1j)(-1 0j)(0 1j) (1 0j)(0 1j)(-1 0j)
3	(1 0j)(0 -1j)(1 0j)(0 1j)(-1 0j)(0 -1j)(-1 0j)(0 -1j)(1 0j)(0 -1j)(-1 0j)(0 -1j)(-1 0j)(0 1j) (-1 0j)(0 -1j)(-1 0j)(0 -1j)(1 0j)(0 1j)(1 0j)(0 1j)(-1 0j)(0 -1j)(-1 0j)(0 -1j)(1 0j)(0 -1j) (1 0j)(0 1j)(1 0j)
4	(1 0j)(0 1j)(1 0j)(0 1j)(1 0j)(0 1j)(1 0j)(0 1j)(-1 0j)(0 -1j)(1 0j)(0 1j)(1 0j)(0 1j) (-1 0j)(0 -1j)(1 0j)(0 -1j)(-1 0j)(0 1j)(-1 0j)(0 -1j)(-1 0j)(0 1j)(-1 0j)(0 -1j)(1 0j)(0 -1j) (-1 0j)(0 -1j)(1 0j)
5	(1 0j)(0 1j)(-1 0j)(0 1j)(1 0j)(0 -1j)(-1 0j)(0 -1j)(1 0j)(0 1j)(1 0j)(0 -1j)(-1 0j)(0 -1j) (-1 0j)(0 -1j)(1 0j)(0 1j)(-1 0j)(0 -1j)(-1 0j)(0 1j)(1 0j)(0 1j)(1 0j)(0 -1j)(1 0j)(0 -1j) (-1 0j)(0 1j)(-1 0j)
6	(-1 0j)(0 1j)(-1 0j)(0 -1j)(1 0j)(0 -1j)(1 0j)(0 1j)(-1 0j)(0 -1j)(-1 0j)(0 -1j)(1 0j)(0 1j) (1 0j)(0 -1j)(1 0j)(0 1j)(1 0j)(0 -1j)(1 0j)(0 1j)(-1 0j)(0 -1j)(1 0j)(0 1j)(1 0j)(0 -1j) (-1 0j)(0 1j)(1 0j)
7	(1 0j)(0 -1j)(-1 0j)(0 -1j)(-1 0j)(0 -1j)(1 0j)(0 -1j)(1 0j)(0 1j)(1 0j)(0 1j)(1 0j)(0 -1j) (-1 0j)(0 1j)(1 0j)(0 1j)(1 0j)(0 1j)(1 0j)(0 -1j)(-1 0j)(0 1j)(-1 0j)(0 1j)(-1 0j)(0 -1j) (-1 0j)(0 1j)(1 0j)
8	(1 0j)(0 1j)(1 0j)(0 -1j)(-1 0j)(0 1j)(1 0j)(0 -1j)(-1 0j)(0 -1j)(-1 0j)(0 -1j)(-1 0j)(0 -1j) (1 0j)(0 -1j)(-1 0j)(0 1j)(1 0j)(0 1j)(-1 0j)(0 -1j)(1 0j)(0 1j)(1 0j)(0 -1j)(-1 0j)(0 1j) (-1 0j)(0 1j)(1 0j)

Table 8: EOE-Gold sequences of length 31.

No.	Sequence
9	(1 0j)(0 1j)(-1 0j)(0 1j)(-1 0j)(0 1j)(-1 0j)(0 -1j)(-1 0j)(0 1j)(1 0j)(0 1j)(1 0j)(0 1j) (1 0j)(0 1j)(1 0j)(0 -1j)(1 0j)(0 1j)(-1 0j)(0 1j)(1 0j)(0 -1j)(1 0j)(0 1j)(1 0j)(0 1j) (1 0j)(0 1j)(1 0j)
10	(1 0j)(0 1j)(-1 0j)(0 -1j)(1 0j)(0 1j)(-1 0j)(0 1j)(-1 0j)(0 1j)(-1 0j)(0 -1j)(-1 0j)(0 -1j) (-1 0j)(0 1j)(-1 0j)(0 1j)(-1 0j)(0 1j)(-1 0j)(0 1j)(-1 0j)(0 -1j)(-1 0j)(0 1j)(-1 0j)(0 -1j) (1 0j)(0 -1j)(1 0j)
11	(1 0j)(0 1j)(-1 0j)(0 -1j)(-1 0j)(0 -1j)(-1 0j)(0 1j)(1 0j)(0 1j)(-1 0j)(0 1j)(1 0j)(0 1j) (1 0j)(0 -1j)(-1 0j)(0 -1j)(1 0j)(0 -1j)(-1 0j)(0 1j)(-1 0j)(0 1j)(-1 0j)(0 -1j)(-1 0j)(0 1j) (-1 0j)(0 -1j)(-1 0j)
12	(-1 0j)(0 1j)(-1 0j)(0 -1j)(-1 0j)(0 1j)(1 0j)(0 1j)(1 0j)(0 -1j)(-1 0j)(0 1j)(-1 0j)(0 -1j) (-1 0j)(0 1j)(1 0j)(0 -1j)(-1 0j)(0 1j)(1 0j)(0 1j)(-1 0j)(0 1j)(1 0j)(0 -1j)(1 0j)(0 1j) (1 0j)(0 1j)(-1 0j)
13	(-1 0j)(0 -1j)(-1 0j)(0 -1j)(-1 0j)(0 1j)(-1 0j)(0 -1j)(1 0j)(0 -1j)(1 0j)(0 1j)(-1 0j)(0 1j) (1 0j)(0 -1j)(-1 0j)(0 1j)(-1 0j)(0 -1j)(-1 0j)(0 -1j)(-1 0j)(0 1j)(1 0j)(0 1j)(1 0j)(0 -1j) (1 0j)(0 -1j)(1 0j)
14	(1 0j)(0 -1j)(1 0j)(0 -1j)(-1 0j)(0 1j)(-1 0j)(0 1j)(-1 0j)(0 -1j)(1 0j)(0 -1j)(-1 0j)(0 1j) (-1 0j)(0 1j)(1 0j)(0 -1j)(1 0j)(0 -1j)(1 0j)(0 1j)(1 0j)(0 1j)(1 0j)(0 1j)(-1 0j)(0 -1j) (-1 0j)(0 -1j)(-1 0j)
15	(-1 0j)(0 1j)(1 0j)(0 1j)(-1 0j)(0 1j)(-1 0j)(0 1j)(1 0j)(0 1j)(1 0j)(0 -1j)(1 0j)(0 1j) (-1 0j)(0 -1j)(-1 0j)(0 1j)(-1 0j)(0 1j)(1 0j)(0 -1j)(-1 0j)(0 -1j)(1 0j)(0 1j)(-1 0j)(0 1j) (-1 0j)(0 1j)(-1 0j)
16	(-1 0j)(0 -1j)(-1 0j)(0 1j)(1 0j)(0 1j)(-1 0j)(0 1j)(1 0j)(0 -1j)(-1 0j)(0 -1j)(1 0j)(0 -1j) (-1 0j)(0 -1j)(1 0j)(0 -1j)(1 0j)(0 -1j)(-1 0j)(0 -1j)(1 0j)(0 1j)(-1 0j)(0 1j)(-1 0j)(0 1j) (1 0j)(0 1j)(1 0j)
17	(1 0j)(0 -1j)(1 0j)(0 -1j)(1 0j)(0 -1j)(-1 0j)(0 1j)(1 0j)(0 -1j)(1 0j)(0 1j)(1 0j)(0 -1j) (1 0j)(0 -1j)(1 0j)(0 1j)(-1 0j)(0 1j)(1 0j)(0 1j)(1 0j)(0 -1j)(1 0j)(0 -1j)(-1 0j)(0 1j) (1 0j)(0 -1j)(1 0j)
18	(1 0j)(0 1j)(1 0j)(0 1j)(-1 0j)(0 -1j)(1 0j)(0 1j)(1 0j)(0 -1j)(1 0j)(0 -1j)(-1 0j)(0 -1j) (1 0j)(0 1j)(1 0j)(0 1j)(1 0j)(0 -1j)(-1 0j)(0 -1j)(-1 0j)(0 -1j)(-1 0j)(0 1j)(1 0j)(0 1j) (1 0j)(0 -1j)(-1 0j)
19	(-1 0j)(0 1j)(-1 0j)(0 1j)(1 0j)(0 1j)(1 0j)(0 -1j)(1 0j)(0 -1j)(1 0j)(0 -1j)(1 0j)(0 1j) (1 0j)(0 1j)(-1 0j)(0 1j)(1 0j)(0 1j)(1 0j)(0 1j)(1 0j)(0 1j)(-1 0j)(0 -1j)(-1 0j)(0 -1j) (1 0j)(0 -1j)(-1 0j)
20	(-1 0j)(0 -1j)(-1 0j)(0 -1j)(1 0j)(0 -1j)(-1 0j)(0 -1j)(-1 0j)(0 -1j)(1 0j)(0 -1j)(1 0j)(0 -1j) (-1 0j)(0 1j)(-1 0j)(0 -1j)(1 0j)(0 1j)(-1 0j)(0 -1j)(-1 0j)(0 -1j)(1 0j)(0 -1j)(1 0j)(0 1j) (-1 0j)(0 -1j)(-1 0j)
21	(-1 0j)(0 -1j)(1 0j)(0 -1j)(-1 0j)(0 -1j)(1 0j)(0 1j)(-1 0j)(0 1j)(1 0j)(0 -1j)(1 0j)(0 -1j) (1 0j)(0 -1j)(-1 0j)(0 -1j)(-1 0j)(0 1j)(-1 0j)(0 1j)(1 0j)(0 1j)(-1 0j)(0 1j)(1 0j)(0 -1j) (1 0j)(0 1j)(-1 0j)
22	(-1 0j)(0 -1j)(1 0j)(0 1j)(-1 0j)(0 1j)(1 0j)(0 -1j)(1 0j)(0 1j)(-1 0j)(0 -1j)(1 0j)(0 -1j) (1 0j)(0 1j)(1 0j)(0 -1j)(-1 0j)(0 -1j)(-1 0j)(0 1j)(-1 0j)(0 -1j)(1 0j)(0 -1j)(-1 0j)(0 -1j) (-1 0j)(0 -1j)(1 0j)
23	(1 0j)(0 -1j)(1 0j)(0 1j)(1 0j)(0 1j)(-1 0j)(0 -1j)(-1 0j)(0 -1j)(-1 0j)(0 1j)(1 0j)(0 -1j) (1 0j)(0 1j)(-1 0j)(0 1j)(-1 0j)(0 -1j)(1 0j)(0 1j)(-1 0j)(0 1j)(-1 0j)(0 1j)(1 0j)(0 1j) (-1 0j)(0 1j)(-1 0j)
24	(-1 0j)(0 1j)(1 0j)(0 1j)(1 0j)(0 -1j)(-1 0j)(0 1j)(-1 0j)(0 1j)(1 0j)(0 1j)(-1 0j)(0 -1j) (1 0j)(0 1j)(-1 0j)(0 -1j)(1 0j)(0 -1j)(1 0j)(0 -1j)(-1 0j)(0 1j)(1 0j)(0 -1j)(-1 0j)(0 -1j) (1 0j)(0 1j)(1 0j)

Table 8: EOE-Gold sequences of length 31.

No.	Sequence
25	(1 0j)(0 -1j)(-1 0j)(0 1j)(1 0j)(0 -1j)(1 0j)(0 1j)(1 0j)(0 1j)(-1 0j)(0 -1j)(-1 0j)(0 1j) (1 0j)(0 1j)(-1 0j)(0 -1j)(-1 0j)(0 1j)(1 0j)(0 -1j)(1 0j)(0 1j)(1 0j)(0 1j)(1 0j)(0 1j) (-1 0j)(0 -1j)(1 0j)
26	(1 0j)(0 1j)(1 0j)(0 -1j)(1 0j)(0 -1j)(1 0j)(0 -1j)(1 0j)(0 -1j)(-1 0j)(0 1j)(1 0j)(0 1j) (-1 0j)(0 1j)(-1 0j)(0 -1j)(-1 0j)(0 -1j)(-1 0j)(0 -1j)(1 0j)(0 -1j)(1 0j)(0 1j)(-1 0j)(0 -1j) (1 0j)(0 1j)(-1 0j)
27	(-1 0j)(0 1j)(-1 0j)(0 1j)(-1 0j)(0 -1j)(1 0j)(0 -1j)(-1 0j)(0 -1j)(1 0j)(0 1j)(-1 0j)(0 -1j) (-1 0j)(0 -1j)(-1 0j)(0 -1j)(-1 0j)(0 -1j)(1 0j)(0 1j)(1 0j)(0 -1j)(-1 0j)(0 1j)(-1 0j)(0 1j) (-1 0j)(0 -1j)(1 0j)
28	(1 0j)(0 -1j)(-1 0j)(0 -1j)(1 0j)(0 1j)(1 0j)(0 -1j)(-1 0j)(0 1j)(1 0j)(0 -1j)(-1 0j)(0 1j) (1 0j)(0 -1j)(1 0j)(0 -1j)(-1 0j)(0 -1j)(1 0j)(0 -1j)(-1 0j)(0 -1j)(-1 0j)(0 -1j)(-1 0j)(0 1j) (1 0j)(0 1j)(-1 0j)
29	(-1 0j)(0 1j)(1 0j)(0 -1j)(-1 0j)(0 -1j)(-1 0j)(0 -1j)(-1 0j)(0 1j)(-1 0j)(0 -1j)(1 0j)(0 1j) (-1 0j)(0 1j)(1 0j)(0 1j)(-1 0j)(0 -1j)(1 0j)(0 -1j)(1 0j)(0 1j)(-1 0j)(0 -1j)(1 0j)(0 1j) (1 0j)(0 -1j)(1 0j)
30	(1 0j)(0 -1j)(-1 0j)(0 1j)(-1 0j)(0 1j)(1 0j)(0 1j)(-1 0j)(0 1j)(-1 0j)(0 1j)(1 0j)(0 -1j) (-1 0j)(0 -1j)(-1 0j)(0 1j)(1 0j)(0 -1j)(1 0j)(0 -1j)(1 0j)(0 -1j)(1 0j)(0 -1j)(1 0j)(0 -1j) (1 0j)(0 -1j)(-1 0j)
31	(-1 0j)(0 1j)(1 0j)(0 -1j)(1 0j)(0 1j)(-1 0j)(0 -1j)(1 0j)(0 1j)(-1 0j)(0 1j)(-1 0j)(0 -1j) (1 0j)(0 -1j)(1 0j)(0 -1j)(1 0j)(0 1j)(1 0j)(0 -1j)(1 0j)(0 -1j)(-1 0j)(0 1j)(1 0j)(0 -1j) (-1 0j)(0 -1j)(-1 0j)
32	(-1 0j)(0 -1j)(-1 0j)(0 1j)(-1 0j)(0 -1j)(-1 0j)(0 1j)(-1 0j)(0 -1j)(-1 0j)(0 1j)(-1 0j)(0 1j) (1 0j)(0 1j)(1 0j)(0 1j)(-1 0j)(0 1j)(-1 0j)(0 -1j)(1 0j)(0 -1j)(-1 0j)(0 -1j)(-1 0j)(0 -1j) (-1 0j)(0 1j)(-1 0j)
33	(-1 0j)(0 -1j)(1 0j)(0 -1j)(1 0j)(0 1j)(1 0j)(0 1j)(1 0j)(0 1j)(1 0j)(0 1j)(-1 0j)(0 1j) (-1 0j)(0 1j)(-1 0j)(0 1j)(1 0j)(0 -1j)(-1 0j)(0 1j)(1 0j)(0 -1j)(-1 0j)(0 -1j)(1 0j)(0 1j) (-1 0j)(0 1j)(1 0j)

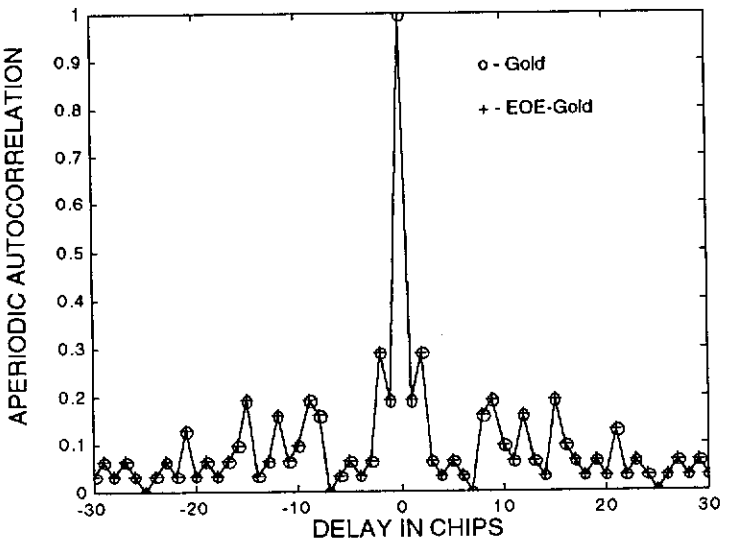

Figure 39: Magnitude of aperiodic autocorrelation function for the sequence $\{\hat{a}_n^{(6)}\}$ of Table 8 and for the corresponding Gold sequence.

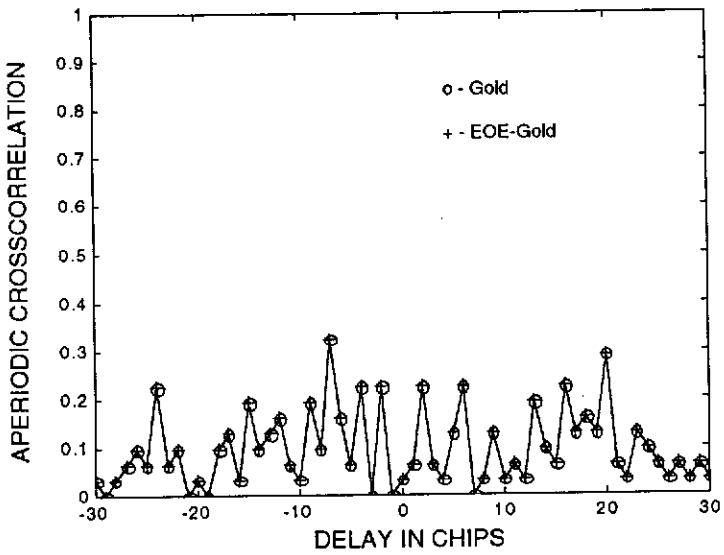

Figure 40: Magnitude of aperiodic crosscorrelation function between the sequences $\{\hat{a}_n^{(1)}\}$ and $\{\hat{a}_n^{(5)}\}$ of Table 8 and between the corresponding Gold sequences.

To complete the comparison of the behaviour of aperiodic autocorrelation functions of EOE-Gold and Binary Gold sequences the example plots of the magnitudes of these functions f are given in Figure 39 and Figure 40. It is clearly visible that the plots obtained for both sequence sets (Gold and EOE-Gold) are identical.

4.2.4 Opperman-Vucetic Sequences

Opperman and Vucetic in [79] have proposed the new family of complex sequences of length N, $U_{m,p,s}(N)$, with sequences $\{\hat{u}_n^{(r)}\}$ having their elements defined by the formula:

$$\hat{u}_n^{(r)} = (-1)^{rn}\exp\left[\frac{j\pi(r^m n^p + n^s)}{N}\right], \quad gdc(r,N) = 1, \quad 1 \le n \le N, \tag{120}$$

where m, p, and s are any real numbers. The definition equation (120) is so general that it includes some well known classes of sequences, like for example FZC sequences, which can be generated by $m = 2, p = 1, s = -\infty$ [79].

The sets of sequences defined by (120) can achieve impressive range of correlation properties with the improvement in crosscorrelation properties of a set ususally

achieved on the expense of significant worsening of autocorrelation properties, and vice-versa.

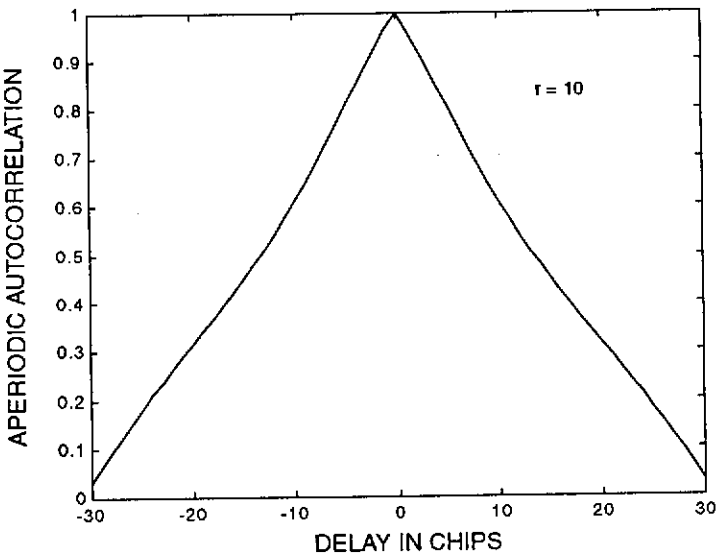

Figure 41: Example plot of magnitude of the normalised aperiodic autocorrelation function for the Opperman-Vucetic sequences of length 31 generated by $m = 0.9, p = 1, s = 1.325$.

To illustrate the correlational properties of Opperman-Vucetic (OV) sequences, the example plots of magnitudes of the aperiodic ACF and CCF are given in Figure 41 and Figure 42, respectively, for the set of length $N = 31$, generated by $m = 0.9, p = 1, s = 1.325$. The set is characterised by the parameters $R_{CC} = 0.7846, R_{AC} = 16.7653$.

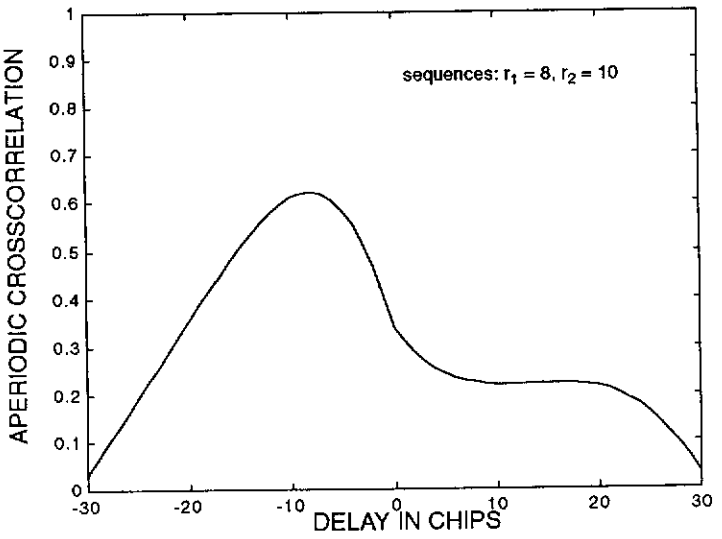

Figure 42: Example plot of magnitude of the normalised aperiodic crosscorrelation function for the Opperman-Vucetic sequences of length 31 generated by $m = 0.9, p = 1, s = 1.325$.

We have also generated another set of sequences of the same length using the parameters $m = 1.075, p = 1, s = 2$. The example plots of magnitudes of the aperiodic ACF and CCF are given in Figure 43 and Figure 44, respectively. The correlation measures obtained for this set are $R_{CC} = 0.9975, R_{AC} = 0.1126$.

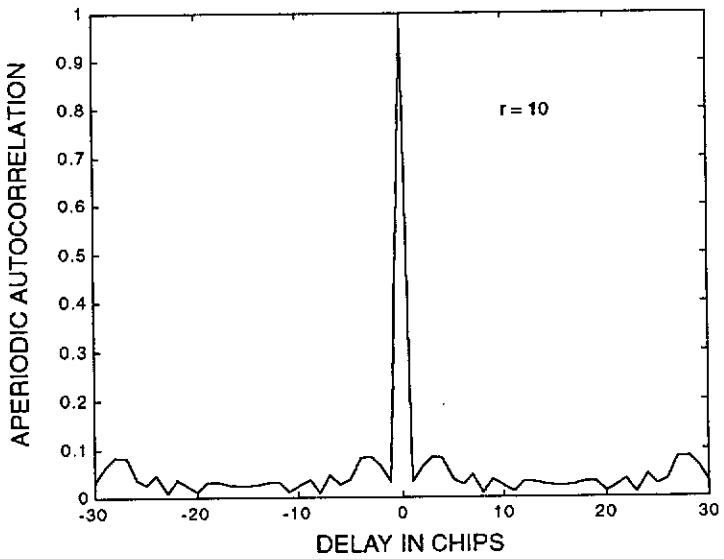

Figure 43: Example plot of magnitude of the normalised aperiodic autocorrelation function for the Opperman-Vucetic sequences of length 31 generated by $m = 1.075, p = 1, s = 2$.

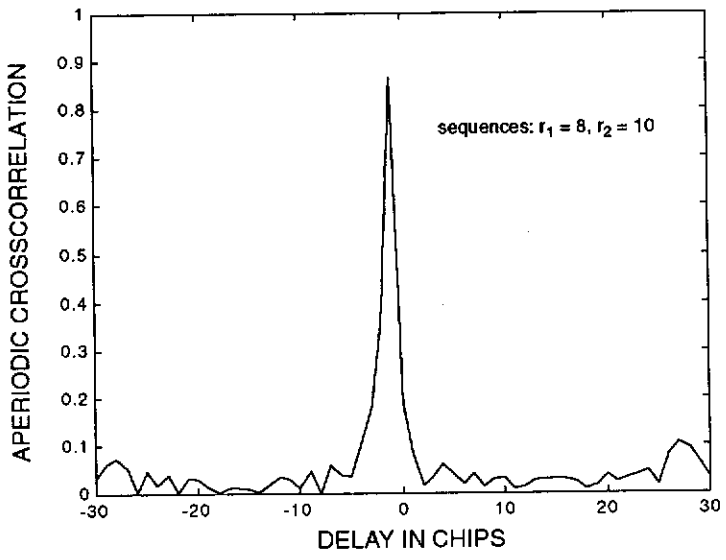

Figure 44: Example plot of magnitude of the normalised aperiodic crosscorrelation function for the Opperman-Vucetic sequences of length 31 generated by $m = 1.075, p = 1, s = 2$.

4.3 Sequence comparison

There are several methods of comparing sets of spreading sequences. A very good classification including comparison of the most of known sequences can be found in [29]. However, from the viewpoint of this work, i.e. application of sequences to DS CDMA high data rate wireless networks, the most important are the following parameters:

- length of the sequence N,
- size of the set M,
- average mean-square value of crosscorrelation function for every sequence in the set R_{CC},
- average mean-square value of autocorrelation function for every sequence in the set R_{AC}.

The values of the abovementioned parameters for the example sequence sets considered in this chapter are given in Table 9 with the parameters R_{CC} and R_{AC} calculated for the case of one sample per chip.

Table 9: Parameters of some sequence sets.

Name of the set	Length N	Size M	R_{CC}	R_{AC}
Walsh	16	16	0.7292	4.0625
Gold	31	33	0.9707	1.0064
Gold-like	15	16	0.9627	0.7490
FZC	9	4	1.0763	0.0858
EOE-Gold	31	33	0.9707	1.0064
OV{1.075,1,2}	31	30	0.9975	0.1126
OV{0.9,1,1.325}	31	30	0.7846	16.7653

The parameters R_{CC} and R_{AC} for short sequences, such as those required in high data rate wireless systems, can be considered only as an indication of the expected system performance [58]. In some cases, even with relatively low average bit error rate, error bursts may be so long that an applied error control algorithm is not able to protect

transmitted data. Therefore, while making the final decision about using the particular sequence set, a comprehensive simulation of system performance, i.e. average bit error rate, statistics of errors caused by the multiaccess interference, and in some cases synchronisability of the system needs to be performed.

One of the other characteristics not mentioned so far, is power spectral density of a spread signal. It is highly desired to, achieve similar bandwidth for the signals spread by different sequences in the set.

5. New methods to design polyphase sequences for wireless data applications

In the previous chapter we discussed several families of binary and complex spreading sequences proposed in literature, with some of them, e.g. OV sequences allowing for a good compromise between CCFs and ACFs for the whole set. There are, however, no clear ways how to chose appropriate values of parameters to achieve the desired spectral characteristics. While designing the sequence sets for use in DS CDMA wireless data network, one also needs to look into some specific system requirements:

i. Because for the downlink (base station to mobile transmission) the conditions for synchronous operation can be met, the designed sequences should be orthogonal or almost orthogonal for perfect synchronization. This would allow for cancellation of MAI for the downlink, and for simpler receiver in mobile terminals.

ii. It is highly desirable to achieve the situation where power of spread signals is distributed uniformly in the available bandwidth, therefore ensuring similar level of the frequency diversity for any channel in the system.

In this chapter, we propose a method to design a useful set of sequences for DS CDMA wireless data networks. Based on the fact that use of complex spreading codes introduces a phase modulation into the band-pass signal, we first look into the properties of sequences obtained on the basis of baseband chirps [121], which are one of the analogue signals having very good autocorrelation properties. The similar approach has been used by Popovic [83] in design of his P3 and P4 sequences. Here, however, we will look into design of sequences for any given length N. Ability to do so, is very important from the viewpoint of applying such sequences in wireless data networks for variable data rates. Later we will investigate application of multiple chirps and the linear combinations of them. Finally we show the way how, using a similar approach to that behind EOF sequences, we can significantly improve correlational properties of known orthogonal sequence sets, e.g. Walsh sequences.

5.1 Chirp sequences

5.1.1 Design method

Chirp signals are widely used in radar applications for pulse compression [18], [19], and were also proposed for use in digital communications by several authors, e.g. [8], [28], [56], [86], [101]. They refer to creation of such a waveform where an instantaneous frequency of the signal changes linearly between the lower and upper frequency limits. This is graphically illustrated in Figure 45, which presents the two basic types of chirp pulses and their instantaneous frequency profiles.

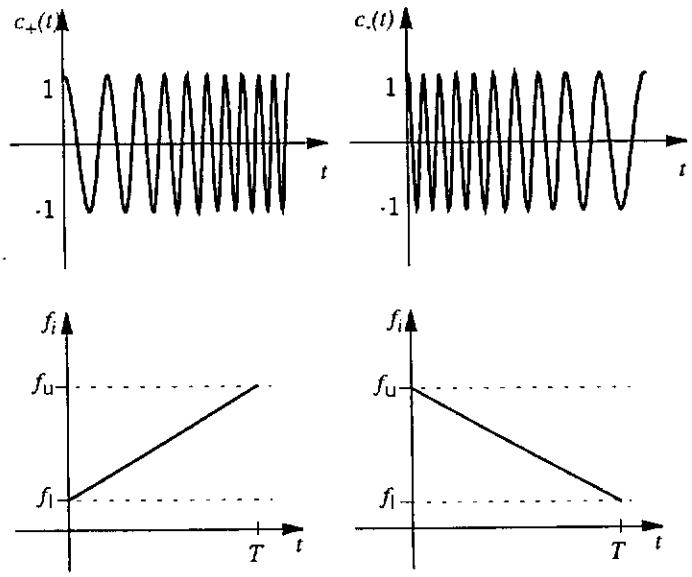

Figure 45: Positive and negative chirp pulses and their instantaneous frequency profiles.

For the positive chirp $c_+(t)$, the instantaneous frequency $f_i(t)$ increases during the pulse duration, according to the formula:

$$f_i(t) = f_l + (f_u - f_l)\frac{t}{T}, \tag{121}$$

where f_l and f_u are the lower and the upper frequency limits, respectively, and T is the duration of the chirp pulse. In the case of the negative chirp $c_-(t)$, the instantaneous

frequency $f_i(t)$ decreases during the pulse duration, accordingly:

$$f_i(t) = f_u - (f_u - f_l)\frac{t}{T}. \tag{122}$$

Introducing a modulation index h, defined as for binary frequency shift keying (FSK) [84], $h = (f_u - f_l)T = \Delta f T$, we can express $f_i(t)$; $0 < t \le T$, as:

$$f_i(t) = \begin{cases} \left(f_c - \frac{h}{2T}\right) + \frac{ht}{T^2}, & \text{for } c_+(t) \\ \left(f_c + \frac{h}{2T}\right) - \frac{ht}{T^2}, & \text{for } c_-(t) \end{cases}, \tag{123}$$

where f_c denotes the central frequency of the chirp pulse, sometimes referred to as the carrier frequency.

Hence, we can describe the waveform $c_+(t)$; $0 < t \le T$, having an amplitude A, by means of:

$$\begin{aligned} c_+(t) &= A\cos\left[2\pi\int_0^t f_i(\tau)d\tau + \phi_0\right] \\ &= A\cos\left[2\pi\int_0^t \left(f_c - \frac{h}{2T} + \frac{h\tau}{T^2}\right)d\tau + \phi_0\right] \end{aligned}, \tag{124}$$

which after performing an integration yields:

$$c_+(t) = A\cos\left[2\pi\left(f_c - \frac{h}{2T}\right)t + \frac{\pi h t^2}{T^2} + \phi_0\right]. \tag{125}$$

By a direct analogy, the $c_-(t)$; $0 < t \le T$ waveform is given by:

$$c_-(t) = A\cos\left[2\pi\left(f_c + \frac{h}{2T}\right)t - \frac{\pi h t^2}{T^2} + \phi_0\right]. \tag{126}$$

In equations (124), (125), and (126), ϕ_0, being an initial phase value is a real constant

$0 \le \phi_0 < 2\pi$.

Using a bandpass signal notation [84], and for simplicity assuming $A = 1$, we can express $c_+(t)$ as:

$$c_+(t) = \begin{cases} \exp[j2\pi h q_p(t)]\exp[j(2\pi f_c t + \phi_0)], & 0 < t \le T \\ 0, & \text{otherwise} \end{cases}, \tag{127}$$

where $q_p(t)$ is an elementary phase pulse given by [121]:

$$q_p(t) = \begin{cases} \dfrac{t^2}{2T^2} - \dfrac{t}{2T}, & 0 < t \le T \\ 0, & \text{otherwise} \end{cases}. \tag{128}$$

Using the same notation, we have:

$$c_-(t) = \begin{cases} \exp[-j2\pi h q_p(t)]\exp[j(2\pi f_c t + \phi_0)], & 0 < t \le T \\ 0, & \text{otherwise} \end{cases}. \tag{129}$$

Therefore, the baseband chirp pulses are given by:

$$b_+(t) = \begin{cases} \exp[j2\pi h q_p(t)], & 0 < t \le T \\ 0, & \text{otherwise} \end{cases} \tag{130}$$

$$b_-(t) = \begin{cases} \exp[-j2\pi h q_p(t)], & 0 < t \le T \\ 0, & \text{otherwise} \end{cases}. \tag{131}$$

Discretising the analog chirp pulses by substituting n for t, and N for T in equations (128) and (130), we can write a formula defining a complex polyphase chirp sequence

$$\{\hat{b}_n(h)\} = (\hat{b}_n(h);\ n = 1, 2, \ldots, N), \tag{132}$$

where:

$$\hat{b}_n(h) = \exp[j2\pi h b_n], \quad n = 1, 2, \ldots, N, \tag{133}$$

$$b_n = \frac{n^2 - nN}{2N^2}, \tag{134}$$

and h can take any arbitrary nonzero real value.

Certainly, both periodic and aperiodic ACFs strongly depend on the value of h. To illustrate this dependency, the plots of magnitudes of aperiodic ACFs for chirp sequences are given in Figure 46 for three values of parameter h.

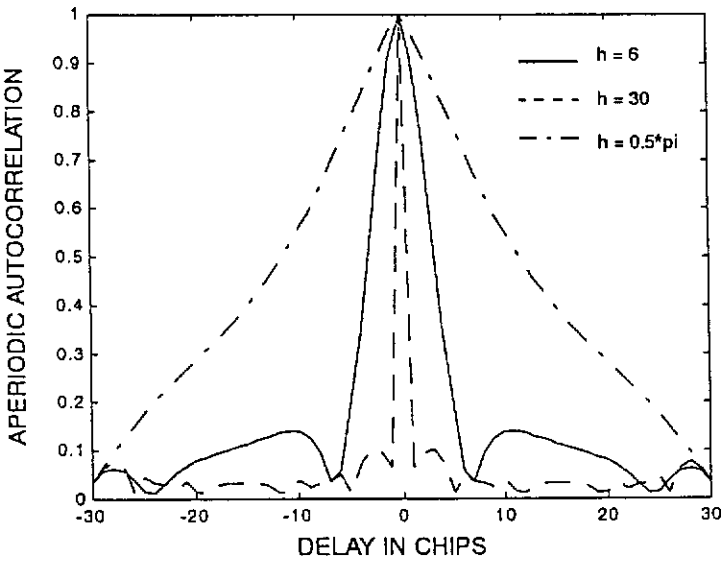

Figure 46: Magnitudes of aperiodic autocorrelation functions for example chirp sequences, $N = 31$.

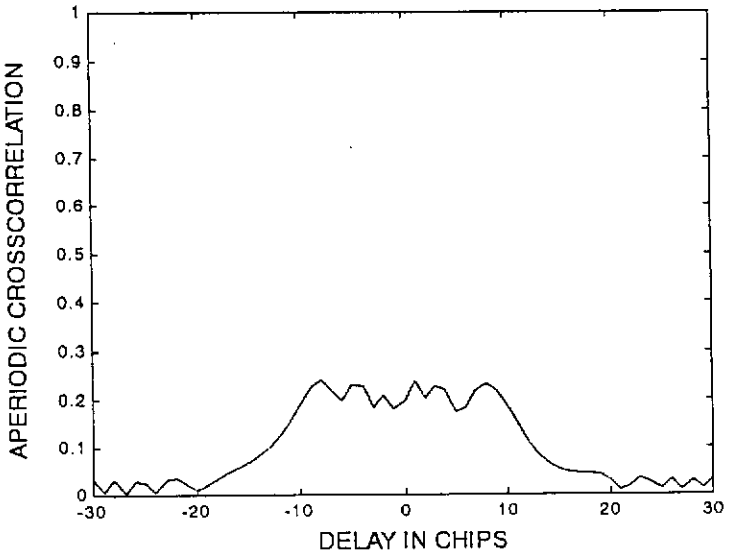

Figure 47: Magnitudes of aperiodic crosscorrelation function between a pair of chirp sequences, $N = 31$, $h_1 = 6$, $h_2 = 30$.

The chirp sequences exhibit also good crosscorrelation properties for some pairs of parameter h values. This is illustrated in Figure 47, where the magnitude of aperiodic CCF is plotted for an example pair of chirp sequences ($h_1 = 6, h_2 = 30$).

The main advantage of chirp sequences compared to other known sets of sequences, lies in that we can easily generate the set for any given length N, while most of the known sets of sequences can be generated only for a certain values of N. The values of parameter h for the sequences can be optimised to achieve:

i. minimum multiaccess interference - by minimising value of R_{CC},

i. the best synchronisability - by minimising value of R_{AC},

ii. minimum peak interference - by minimising the maximum value for the aperiodic CCFs, ($ACCF_{max}$), over the whole set of the sequences.

Usually, by improving one of the above features the other two need to be compromised. Therefore, while searching for the optimum values of parameter h for the whole set of sequences, the acceptable compromise needs to be achieved.

5.1.2 Example

Let us design a set of 16 polyphase chirp sequences $\left\{ \hat{b}_n^{(r)} \right\}$ of length $N = 16$.

Because the parameter h can take any real non-zero value, we chose them according to the following pattern[1]:

$$h^{(r)} = \begin{cases} (r-9)d, & \text{for } r = 1, 2, \ldots, 8 \\ (r-8)d, & \text{for } r = 9, 10, \ldots, 16 \end{cases} . \tag{135}$$

To find the proper value of d, we then calculate the values of R_{CC}, R_{AC}, and $ACCF_{max}$ for $1 \le d \le 20$ with a step of 0.1, calculated for a single sample per chip. The plots of $R_{CC}(d)$, $R_{AC}(d)$, and $ACCF_{max}(d)$, are given in Figure 48, Figure 49,

1. Certainly, any other choice can be considered, and may even lead to better performance.

and Figure 50, respectively. By analysing those plots , we can find a reasonable compromise at $d = 7.3$, with $R_{CC}(7.3) = 1.0041$, $R_{AC}(7.3) = 0.7405$, and $ACCF_{max}(7.3) = 0.4824$.

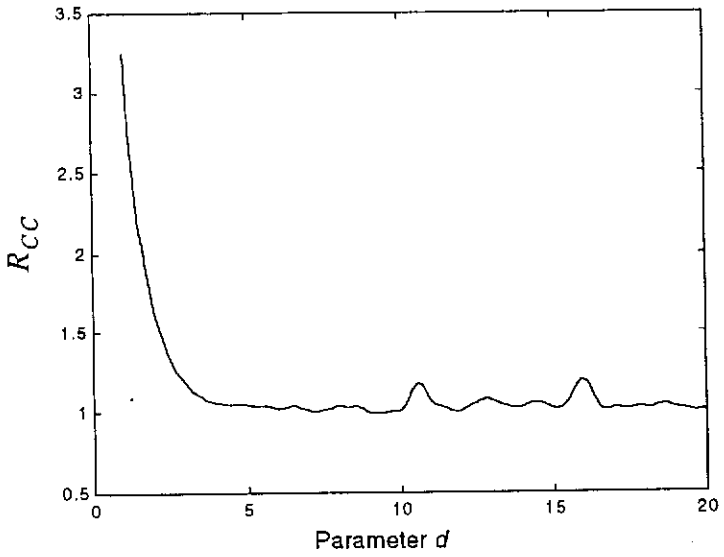

Figure 48: Plot of $R_{CC}(d)$ for the example chirp sequence sets.

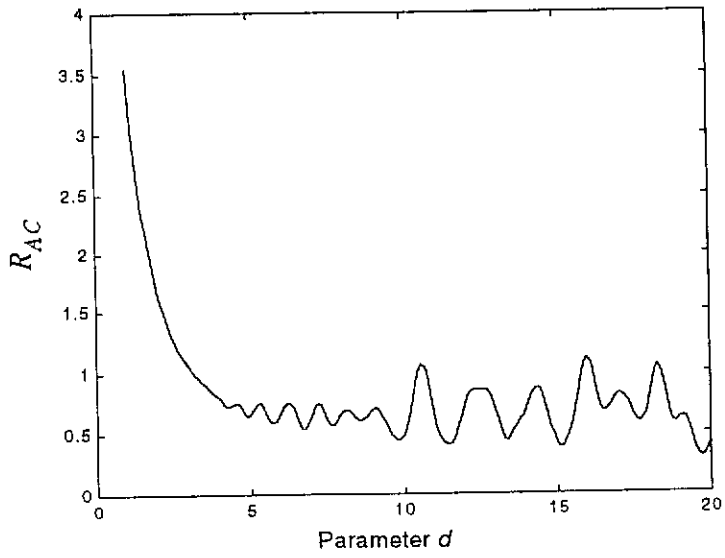

Figure 49: Plot of $R_{AC}(d)$ for the example chirp sequence sets.

For the comparable set of 16 sequences, i.e. Gold-like sequence set of length

$N = 15$, we have the following values: $R_{CC} = 0.9627$, $R_{AC} = 0.7490$, and $ACCF_{max} = 0.6000$.

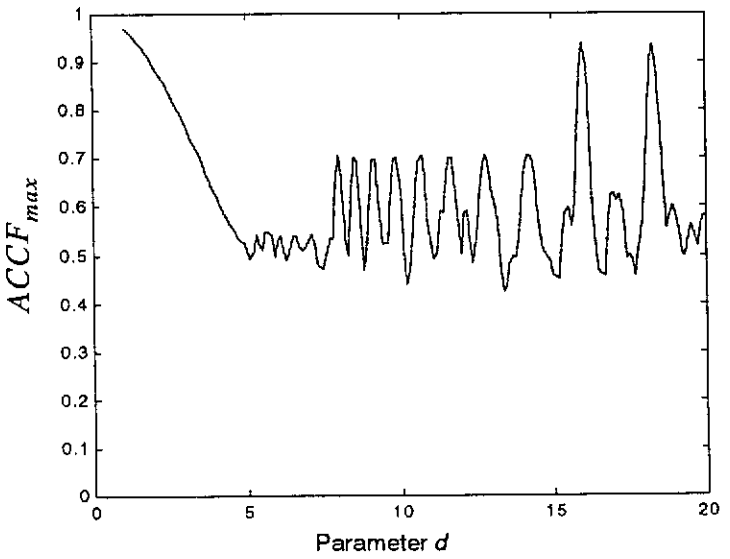

Figure 50: Plot of $ACCF_{max}(d)$ for the example chirp sequence sets.

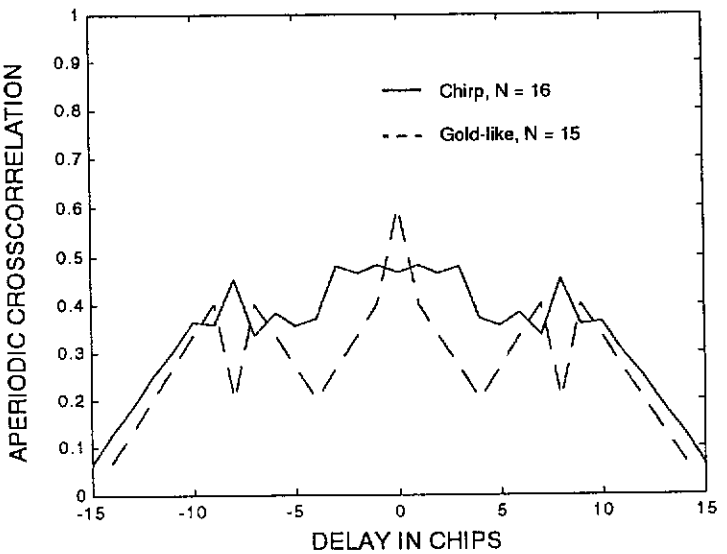

Figure 51: Plots of $ACCF_{max}(\tau)$ for the set of 16 chirp sequences of length $N = 16$ and parameter $d = 7.3$, and for the set of 16 Gold-like sequences of length $N = 15$.

To further compare these two sets of sequences, in Figure 51, we show the plots of

$ACCF_{max}(\tau)$. The plots of Figure 51, indicate that the designed chirp sequence set exhibits better performance than the Gold-like sequence set in the case of a perfect synchronisation.

Additional comparison of these two sets needs to be done from the viewpoint of spectral characteristics of the sequences. There are several different methods of estimating power spectrum of complex signals. They can be classified [47] as nonparametric methods, like the periodogram, the Bartlett and Welch modified periodogram [112] and the Blackman-Tukey methods [12], or parametric methods, e.g. [13], [33], [51], [54], [66]. The nonparametric methods exhibit a low spectral resolution in the case of short records and require windowing to reduce spectral leakage [47]. On the other hand, the very significant disadvantage of the parametric methods are difficulties in deriving an appropriate time series model. Therefore, we have decided to use here the nonparametric Welch method to estimate power spectrum of the spread signal. The method is implemented in a standard MATLAB Signal Processing Toolbox as a function '*psd*' [69].

To obtain a good spectral resolution, we simulated random bipolar, {+1,-1}, data sequences of length 64 bits spread by the spreading sequences, and applied sampling of four samples per chip. For other parameters of the *'psd'* function we used MATLAB default parameters [69], i.e.: FFT length - 256, Hanning window of length 256, 50% overlapping. The results of computations are plotted in Figure 52, Figure 53 for each of the 16 chirp signatures. In addition, Figure 54 shows the spectrum of a compound signal obtained in the case where all 16 chirp sequences are used simultaneously to produce 16 spread signals, transmitted over the same channel. The frequency, on all plots, is normalised to the data rate, so the chip rate is equal to 16.

To compare spectral characteristics of the designed chirp sequences with the spectral characteristics of the Gold-like sequences of length 15, in Figure 55 we also show the spectrum of a compound signal obtained in the case where all 16 Gold-like sequences are used simultaneously to produce 16 spread signals, transmitted over the same channel. It is visible, by comparing Figure 54 and Figure 55, that the designed sequences have similar spectral properties to Gold-like sequences of length 15.

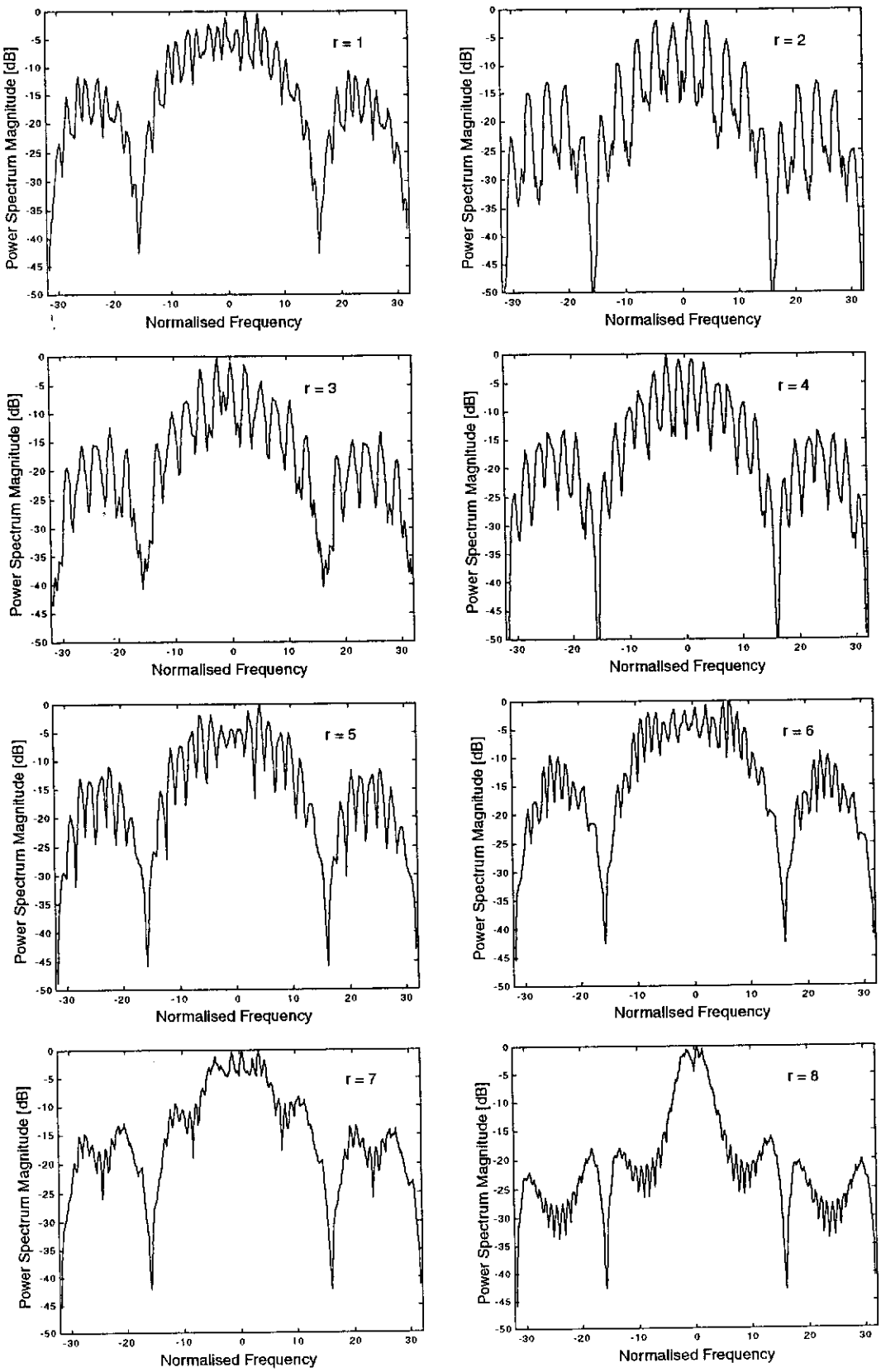

Figure 52: Plots of power spectrum magnitudes for signals obtain by spreading a random bipolar signal by the use of the chirp signatures of length 16, and parameters h defined by the use of equation (135) with $d = 7.3$, $r = 1, 2, ..., 8$.

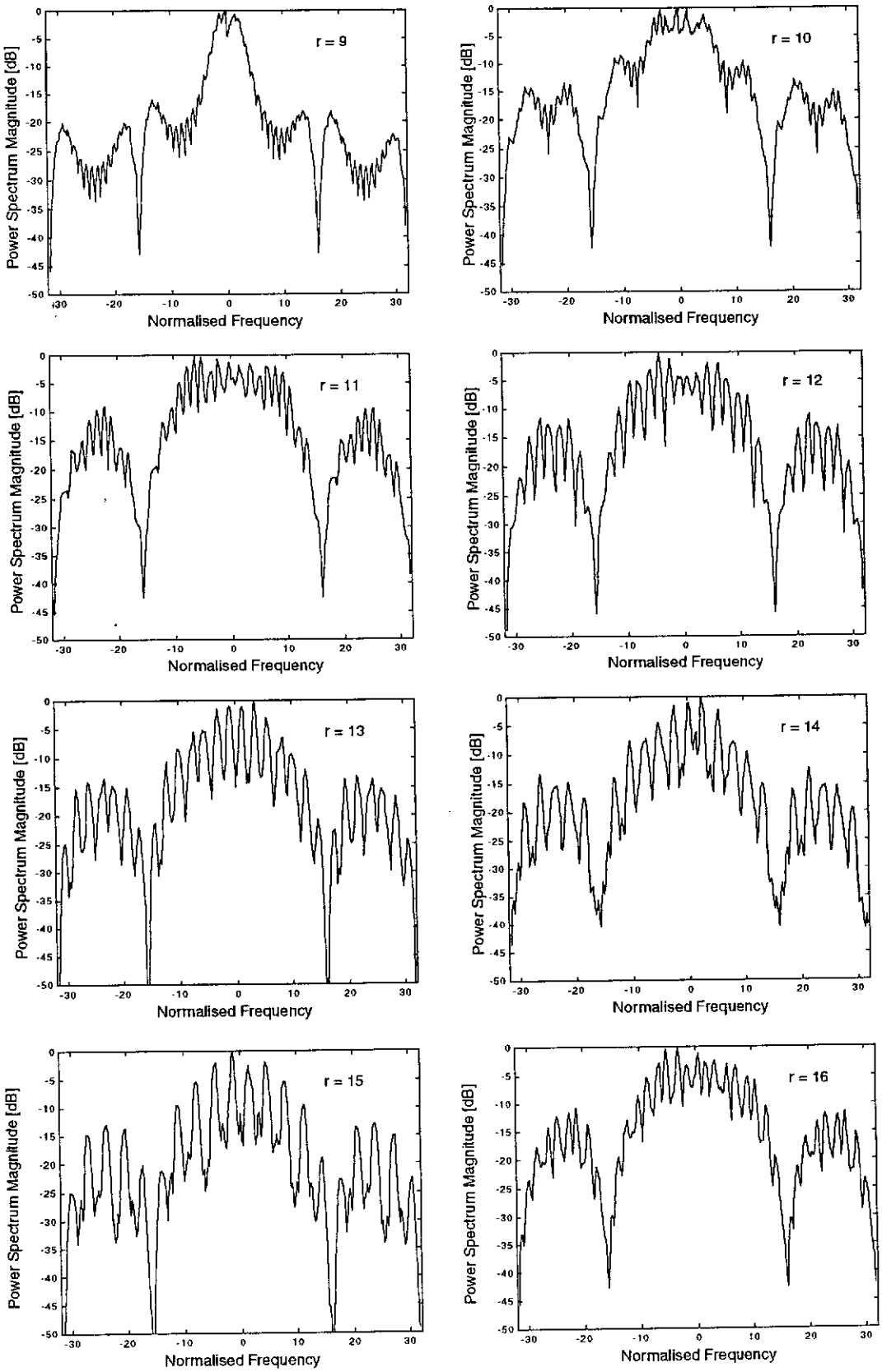

Figure 53: Plots of power spectrum magnitudes for signals obtain by spreading a random bipolar signal by the use of the chirp signatures of length 16, and parameters h defined by the use of equation (135) with $d = 7.3$, $r = 9, ..., 16$.

This time, we used the same normalisation for the frequency, so the chip rate is 15 for the Gold-like sequences. The only significant difference is the position on the frequency axis of the first 'null' in the spectrum, being 16 for chirp sequences of length 16, and 15 for Gold-like sequences of length 15.

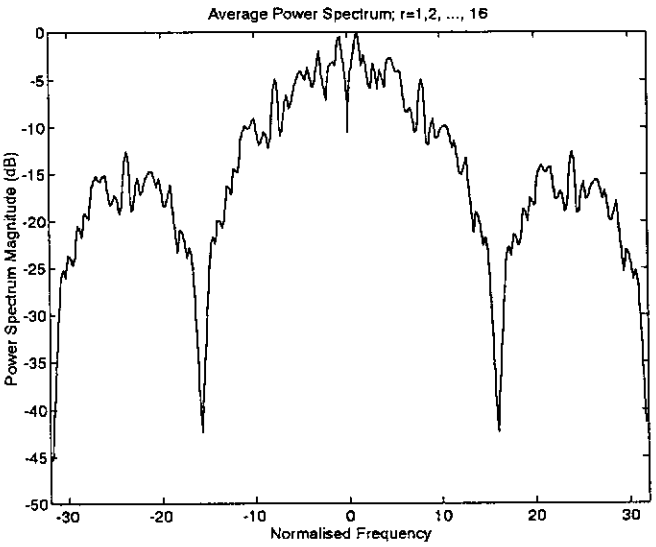

Figure 54: Power spectrum of a compound of 16 signals spread by all 16 different chirp signatures of length 16, and parameters h defined by the use of equation (135) with $d = 7.3$.

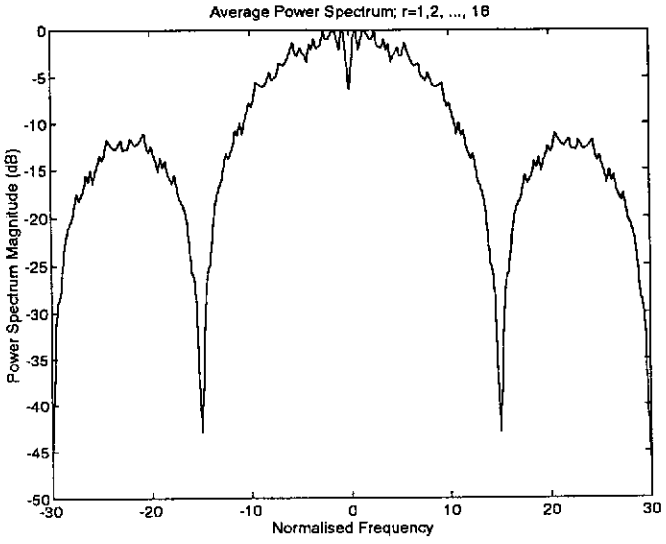

Figure 55: Power spectrum of a compound of 16 signals spread by all 16 different Gold-like signatures.

5.2 Sequences designed by the use of multiple chirps

5.2.1 Design method

In the previous section, we showed that using sequences based on the baseband chirp pulses we can design useful sets of spreading sequences of any arbitrary length. Here, we will consider an extension to this idea, i.e. design of sequence sets comprising sequences designed on the basis of baseband chirp pulses of higher order or even the linear combination of them. To do so, we first introduce a definition of the chirp pulse of order s.

A pulse is referred to as a chirp pulse of the order s, if and only if the first time derivative of its instantaneous frequency (the angular acceleration) is a step function with the number of time intervals where it is constant being equal to s. In addition, if the integral of the instantaneous frequency over the duration of the pulse is equal to zero:

$$\int_0^T f_i(t)dt = 0, \tag{136}$$

then such a pulse is called a baseband chirp pulse of the order s.

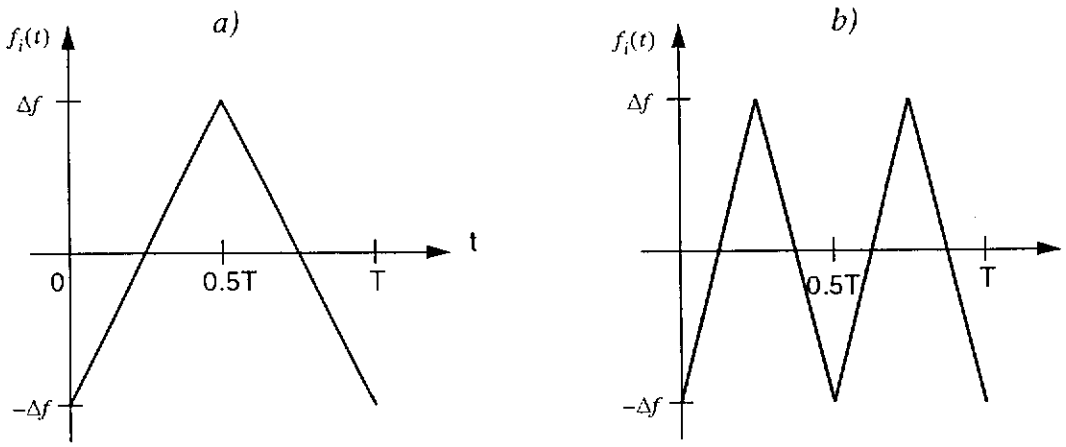

Figure 56: Example baseband chirp pulses of the order: a) 2, b) 4.

As an example, a baseband chirp pulse of orders 2 and 4 are shown in Figure 56.

The presented pulses are symmetrical, in general, however, the chirp pulses do not need to be so regular.

The instantaneous frequency function $f_i(t)$ for the chirp pulse of order 2, depicted in Figure 56 is given by:

$$f_i(t) = \begin{cases} \frac{4t}{T}\Delta f - \Delta f, & 0 < t \le \frac{T}{2} \\ -\frac{4t}{T}\Delta f + 3\Delta f, & \frac{T}{2} < t \le T \\ 0, & \text{otherwise} \end{cases} . \tag{137}$$

Substituting h/T for Δf, as we did in the previous section, yields:

$$f_i(t) = \begin{cases} \frac{4t}{T^2}h - \frac{h}{T}, & 0 < t \le \frac{T}{2} \\ -\frac{4t}{T^2}h + 3\frac{h}{T}, & \frac{T}{2} < t \le T \\ 0, & \text{otherwise} \end{cases} , \tag{138}$$

which, after integration, gives the following expression for the elementary phase pulse $q_p(t)$ for the chirp pulse of order 2:

$$q_p(t) = \begin{cases} \frac{2t^2}{T^2}h - \frac{th}{T}, & 0 < t \le \frac{T}{2} \\ -\frac{2t^2}{T^2}h + 3\frac{th}{T} - 1, & \frac{T}{2} < t \le T \\ 0, & \text{otherwise} \end{cases} . \tag{139}$$

Substituting n for t, and N for T to discretise the pulse $q_p(t)$ given by equation (139), we obtain the formula for the elements d_n of a normalised ($h = 1$) double chirp sequence $\{d_n\}$:

$$d_n = \begin{cases} \dfrac{2n^2}{N^2} - \dfrac{n}{N}, & 0 < n \le \dfrac{N}{2} \\ -\dfrac{2n^2}{N^2} + 3\dfrac{n}{N} - 1, & \dfrac{N}{2} < n \le N \\ 0, & \text{otherwise} \end{cases} . \tag{140}$$

The complex double chirp sequence elements $\hat{d}_n$ are therefore given by:

$$\hat{d}_n = \exp[j2\pi h d_n]; \quad n = 1, 2, \ldots, N \tag{141}$$

In the same way, we can find the formula of the elements q_n of a normalised quadruple chirp sequence $\{q_n\}$, corresponding to the chirp pulse of the order 4. The elements q_n are expressed as:

$$q_n = \begin{cases} \dfrac{4n^2}{N^2} - \dfrac{n}{N}, & 0 < t \le \dfrac{N}{4} \\ -\dfrac{4n^2}{N^2} + 3\dfrac{n}{N} + 1, & \dfrac{N}{4} < t \le \dfrac{N}{2} \\ \dfrac{4n^2}{N^2} - 5\dfrac{n}{N} + \dfrac{3}{2}, & \dfrac{N}{2} < t \le \dfrac{3N}{4} \\ -\dfrac{4n^2}{N^2} + 7\dfrac{n}{N} - 3, & \dfrac{3N}{4} < t \le N \\ 0, & \text{otherwise} \end{cases} , \tag{142}$$

and the elements of the complex quadruple chirp sequnces are given by:

$$\hat{q}_n = \exp[j2\pi h q_n]; \quad n = 1, 2, \ldots, N. \tag{143}$$

Analogically, one can develop the formulae describing any, even irregular, chirp sequences.

Another class of higher order chirp sequences, can be obtained if a superposition of chirp sequences of different orders is used to create the complex polyphase sequence. In the following example, we will show that by using such a superposition we can create sequence sets having better performance.

5.2.2 *Example*

Let us consider a set of 16 complex sequences $\{\hat{s}_n^{(r)}\}$, $r = 1, 2, \ldots, 16$ of length 16 obtained by the use of a superposition of a single and double chirp sequences. Therefore, their elements $\hat{s}_n^{(r)}(h_1^{(r)}, h_2^{(r)})$ are given by:

$$\hat{s}_n^{(r)}(h_1^{(r)}, h_2^{(r)}) = \exp[j2\pi(h_1^{(r)} b_n + h_2^{(r)} d_n)]; \quad r = 1, \ldots, 16, n = 1, \ldots, 16, \quad (144)$$

where the coefficients $h_1^{(r)}$ and $h_2^{(r)}$ can be any real numbers, with the only exception that they cannot be equal both to zero for the same r.

In order to find the acceptable values for the coefficients $h_1^{(r)}$ and $h_2^{(r)}$ for all 16 sequences, let us define them in the following way:

$$h_1^{(r)} = \begin{cases} d_1(r-9), & r = 1, 2, \ldots, 8 \\ d_1(r-8), & r = 9,10, \ldots, 16 \end{cases}, \quad (145)$$

$$h_2^{(r)} = r d_2, \quad r = 1, 2, \ldots, 16, \quad (146)$$

and compute the values of $R_{CC}(d_1, d_2)$, $R_{AC}(d_1, d_2)$, and $ACCF_{max}(d_1, d_2)$ for $1 \le d_1, d_2 \le 20$ with a grid of 0.2. The plots of $R_{CC}(d_1, d_2)$, $R_{AC}(d_1, d_2)$, and $ACCF_{max}(d_1, d_2)$ are given in Figure 57, Figure 58, and Figure 59, respectively.

From the plots of Figure 57, Figure 58, and Figure 59, it is visible that all three functions, $R_{CC}(d_1, d_2)$, $R_{AC}(d_1, d_2)$, and $ACCF_{max}(d_1, d_2)$, are highly irregular functions of d_1 and d_2. As one could expect, the local minima of $R_{CC}(d_1, d_2)$ occur usually for such values of d_1 and d_2 where local maxima of $R_{AC}(d_1, d_2)$ take place.

Since the average mean aperiodic crosscorrelation is generally regarded as more important from the viewpoint of multiaccess interference in DS CDMA systems, we decided here, to chose those values of d_1 and d_2, where the minimum of $R_{CC}(d_1, d_2)$ appears, i.e. $d_1 = 14.2$, and $d_2 = 7.6$.

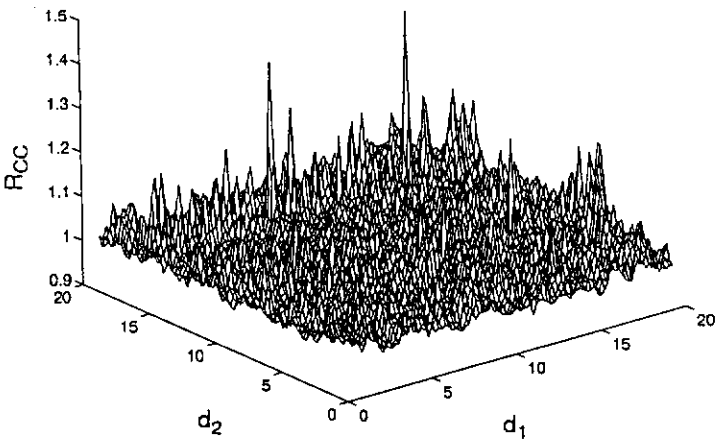

Figure 57: Plot of $R_{CC}(d_1, d_2)$ for the designed sequence set.

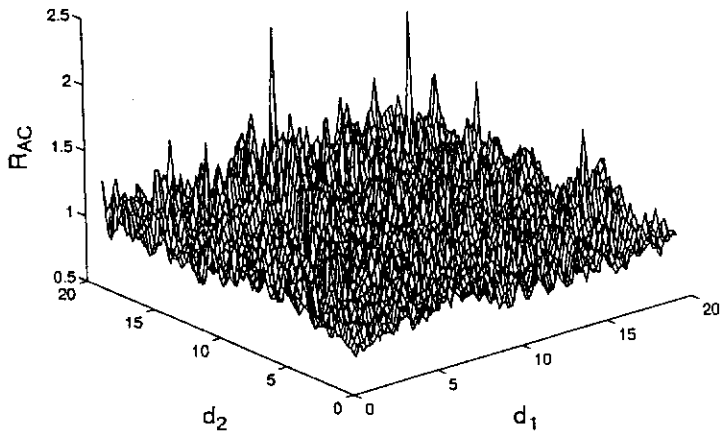

Figure 58: Plot of $R_{AC}(d_1, d_2)$ for the designed sequence set.

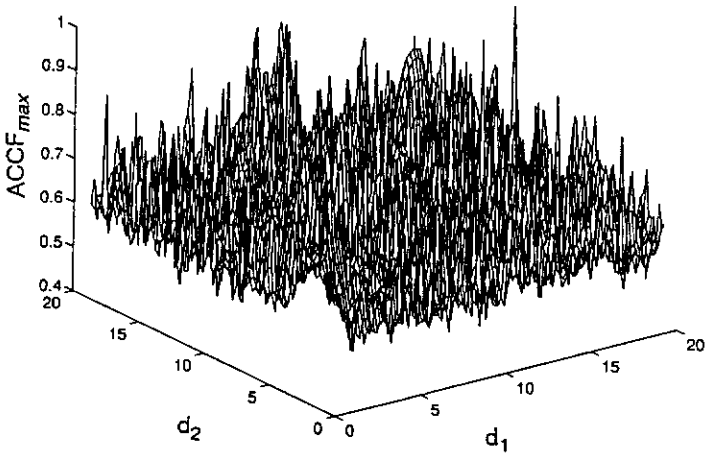

Figure 59: Plot of $ACCF_{max}(d_1, d_2)$ for the designed sequence set.

Table 10: List of coefficients $h_1^{(r)}$ and $h_2^{(r)}$ for the designed sequence set.

r	$h_1^{(r)}$	$h_2^{(r)}$
1	-113.60	7.60
2	-99.40	15.20
3	-85.20	22.80
4	-71.00	30.40
5	-56.80	38.00
6	-42.60	45.60
7	-28.40	53.20
8	-14.20	60.80
9	14.20	68.40
10	28.40	76.00
11	42.60	83.60
12	56.80	91.20
13	71.00	98.80
14	85.20	106.40
15	99.40	114.00
16	113.60	121.60

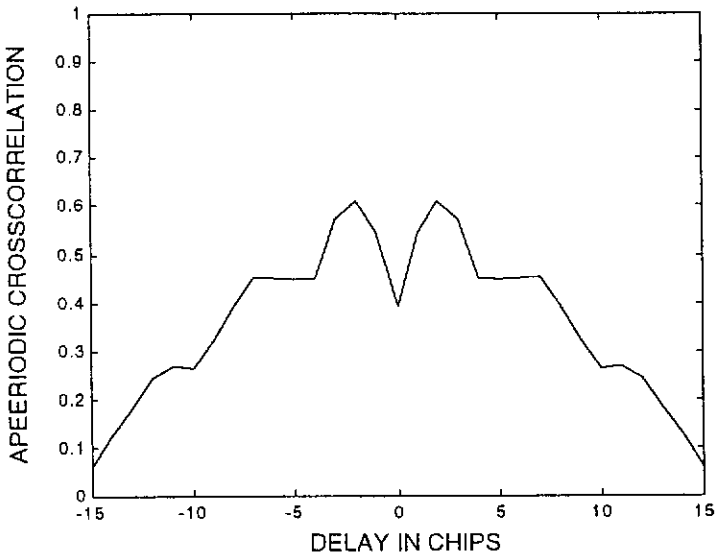

Figure 60: Plot of $ACCF_{max}(\tau)$ for $d_1 = 14.2$, and $d_2 = 7.6$.

This results in $R_{CC}(14.2, 7.6) = 0.9057$, $R_{AC}(14.2, 7.6) = 1.7439$, and $ACCF_{max}(14.2, 7.6) = 0.6085$. The full list of corresponding values of $h_1^{(r)}$ and $h_2^{(r)}$ for all 16 sequences is given in Table 10, and the plot of $ACCF_{max}(\tau)$ for $d_1 = 14.2$, and $d_2 = 7.6$ is given in Figure 60.

Another important set of characteristics for a spreading sequence set is power spectral densities of signals spread by these sequences. The plots of the magnitudes of power spectra for signals spread by each of the 16 sequences are given in Figure 61 and Figure 62. These plots were obtained using the same method as described in the previous section.

Further improvement in the value of R_{CC} can be obtained if coefficients $h_1^{(r)}$ and $h_2^{(r)}$ are optimised for all 16 sequences from the viewpoint of reaching minimum of R_{CC}. Several different methods of optimisation can be used for this purpose, and determining which one is the most efficient exceeds the scope of this thesis. To show however, that reduction in R_{CC} is possible, we have applied the Nelder-Meade simplex search [76] implemented in MATLAB as the function '*fmins*' [68] and described in Appendix 1, chosing the values given in Table 10 as a starting point. More details about the optimisation procedure are given in Apendix 2.

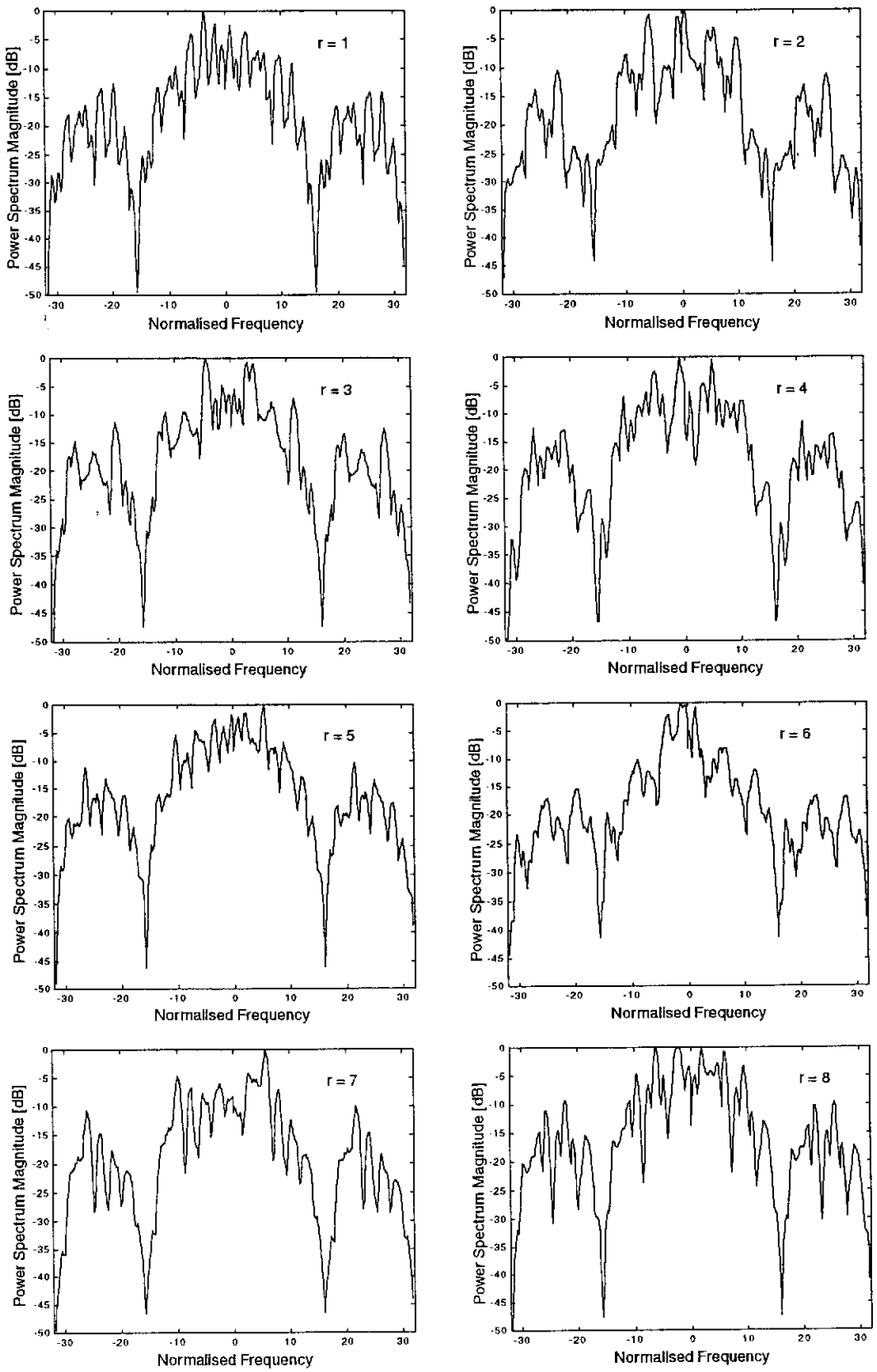

Figure 61: Plots of power spectrum magnitudes for signals obtain by spreading a random bipolar signal by the use of the designed sequences, $r = 1, 2, \ldots, 8$.

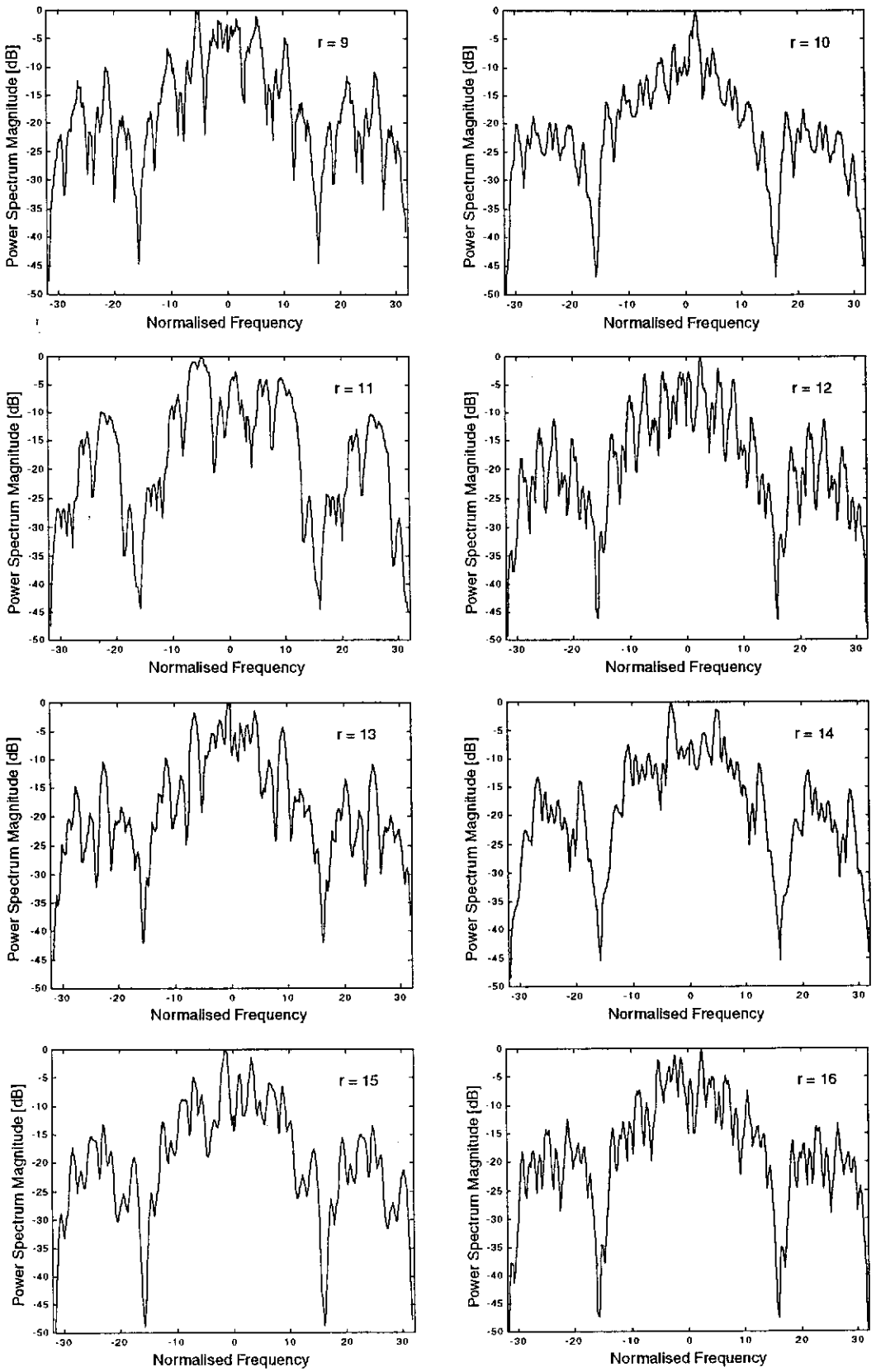

Figure 62: Plots of power spectrum magnitudes for signals obtain by spreading a random bipolar signal by the use of the designed sequences, $r = 9, 10, \ldots, 16$.

Table 11: List of the optimised coefficients $h_1^{(r)}$ and $h_2^{(r)}$.

r	$h_1^{(r)}$	$h_2^{(r)}$	r	$h_1^{(r)}$	$h_2^{(r)}$
1	-112.6513	7.5972	9	13.2249	69.7038
2	-96.7127	15.2773	10	28.2715	78.1511
3	-84.1755	23.5579	11	42.2284	85.7450
4	-71.0210	31.3700	12	57.6174	92.8630
5	-56.8045	36.4517	13	70.2810	98.7896
6	-44.9827	44.2826	14	85.4777	105.8105
7	-27.9950	49.9497	15	96.5492	112.4437
8	-14.5283	63.7458	16	114.0881	121.3066

After the completing optimisation, we were able to achieve $R_{CC} = 0.8441$. However, as expected the abovementioned gain was counteracted by deterioration in the synchronisability performance due to $R_{AC} = 2.4875$. The list of the optimised coefficients $h_1^{(r)}$ and $h_2^{(r)}$ is given in Table 11.

In Figure 63 we present two example plots of the magnitude of aperiodic CCF between the sequences $(1, 2)$ and $(1, 16)$, having their parameters $h_1^{(r)}$ and $h_2^{(r)}$ according to Table 11.

Even though the value of $R_{AC} = 2.4875$, the aperiodic ACFs for all of the sequences are still reasonable, exhibiting significant peaks at zero. The example plots of the magnitudes of ACFs for three different sequences are given in Figure 64. Certainly, one can optimise the coefficients $h_1^{(r)}$ and $h_2^{(r)}$, in order to minimise other parameters like R_{AC}. Also, one can chose different starting point for the optimisation.

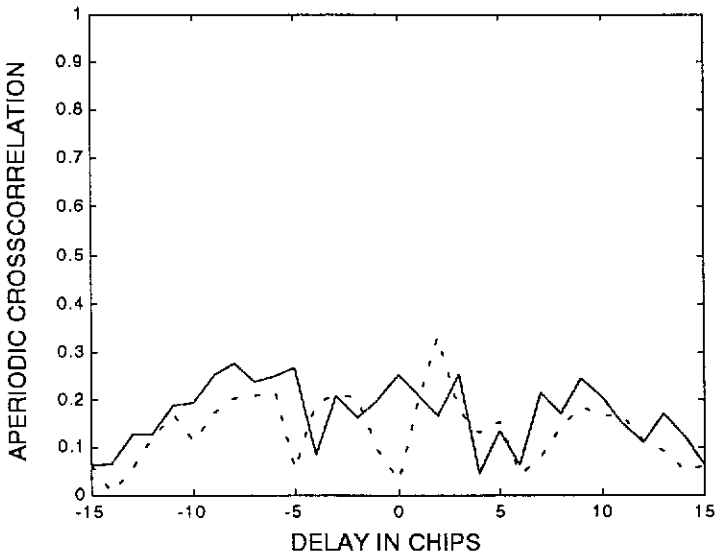

Figure 63: Magnitudes of the aperiodic CCFs between the sequences: (1,2) - solid line, and (1,16) - dotted line, having their parameters $h_1^{(r)}$ and $h_2^{(r)}$ according to Table 11.

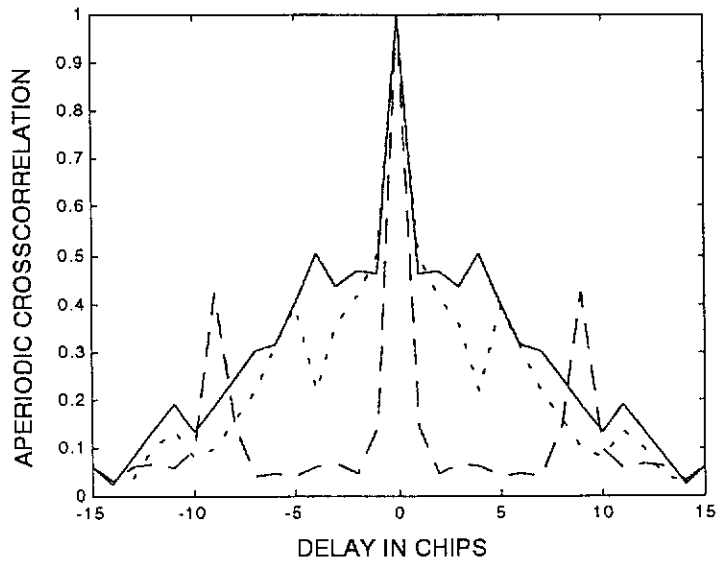

Figure 64: Magnitudes of aperiodic ACFs for $r = 1, 8,$ and 16.

5.3 Modified Walsh sequences

5.3.1 Design method

In [114], we have described the method to reduce ISI and MAI for non-synchronized CDMA signals by means of a modification to the carrier waveform. The modified carrier has been obtained by a regular distortion to the frequency of the original carrier, resulting in the ith user line signal $s^{(i)}(t)$ expressed by:

$$s^{(i)}(t) = b^{(i)}(t) \cdot \cos\left[\omega_c t + \int_0^t w^{(i)}(\tau)d\tau + \phi^{(i)}(t)\right], \tag{147}$$

where $w^{(i)}(t)$ is a frequency distorting function, which can be optimized to minimize the cross-correlations between users, and to minimize the off-peak auto-correlation of the ith line signal, $\phi^{(i)}(t)$ is an information carrying phase component.

A base-band approach [118] follows from the fact that for the real spreading signal $b^{(i)}(t)$ being a physical representation of a real spreading sequence $\{\hat{b}_n^{(i)}\}$; $n = 1, 2, \ldots, N$, equation (147) can be rewritten in the exponential form as:

$$s^{(i)}(t) = b^{(i)}(t) \cdot Re\left\{e^{j\omega_c t}\exp\left[j\int_0^t w^{(i)}(\tau)d\tau\right]e^{\phi^{(i)}(t)}\right\}. \tag{148}$$

The complex envelope [84] $\sigma(t)$ of such a signal is given by:

$$\sigma(t) = b^{(i)}(t)\exp\left[j\int_0^t w^{(i)}(\tau)d\tau\right]e^{\phi^{(i)}(t)} = c^{(i)}(t)e^{\phi^{(i)}(t)}, \tag{149}$$

Because signal is usually processed using digital signal processing (DSP) technology in the receiver, instead of the analogue spreading waveform:

$$c^{(i)}(t) = b^{(i)}(t)\exp\left[j\int_0^t w^{(i)}(\tau)d\tau\right] \tag{150}$$

one can use the polyphase complex spreading sequence $\{\hat{c}_n^{(i)}\}$; $n = 1, 2, \ldots, N'$. The length N' of the signature $\{\hat{c}_n^{(i)}\}$ is equal to the length of the original sequence $\{\hat{b}_n^{(i)}\}$ multiplied by the number of samples per chip used in the receiver, s. The elements $\hat{c}_n^{(i)}$ of the sequence $\{\hat{c}_n^{(i)}\}$ are calculated according to the formula:

$$\hat{c}_n^{(i)} = w_n^{(i)} \hat{b}_m^{(i)}, \; m = \left\lfloor \frac{n-1}{s} \right\rfloor + 1, \; n = 1, \ldots, N', \tag{151}$$

with the factors $w_n^{(i)}$ obtained by discretising the function $W^{(i)}(t)$:

$$W^{(i)}(t) = \exp\left[j \int_0^t w^{(i)}(\tau) d\tau \right] \tag{152}$$

by substituting n for t and N' for T.

5.3.2 *Example*

In order to optimise the spreading sequences for the use in a 13 channel DS CDMA ATM WLAN [30], we have chosen a subset of 13 orthogonal Walsh sequences $\{\hat{h}_n^{(i)}\}$ of length $N = 16$, where their elements $\hat{h}_n^{(r)}$ are the rth rows of a Hadamard matrix H_{16} for $r = 2, \ldots, 8, 10, 11, 12, 14, 15, 16$.

To minimise the crosscorrelation between any pair of the spreading signatures, independently of the relative delay, we applied the described method with the functions $w^{(i)}(t)$, $i = 1, 2, \ldots, 13$, being of the form:

$$w^{(i)}(t) = 2\pi[\alpha^{(i)}\zeta(t/16) + \beta^{(i)}\zeta(t/8) + \gamma^{(i)}\zeta(t/4)], \tag{153}$$

where the triangular wave $\zeta(t)$ is defined as:

$$\zeta(t) = \sum_{n=-\infty}^{\infty} \lambda(t-n), \tag{154}$$

and

$$\lambda(t) = \begin{cases} 0, & t < 0 \\ \frac{4t}{T} - \frac{1}{T}, & 0 \le t < 0.5T \\ -\frac{4t}{T} + \frac{3}{T}, & 0.5T \le t < T \\ 0, & t \ge T \end{cases} \tag{155}$$

with T being the duration of a data bit.

The values of the coefficients $\alpha^{(i)}$, $\beta^{(i)}$, $\gamma^{(i)}$, $i = 1, \ldots, 13$ were optimised [118] to find their values minimising $R_{CC}(A)$:

$$A = \begin{bmatrix} \alpha^{(1)} & \ldots & \alpha^{(13)} \\ \beta^{(1)} & \ldots & \beta^{(13)} \\ \gamma^{(1)} & \ldots & \gamma^{(13)} \end{bmatrix}. \tag{156}$$

Since the function to be minimised is highly irregular having many local maxima and minima, we have used the following algorithm to find the solution:

i. In the first step of the optimisation we set:

$$\begin{cases} \alpha^{(i)} = \alpha\ , \ i = 1, 2, \ldots, 13 \\ \beta^{(i)} = \beta\ , \ i = 1, 2, \ldots, 13 \\ \gamma^{(i)} = \gamma\ , \ i = 1, 2, \ldots, 13 \end{cases} \tag{157}$$

and calculated the values of $R_{CC}(A)$ for $-20 \le \alpha, \beta, \gamma \le 20$ with grid step being equal to 0.2 for each of the parameters α, β, and γ.

ii. Next we perform optimization for all 39 variables using the Nelder-Meade simplex search [76] implemented in MATLAB as the function *'fmins'* [68] (see Appendix 1). For the starting point, we choose

$$A^* = \begin{bmatrix} \alpha^* \\ \beta^* \\ \gamma^* \end{bmatrix} \otimes \begin{bmatrix} 1 & 1 & 1 & 1 & 1 & 1 & 1 & 1 & 1 & 1 & 1 & 1 & 1 \end{bmatrix}, \tag{158}$$

where: $\otimes$ denotes the Kronecker product, α^*, β^*, and γ^* are the values of α, β, and γ, respectively, for which $R_{CC}(A)$ reaches the minimum in the previous step. More details of the optimisation procedure can be found in Appendix 3.

The values of the coefficients $\alpha^{(i)}$, $\beta^{(i)}$, $\gamma^{(i)}$, $i = 1, \ldots, 13$ for which $R_{CC}(A)$ reaches a local minimum of 0.8167, and $R_{AC}(A) = 1.2888$, are given in Table 12.

Table 12: Optimised values of coefficients $\alpha^{(i)}$, $\beta^{(i)}$, $\gamma^{(i)}$.

i	$\alpha^{(i)}$	$\beta^{(i)}$	$\gamma^{(i)}$
1	2.4029	1.2238	-2.5695
2	10.5088	2.2025	1.6241
3	0.0276	1.8266	0.3233
4	7.4261	-0.5551	3.4070
5	3.3230	-3.1656	-0.0607
6	5.4877	0.1337	3.7314
7	-4.4534	-3.3895	-1.5841
8	3.6984	-4.4512	0.1607
9	5.5630	-2.9983	-3.5744
10	-5.3085	6.7429	0.0321
11	-5.2342	-3.1874	-0.4403
12	0.7175	-0.3491	0.8905
13	-0.7613	5.8160	2.8800

In Figure 65 and Figure 66 we show example plots of aperiodic ACFs and CCFs, for the designed set of sequences, respectively. The maximum value of aperiodic CCFs over the whole set of sequences is given in Figure 67.

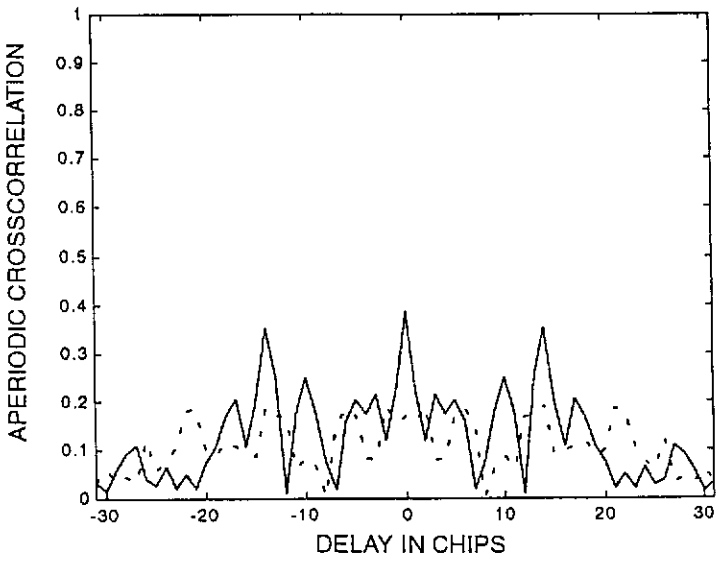

Figure 65: Example plots of the magnitude of aperiodic crosscorrelation functions between the sequences: $\{\hat{c}_n^{(1)}\}$ and $\{\hat{c}_n^{(7)}\}$ - solid line, and $\{\hat{c}_n^{(3)}\}$ and $\hat{c}_n^{(10)}\}$ - dotted line.

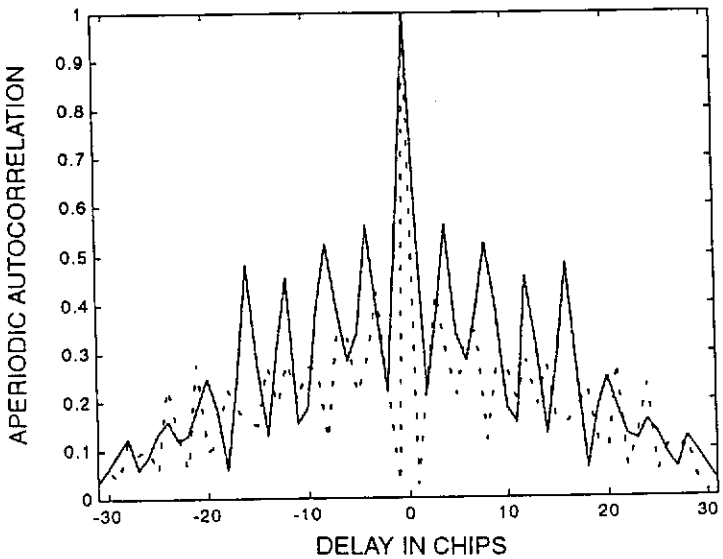

Figure 66: Example plots of the magnitude of aperiodic autocorrelation functions for the sequences $\{\hat{c}_n^{(3)}\}$ - solid line, and $\{\hat{c}_n^{(9)}\}$ - dotted line.

From Figure 65, and in particular from Figure 67, it is visible that even though the original set of Walsh sequences is a set of orthogonal sequences, $ACCF_{max}(\tau)$ is not equal to zero for $\tau = 0$, and therefore the designed sequences are no longer orthogonal. On the other hand, we have achieved a significant improvement as far as the auto-

correlation properties of the set are concerned, compared to the original set of Walsh sequences.

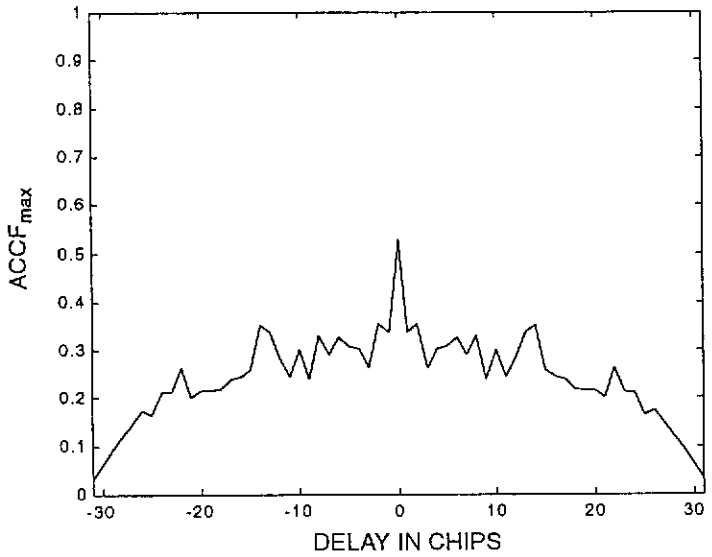

Figure 67: Plot of $ACCF_{max}(\tau)$ for the designed set of sequences.

As usual, among the very important characteristics of the set of spreading sequences are power spectra of the signals spread by those sequences. Using the same method as described in Section 5.2, we calculated power spectra for the random bipolar signals of length 64 data bits, spread by each of the designed signatures. The plots of the computed power spectra magnitudes are given in Figure 68, and Figure 69. From these plots, it is clear that the bandwidth required to transmit such signals is about twice as wide as in the case of 16 chip sequences considered in the two previous sections. Therefore, the lower value of R_{CC} in this case can be, at least partially, attributed to the increase in the bandwidth occupancy.

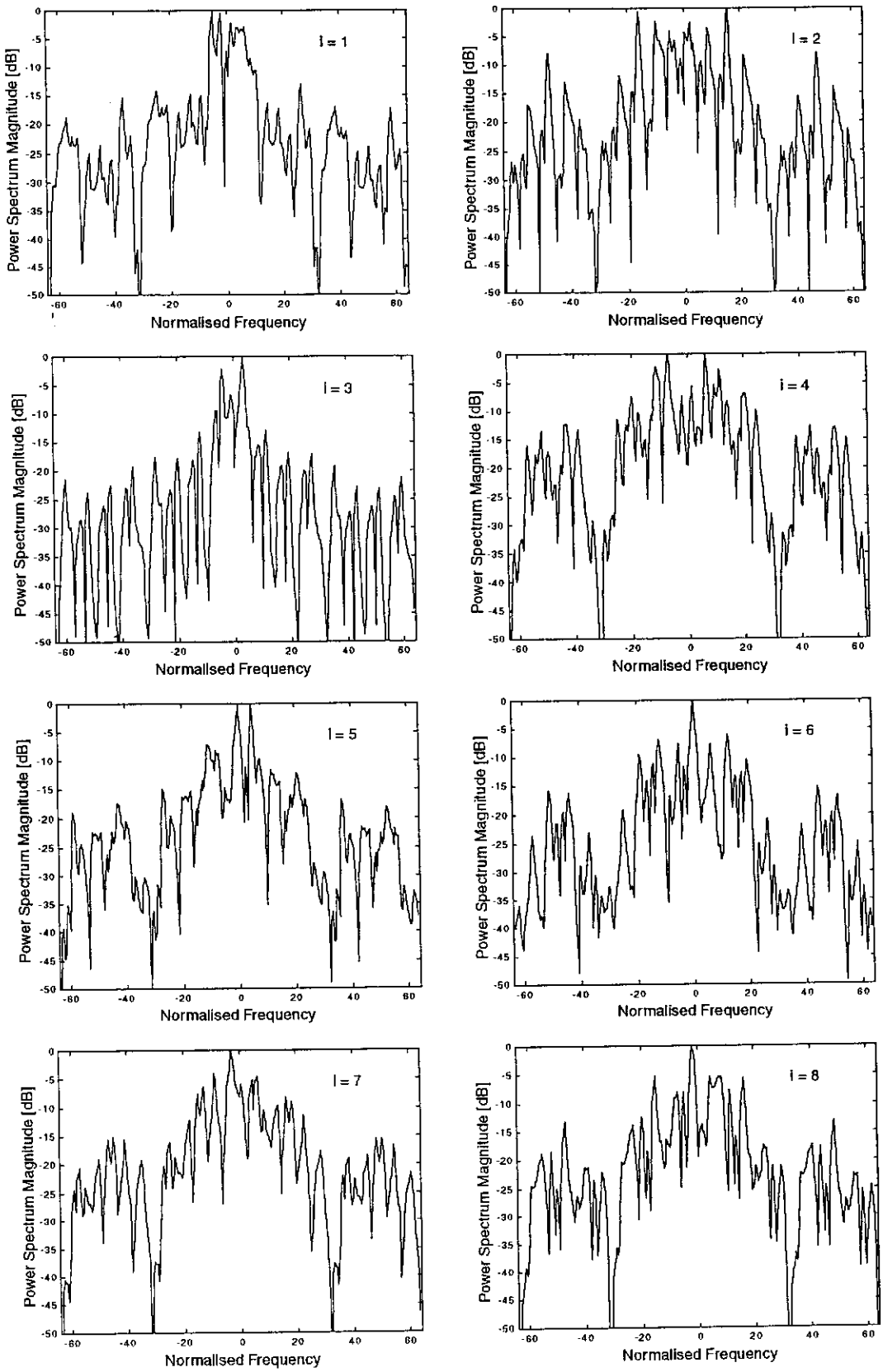

Figure 68: Power spectra magnitudes for the signals spread by Walsh sequences $\{\hat{c}_n^{(i)}\}$ modified by the superposition of triangular functions, $i = 1, 2, \ldots, 8$.

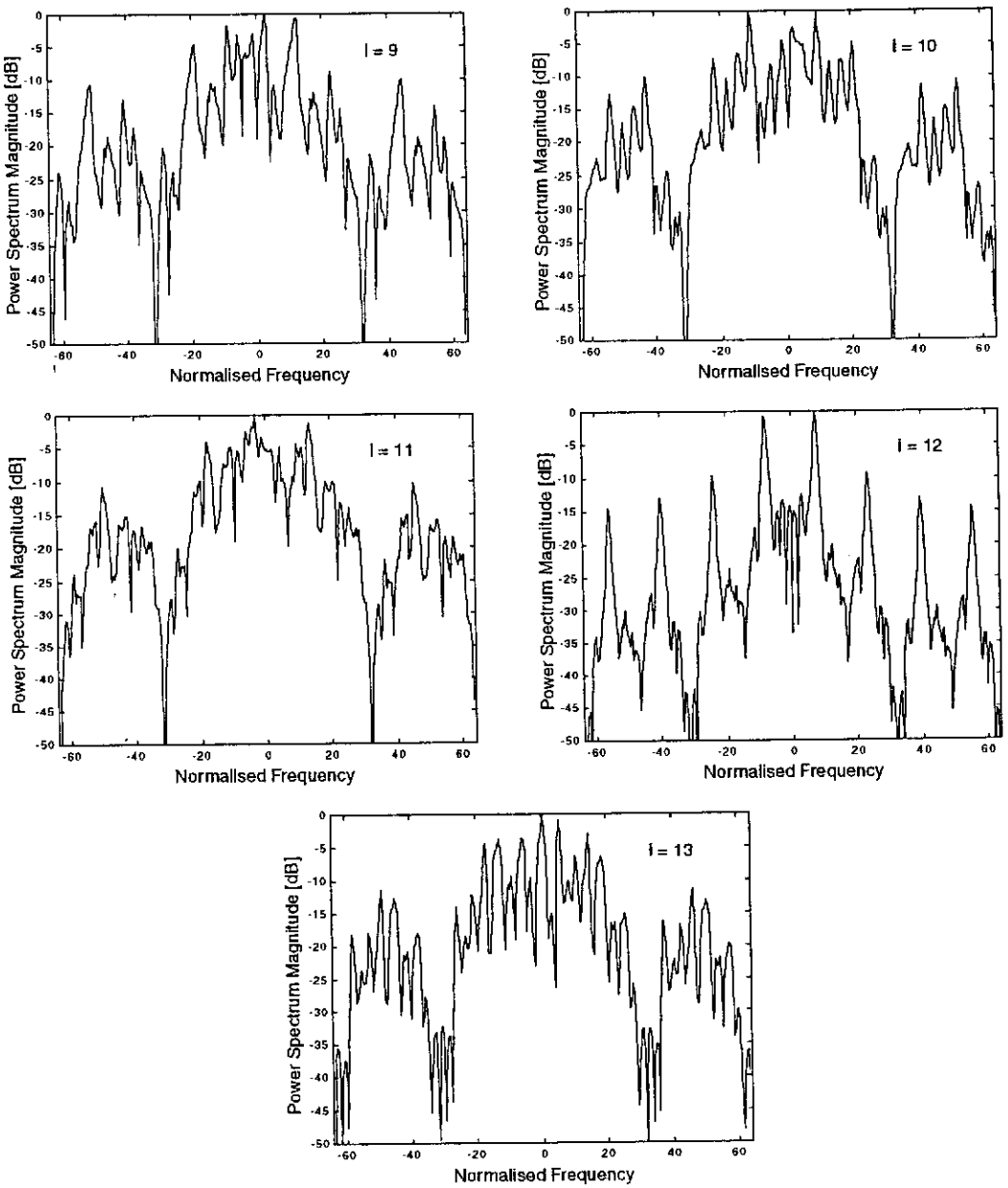

Figure 69: Power spectra magnitudes for the signals spread by Walsh sequences $\{\hat{c}_n^{(i)}\}$ modified by the superposition of triangular functions, $i = 9, \ldots, 13$.

5.4 Sets of orthogonal polyphase spreading sequences

5.4.1 Design method

At the beginning of this chapter, we indicated that one of our goals in developing the new methods to design sets of spreading sequences for high capacity wireless data DS CDMA networks is achieving orthogonality of the sequences in the case of perfect synchronisation. Using similar approach to that employed in design of EOE sequences [34], we can keep orthogonality of sequences, if the elements $\hat{o}_n^{(i)}$ of the sequences $\hat{o}_n^{(i)}\}$, $i = 1, 2, \ldots, M$, are given by:

$$\hat{o}_n^{(i)} = w_n \hat{b}_n^{(i)}, \; n = 1, 2, \ldots, N, \tag{159}$$

where

$$w_n = \exp[j2\pi(h_1 b_n + h_2 d_n)], \tag{160}$$

b_n and d_n are defined by equations (134) and (140), respectively, and $\hat{b}_n^{(i)}$ are the elements of orthogonal sequences $\{\hat{b}_n^{(i)}\}$, $i = 1, \ldots, M$.

We will prove now the following theorem:

Theorem: If two sequences $\{\hat{a}_n^{(1)}\}$, and $\{\hat{a}_n^{(2)}\}$ of length N are orthogonal, then the sequences $\hat{d}_n^{(1)}$, and $\{\hat{d}_n^{(2)}\}$ having their elements of the form:

$$\begin{aligned} \hat{d}_n^{(1)} &= w_n \hat{a}_n^{(1)} \\ \hat{d}_n^{(2)} &= w_n \hat{a}_n^{(2)} \\ n &= 1, 2, \ldots, N \end{aligned} \tag{161}$$

are also orthogonal, if

$$w_n w_n^* = 1, n = 1, \ldots, N, \tag{162}$$

where w_n^* denotes the complex conjugate of w_n.

Proof: Two complex valued sequences $\{\hat{a}_n^{(1)}\}$ and $\{\hat{a}_n^{(2)}\}$ are said to be orthogonal if and only if their aperiodic crosscorrelation $c_{a1,\,a2}(\tau)$ is equal to zero for $\tau = 0$:

$$c_{a1,\,a2}(0) = \frac{1}{N}\sum_{n=1}^{N} \hat{a}_n^{(1)}[\hat{a}_n^{(2)}]^* = 0. \tag{163}$$

Utilising equation (161), we can write the aperiodic crosscorrelation $c_{d1,\,d2}(0)$ between the sequences $\{\hat{d}_n^{(1)}\}$, and $\{\hat{d}_n^{(2)}\}$ as:

$$\begin{aligned} c_{d1,\,d2}(0) &= \frac{1}{N}\sum_{n=1}^{N} w_n\hat{a}_n^{(1)}[w_n\hat{a}_n^{(2)}]^* \\ &= \frac{1}{N}\sum_{n=1}^{N} w_n w_n^*\,\hat{a}_n^{(1)}[\hat{a}_n^{(2)}]^* \\ &= \frac{1}{N}\sum_{n=1}^{N} \hat{a}_n^{(1)}[\hat{a}_n^{(2)}]^* \\ &= c_{a1,\,a2}(0) = 0 \end{aligned} \tag{164}$$

Therefore, the sequences $\{\hat{d}_n^{(1)}\}$, and $\{\hat{d}_n^{(2)}\}$ are orthogonal.

Because the factor w_n given by equation (160) fulfils the condition (162), then by keeping it constant for all sequences $\{\hat{b}_n^{(i)}\}$, we can maintain the orthogonality of the sequences $\{\hat{o}_n^{(i)}\}$.

5.4.2 Example

Using the same subset of the orthogonal Walsh sequences as in Section 5.3, design a set of orthogonal polyphase sequences of length $N = 16$.

In order to find the appropriate values for the coefficients h_1 and h_2, we calculated

the value of R_{CC} for $0 \le h_1 \le 30$ and $0 \le h_2 \le 30$, with the grid of 0.2. The results are plotted in Figure 70. In the investigated region, R_{CC} reaches the minimum of 0.8532 for $h_1 = 15.8$ and $h_2 = 24.4$. For those values of h_1 and h_2 the R_{AC} takes the value of 1.5962, and the plot of $R_{AC}(h_1, h_2)$ is given in Figure 71.

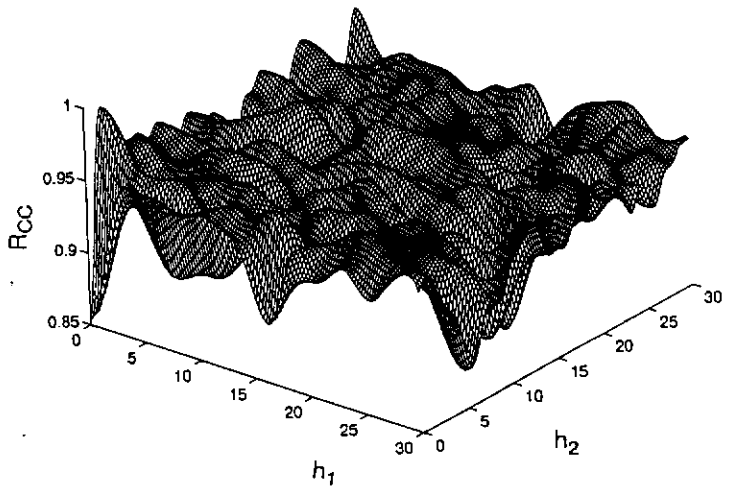

Figure 70: Plot of $R_{CC}(h_1, h_2)$ for the designed set of sequences $\{\hat{o}_n^{(i)}\}$, $i = 1, \ldots, 13$.

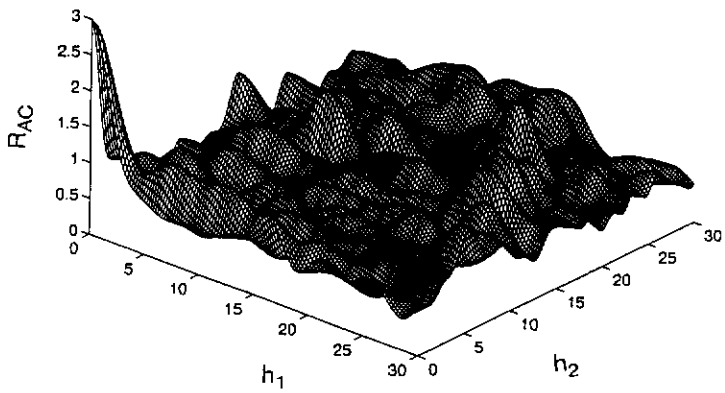

Figure 71: Plot of $R_{AC}(h_1, h_2)$ for the designed set of sequences $\{\hat{o}_n^{(i)}\}$, $i = 1, \ldots, 13$.

To show that the designed set of sequences is orthogonal, we plotted $ACCF_{max}(\tau)$ in Figure 72, where it is clearly visible that $ACCF_{max}(0) = 0$. The same is visible in Figure 73, where we plotted the magnitudes of aperiodic CCFs for two example pairs of designed sequences. The autocorrelation properties of the designed set of sequences are also good, and to illustrate this we plotted magnitudes of ACFs for two example sequences in Figure 74.

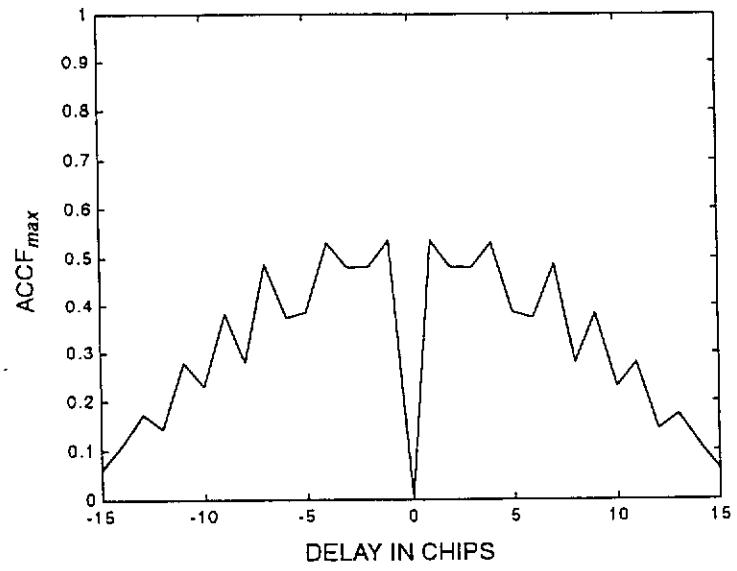

Figure 72: Plot of $ACCF_{max}(\tau)$ for the designed set of sequences $\{\hat{o}_n^{(i)}\}$, $i = 1, \ldots, 13$

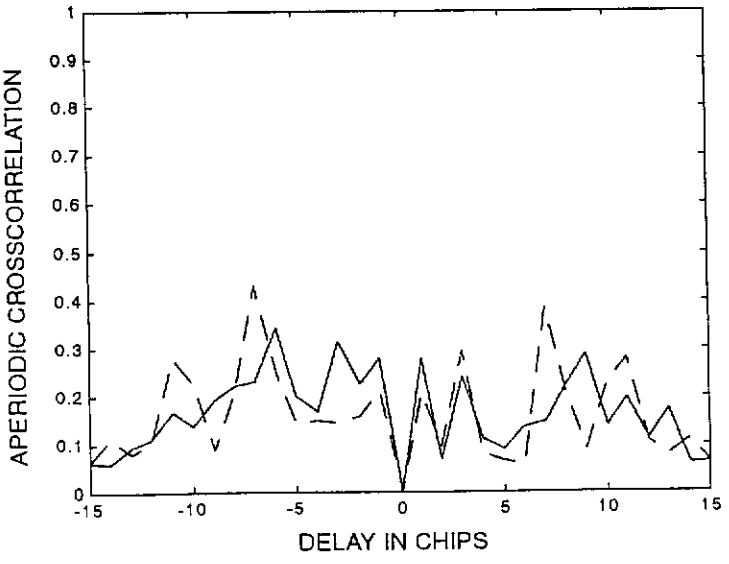

Figure 73: Magnitudes of the aperiodic CCFs between the sequences: (1,10) - solid line, and (4,11) - dashed line.

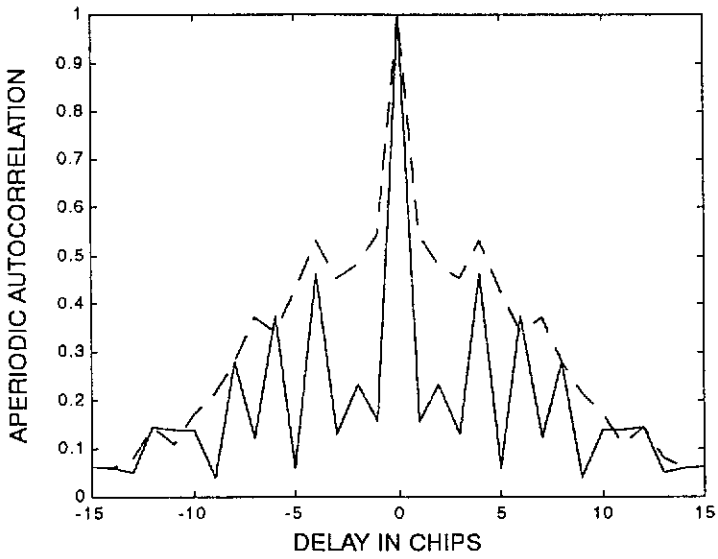

Figure 74: Magnitudes of the aperiodic ACFs for the sequences: 4 - solid line, and 10 - dashed line.

As with the previously designed sequence sets, we will now look into the power spectra of random bipolar signals spread by means of the designed sequences. The plots of the power spectra magnitudes of such signals are given in Figure 75, and Figure 76. They were computed using the same method as the one used throughout this chapter. From the plots of Figure 75 and Figure 76, it is visible that the first nulls in the power spectra magnitudes is at the normalised frequencies ± 16, which is half that of the sequences considered in Section 5.3.

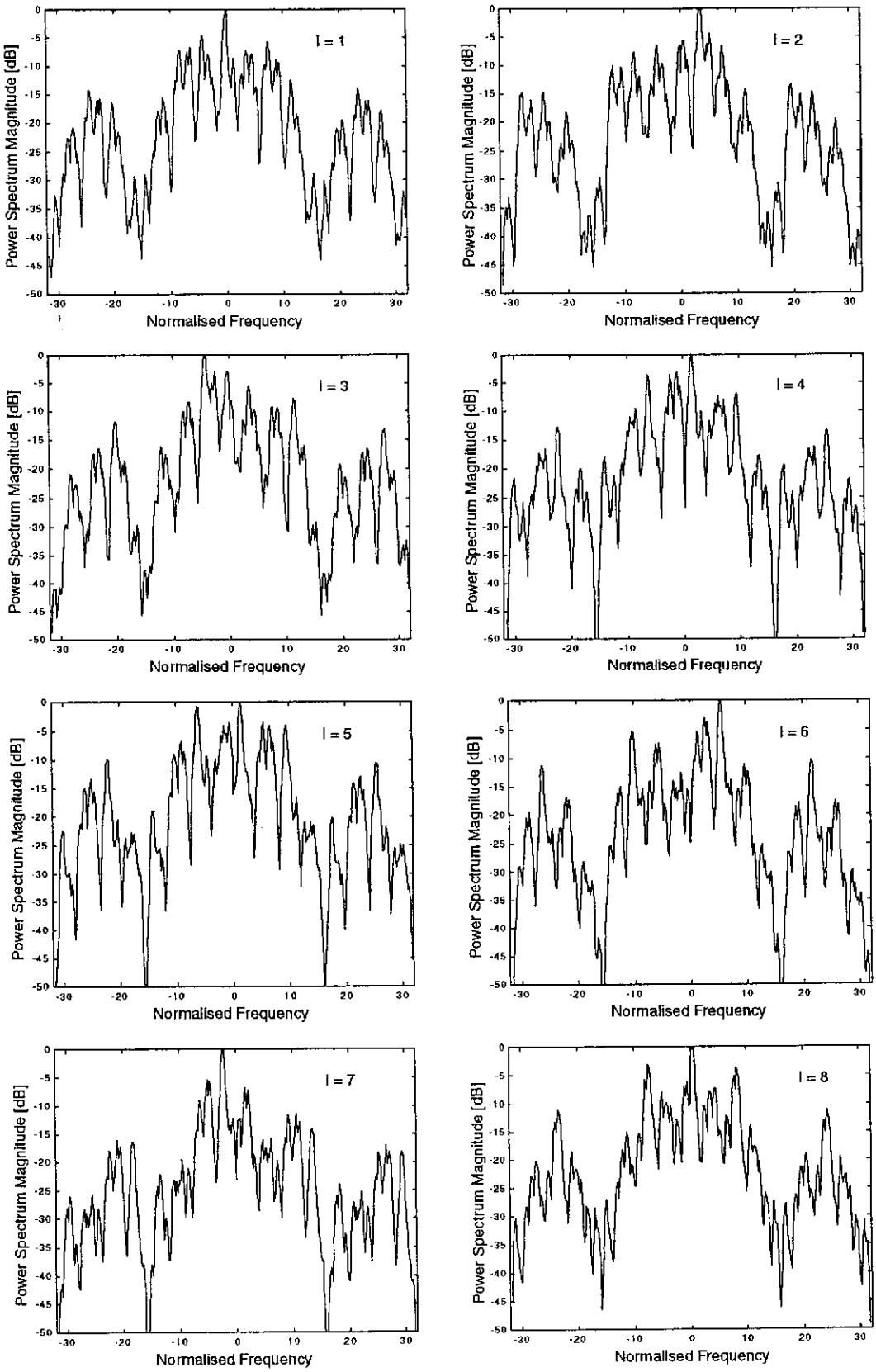

Figure 75: Power spectra magnitudes for signals spread by the sequences $\{\hat{o}_n^{(i)}\}$; $i = 1, ..., 8$.

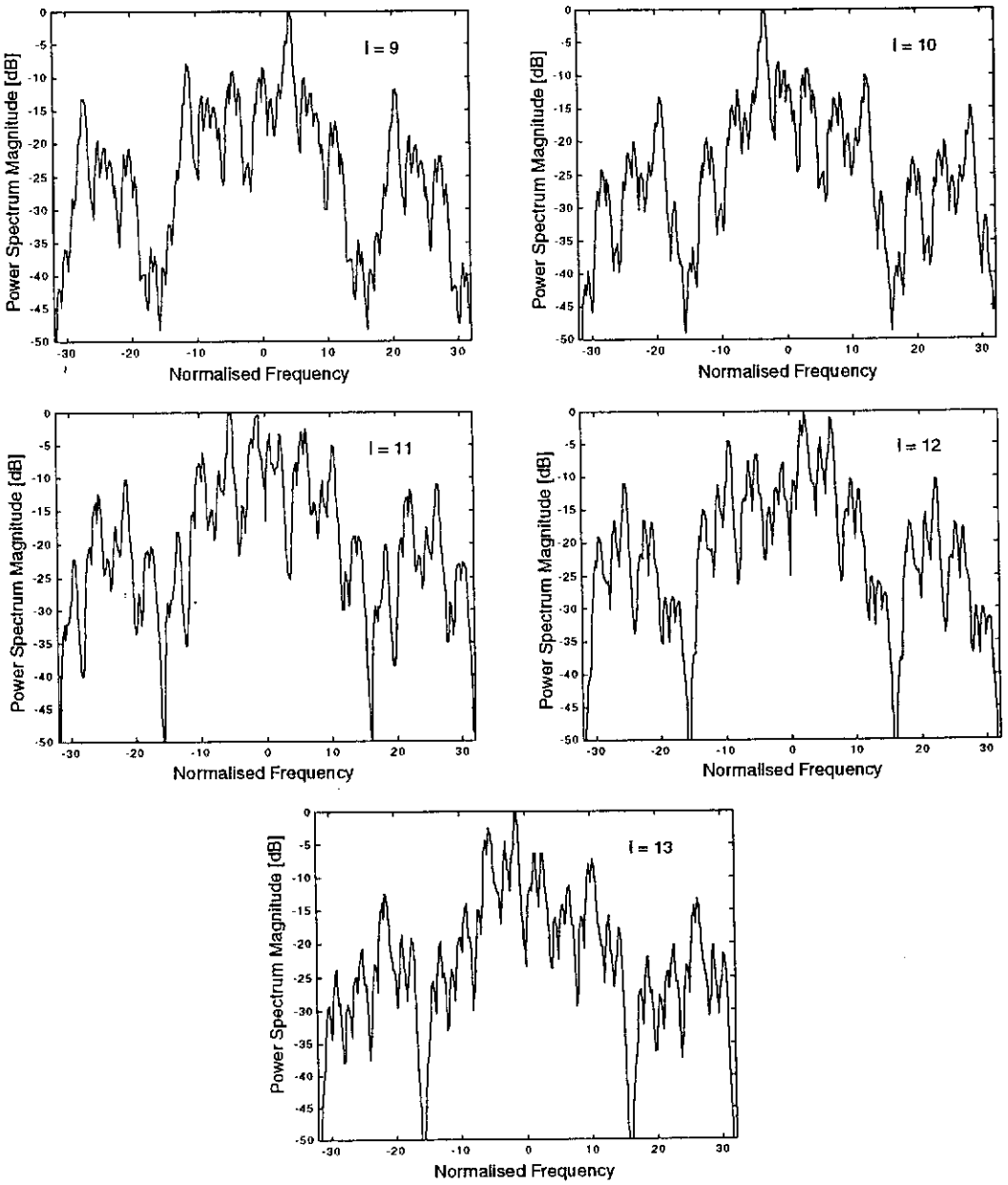

Figure 76: Power spectra magnitudes for signals spread by the sequences $\{\hat{o}_n^{(i)}\}$; $i = 9, ..., 13$.

5.5 Summary

In this chapter we have introduced four new methods to design spreading sequences for DS CDMA wireless data networks:

i. chirp sequences, (Section 5.1),

ii. sequences being superposition of chirp sequences of different order, (Section 5.2),

iii. modified non-orthogonal Walsh sequences, (Section 5.3),

iv. orthogonal polyphase sequences, (Section 5.4).

The example sets of designed sequences exhibit good correlational properties reflected in the values of R_{CC} and R_{AC}, and also the last method can give us the set of orthogonal sequences with good correlation properties. The major benefit of the two first methods lies in the fact that we can design sequences of any arbitrary length with the reasonable values of R_{CC} and R_{AC}. In the next chapter we will follow our investigations and present the results of simulated bit error rates for DS CDMA system if the sequences designed in this chapter are used.

6. Multiuser performance of the designed sequences

In this chapter we will use some of the sequence sets designed in the previous chapter to simulate the multiuser DS CDMA system and to obtain the bit error rate (BER) characteristics of such systems, depending on the number of simultaneous users and the noise level. While simulating the DS CDMA systems we will not be taking to account other factors which can influence the BER, for example imperfect sequence acquisition, and the impact of the near/far effect [26], [87].

In the first section of this chapter we describe the simulation procedure, and in the following sections we present results of the simulation for the DS CDMA systems utilising three of the sequence sets developed in the previous chapter, compared with the results obtained for the system employing a set of 15-chip Gold-like sequences [29].

6.1 Simulation procedure

In order to finally assess the usefulness of a designed spreading sequence set, particularly in the case of small sets of short sequences, one needs to simulate operation of the CDMA multiuser system utilising those sequences. In such a way, one can sensibly approximate BER caused by multiaccess interference (MAI), noise, or multipath propagation.

We have assumed that data transmitted in any of the active channels is random, grouped into encapsulated wireless ATM (WATM) frames comprising 424 bits of an ATM cell plus 100 bits of a wireless overhead [30]. With ATM being the widely accepted standard for broadband networking, it is highly desirable for new broadband wireless networks to interwork seamlessly with existing and emerging fixed ATM networks. Accordingly, the ATM Forum is working towards the specification of a wireless ATM (WATM) standard to support both terminal mobility and wireless access with minimal modifications to the existing ATM technology [20]. We have considered such frames not because we wanted to associate the methods developed in the thesis with WATM technology, but because with such a short packet we could assume the channel to be static for the duration of a whole packet. However, any other frame formats can be considered.

Because the simulated system has been considered as an asynchronous system,

only the examined channel has been kept synchronised with the corresponding reference sequence generated at the receiver while the interfering m channels have been randomly delayed with respect to the examined channel. Those random delays τ_i, $i = 1, \ldots, m$, have been chosen as integer multiplies of 0.5, and satisfying the condition:

$$0 \leq \tau < N, \tag{165}$$

where N is the length of the spreading sequences.

Since in a real system phases of the generators used in all of the transmitting terminals can be different, we multiplied each of the interferers' signals by a coefficient:

$$\rho_i = \exp(j\phi_i), \tag{166}$$

where ϕ_i is a constant chosen randomly from the interval $[0, 2\pi)$.

In order to simplify the simulations, we have kept those randomly chosen coefficients τ_i, ϕ_i, $i = 1, \ldots, m$, constant throughout the transmission of a single WATM frame in the examined channel, with drawing of them repeated before every new transmission of a single WATM frame being simulated.

Generally, the MAI caused by the signals obtained by spreading data with different sequences is different. Therefore, for each of the simulated frame transmissions in the examined channel, the sequences used by the interferers has been chosen randomly from the set of all possible spreading sequences utilised in the system, disregarding the one used by the channel under examination.

To avoid being drawn into considering the problems associated with the near/far-effect, we have assumed a very stringent power control, keeping powers of all signals arriving at the receiver at the same level. Failure to do so, could dim the process of drawing the conlusions about usefulness of the designed sequences, not mention the significant increase in complexity of simulation routines and a processing time for simulation.

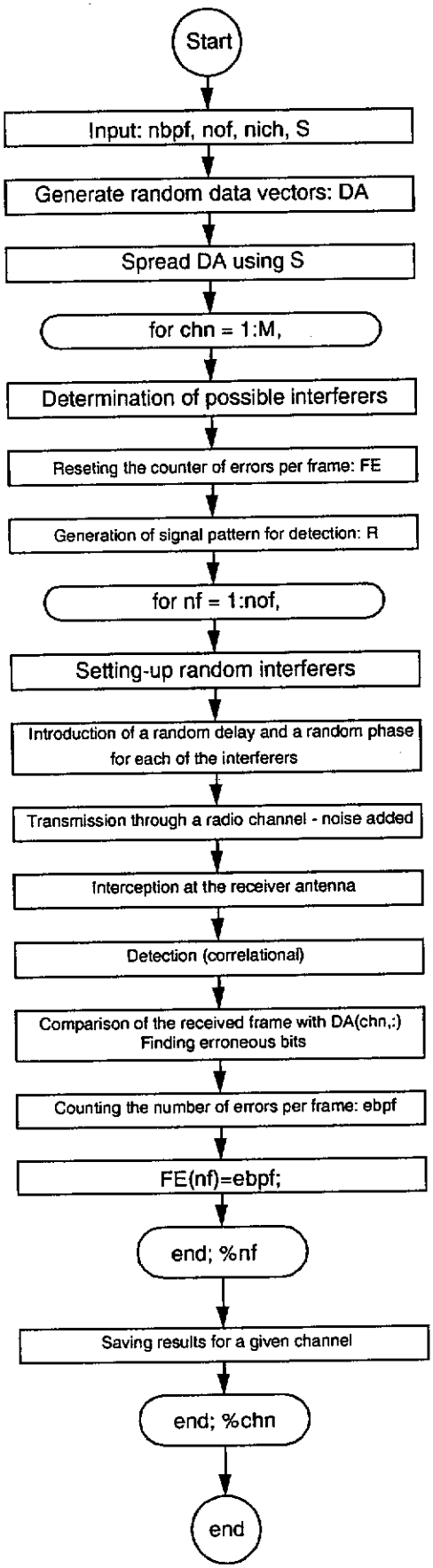

Note:

S - sequence set,
nbpf - number bits per frame,
nof - number of frames to be simulated,
nich - number of interferers
M - number of spreading sequences.

Figure 77: Simplified flow chart of the simulation program.

All simulation programs have been written in MATLAB, and run on UltraSparc SUN workstation. It is, however difficult to make any comments on the time required for simulations, because the workstation has been used by other users too. The simplified flow chart of the simulation program is shown in Figure 77. The program can be easy extended to accommodate different channel models and interferers' powers can be also adjusted to cater for near-far-effect.

The simulation program has been run for different sets of spreading sequences, with the number of possible interferers being changed from 1 to M-1, where M has been the total number of spreading sequences in the given set. All results have been stored, and later processed to obtain histograms of the number of errors in the received WATM frames, as well as the average BER as functions of the number of interferers.

The simulation results for four different spreading sequence sets, including 15 chip Gold-like sequences described in Section 4.1.3, and the sequences developed in Chapter 5, i.e. 16-chip poly-chirp sequences, 16-chip modified orthogonal Walsh sequences, and 32 -chip non-orthogonal modified Walsh sequences, are given in the next four sections of this chapter. In all cases we have simulated the situation of 1000 independent WATM frames transmitted through the system.

Apart from the presence of MAI, we have assumed the presence of white Gausian noise in the channel. We have repeated the simulations for two values of noise level, resulting in $E_b/N_0 = 20$ dB and $E_b/N_0 = 8$ dB , where N_0 is single sided power spectral density of white noise, and E_b is energy per information bit [84], [96].

6.2 System utilising 15-chip Gold-like sequences

In order to evaluate performance of the developed sets of spreading sequences we decided to compare their performance with the performance of the set of Gold-like sequences of 15-chip length. We have chosen 15-chip Gold-like sequences because of their length, and therefore the spreading ratio are similar to those of 16-chip poly-chirp sequences or 16-chip modified orthogonal Walsh sequences. The simulation results are presented in Figure 78 through to Figure 85. Apart from the overall system performance given in Figure 84 and Figure 85, we present the results achieved for the channels exhibiting the highest and the lowest BER. We refer to them hereafter as 'the worst channel' and 'the best channel', respectively.

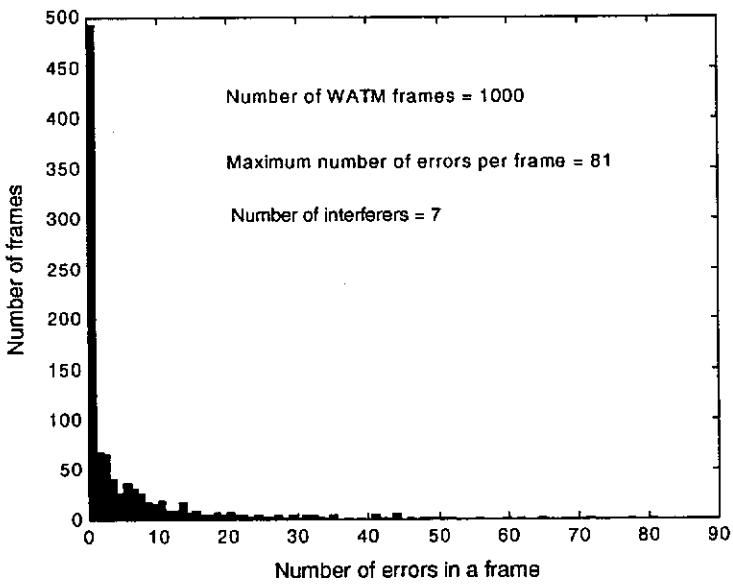

Figure 78: Histogram of the numbers of errors during simulated transmission of 1000 WATM frames for 7 interferers, $E_b/N_0 = 20$ dB, in the case of the worst channel.

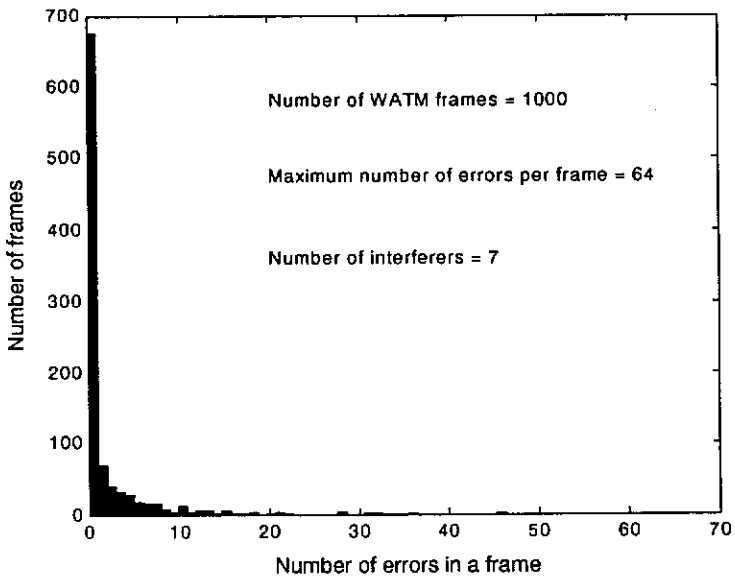

Figure 79: Histogram of the numbers of errors during simulated transmission of 1000 WATM frames for 7 interferers, $E_b/N_0 = 20$ dB, in the case of the best channel.

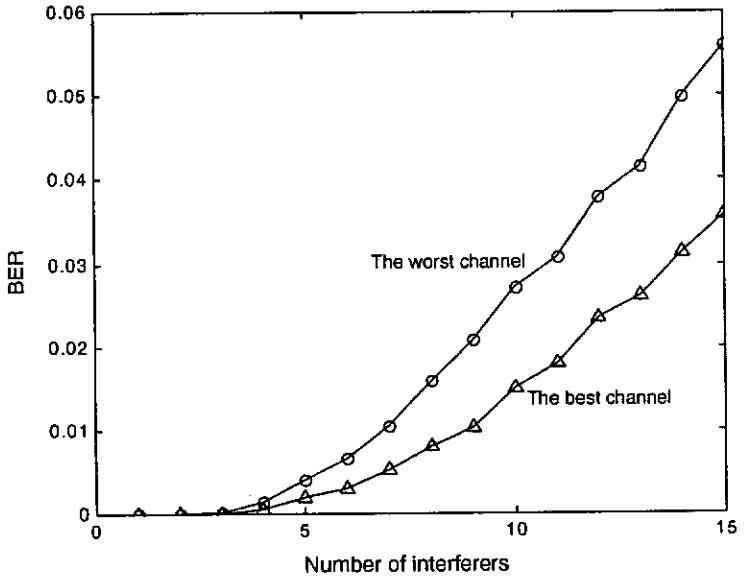

Figure 80: Plots of the BER for a system utilising 15-chip Gold-like sequences as functions of the number of interfering channels for the best and the worst channel out of 16 possible channels; $E_b/N_0 = 20$ dB.

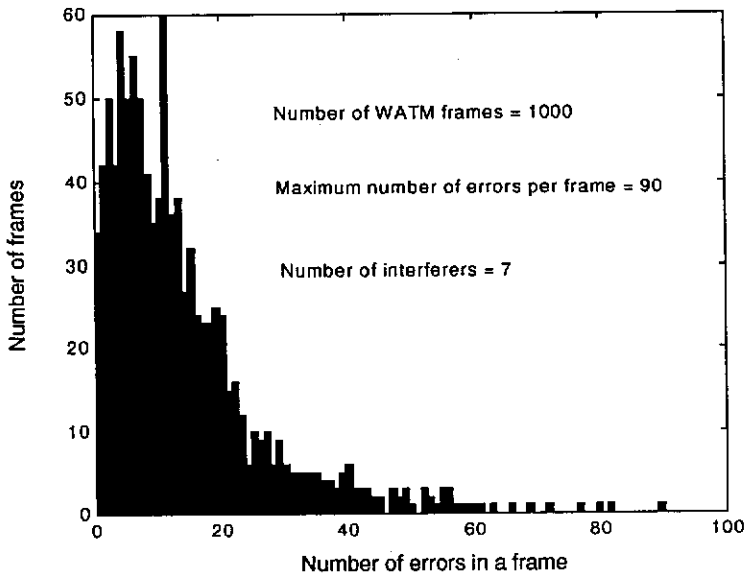

Figure 81: Histogram of the numbers of errors during simulated transmission of 1000 WATM frames for 7 interferers, $E_b/N_0 = 8$ dB, **in the case of the worst channel.**

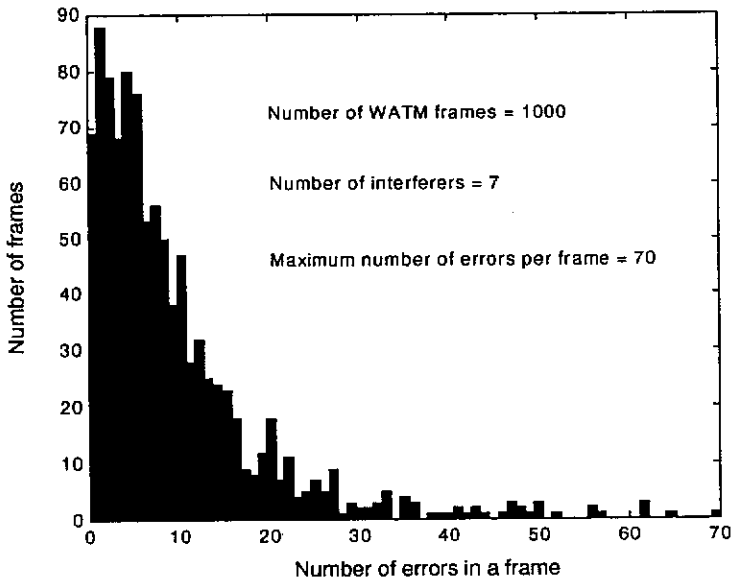

Figure 82: Histogram of the numbers of errors during simulated transmission of 1000 WATM frames for 7 interferers, $E_b/N_0 = 8$ dB, in the case of the best channel.

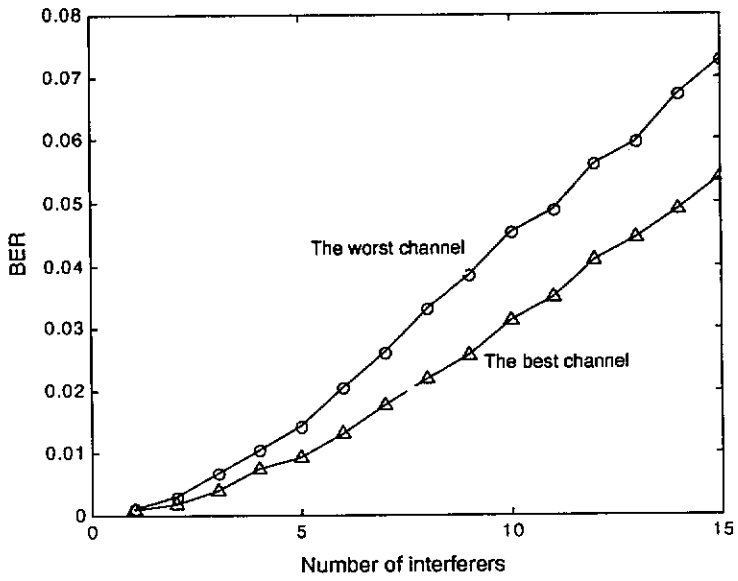

Figure 83: Plots of the BER for a system utilising 15-chip Gold-like sequences as functions of the number of interfering channels for the best and the worst channel out of 16 possible channels; $E_b/N_0 = 8$ dB.

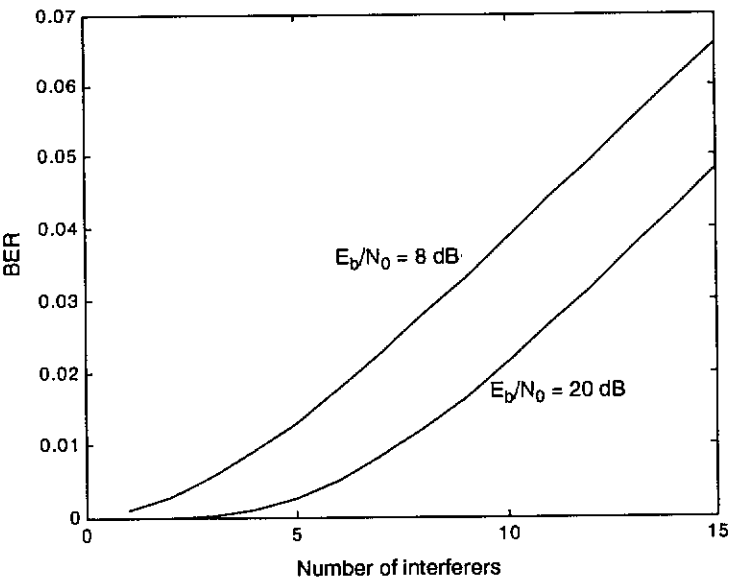

Figure 84: Plots of the BER for a system utilising 15-chip Gold-like sequences as functions of the number of interfering channels, averaged over 16 possible channels.

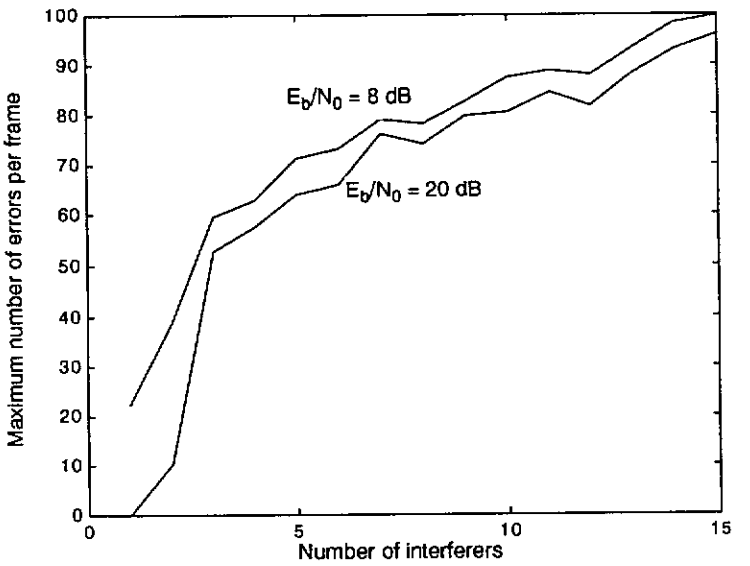

Figure 85: Plots of maximum number of errors per WATM frame for a system utilising 15-chip Gold-like sequences as functions of the number of interfering channels.

From the presented plots it is clear that BER very strongly depends on the number of interferers. Because there is a significant difference in the performance of the best and the worst channels, it means that BER also strongly depends on the sequence used to spread the data. Additionally, BER depends on E_b/N_0. In average, that 12 dB dif-

ference in the value of E_b/N_0, equates to 3 additional interferers if the cases of E_b/N_0 = 8 dB and E_b/N_0 = 20 dB are compared. Similar differences are obtained if performance of the best and the worst channel are compared.

Generally, considering the BER characteristics, we can conclude that for $BER \leq 0.01$ we need to assure less than 5 concurent users if E_b/N_0 = 8 dB, and less than 8 concurent users if E_b/N_0 = 20 dB.

These results, however, are somehow cloded by taking into account the maximum number of errors per WATM frame. The plots of Figure 85 indicate that with the number of concurent users exceeding 3, the maximum number of errors per frame can be too high for detection if a 100 bit overhead is used. Thus such a system might release erroneous frames, diminishing system reliability.

6.3 System utilising 16-chip multiple chirp sequences

In this section we consider the performance of a 16 channel DS CDMA system utilising 16-chip chirp-double-chirp sequences developed in the Section 5.2.2. The same set of simulations, as for the 15-chip Gold-like sequences has been repeated, and the results are presented in Figure 86 to Figure 93 in the same order as in the previous section.

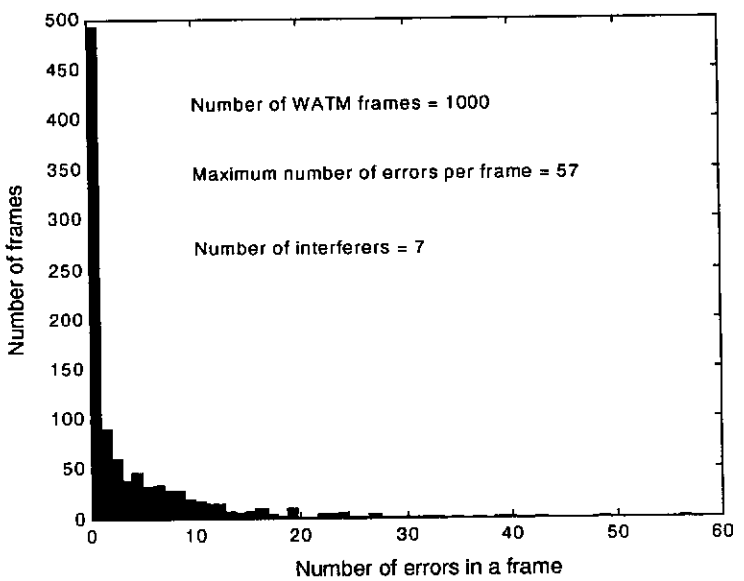

Figure 86: Histogram of the numbers of errors during simulated transmission of 1000 WATM frames for 7 interferers, E_b/N_0 = 20 dB, in the case of the worst channel.

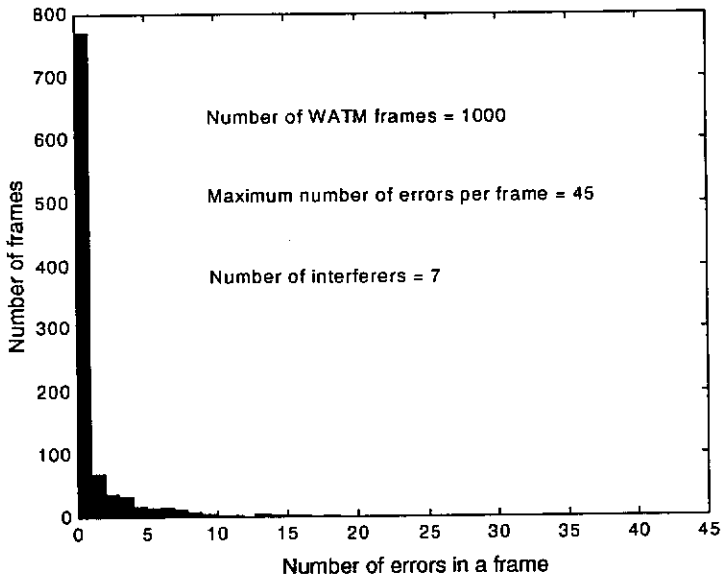

Figure 87: Histogram of the numbers of errors during simulated transmission of 1000 WATM frames for 7 interferers, $E_b/N_0 = 20$ dB, in the case of the best channel.

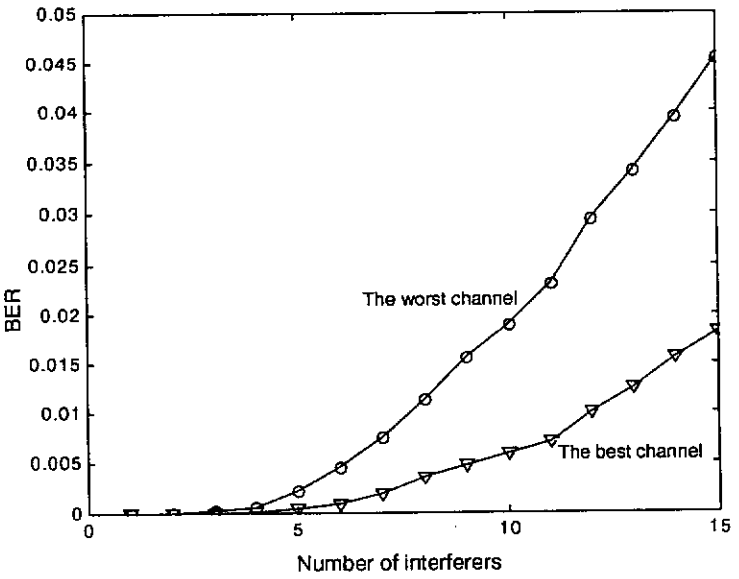

Figure 88: Plots of the BER for a system utilising 16-chip chirp-double-chirp sequences as functions of the number of interfering channels for the best and the worst channel out of 16 possible channels; $E_b/N_0 = 20$ dB.

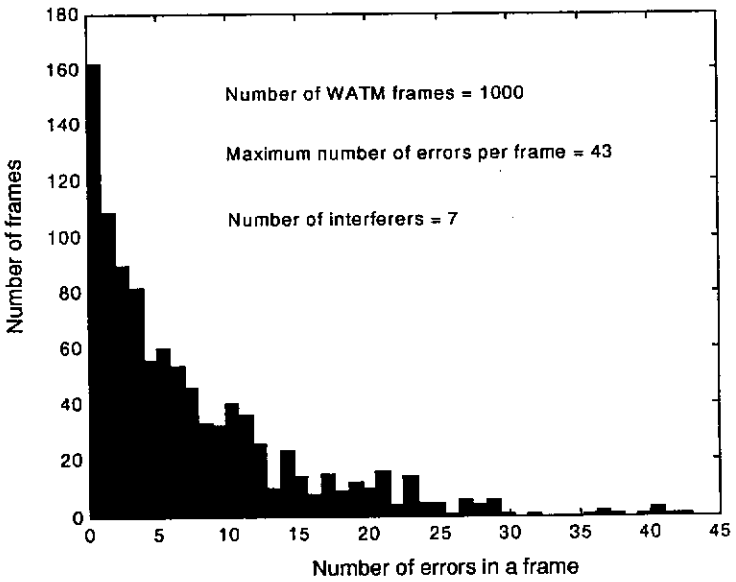

Figure 89: Histogram of the numbers of errors during simulated transmission of 1000 WATM frames for 7 interferers, $E_b/N_0 = 8$ dB, in the case of the worst channel.

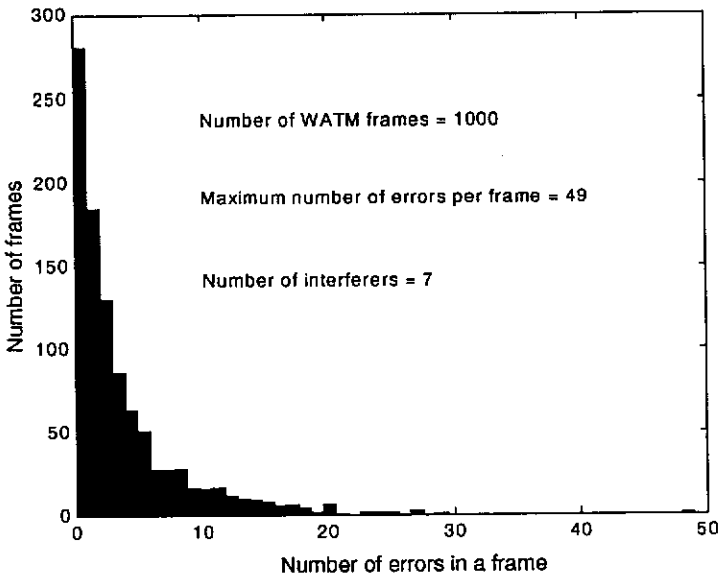

Figure 90: Histogram of the numbers of errors during simulated transmission of 1000 WATM frames for 7 interferers, $E_b/N_0 = 8$ dB, in the case of the best channel.

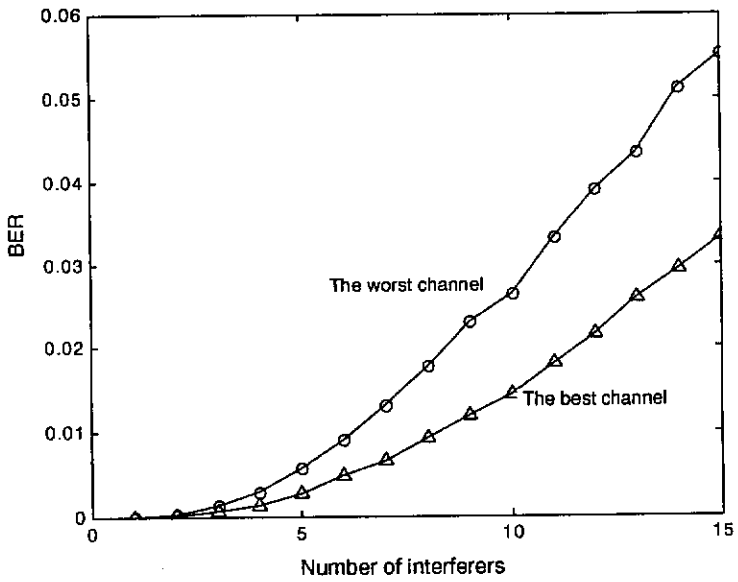

Figure 91: Plots of the BER for a system utilising 16-chip chirp-double-chirp sequences as functions of the number of interfering channels for the best and the worst channel out of 16 possible channels; $E_b/N_0 = 8$ dB.

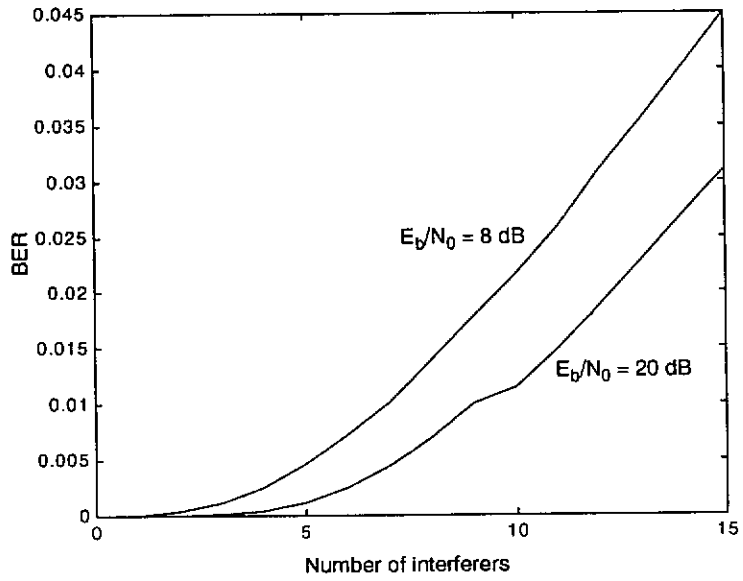

Figure 92: Plots of the BER for a system utilising 16-chip chirp-double-chirp sequences as functions of the number of interfering channels, averaged over 16 possible channels.

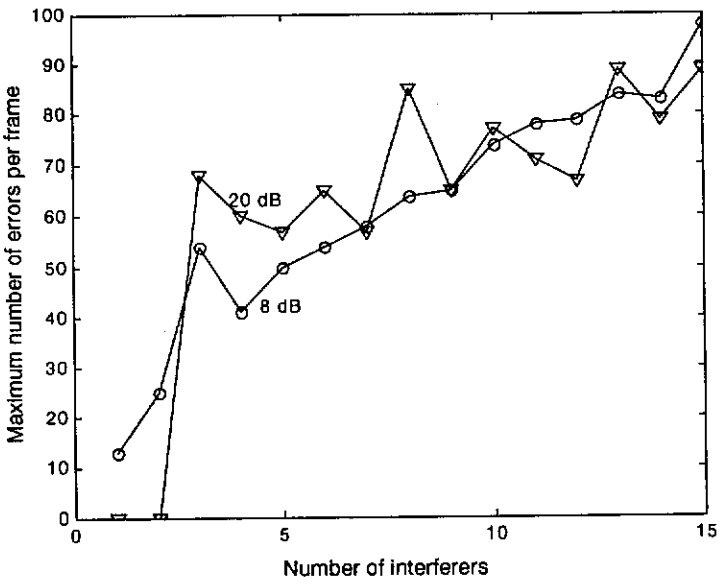

Figure 93: Plots of maximum number of errors per WATM frame for a system utilising 16-chip chirp-double-chirp sequences as functions of the number of interfering channels.

From the presented results it is visible that for the examined system utilising 16-chip chirp-double-chirp sequences the dependency of the BER on the number of interferers and on the value of E_b/N_0 is similar as that for the system utilising 15-chip Gold-like sequences. However, the values of BER for the system utilising 16-chip chirp-double-chirp sequences are more than 25% lower than the equivalent values obtained for the system utilising 15-chip Gold-like sequences. The values of, $BER \leq 0.01$ in the case considered here, can be achieved for 7 simultaneous users if $E_b/N_0 = 8$ dB and 10 simultaneous users in the case of $E_b/N_0 = 20$ dB. Therefore, the system utilising 16-chip chirp-double-chirp sequences can support more simultaneous users than the one utilising 15-chip Gold-like sequences. This is particularly evident for the lower values of E_b/N_0.

Both of the system considered so far have the similar properties, from the viewpoint of the maximum number of errors per WATM frame characteristics. As result, one should expect the similar reliability problems in both cases. However, the developed set of 16-chip chirp-double-chirp sequences has significantly better properties with respect to the average *BER* than the set of 15-chip Gold-like sequences, which results in a possible increase of system capacity. Another benefit of the chirp-double-chirp sequences is the fact that they can be designed for any arbitrary length.

6.4 System utilising 16-chip orthogonal Walsh-chirp sequences

In this section, we consider a system utilising 16-chip orthogonal Walsh-chirp sequences developed in Section 5.4.2. The set of system simulations, the same as for the system considered in the two previous sections, has been performed and the results are presented in Figure 94 to Figure 101.

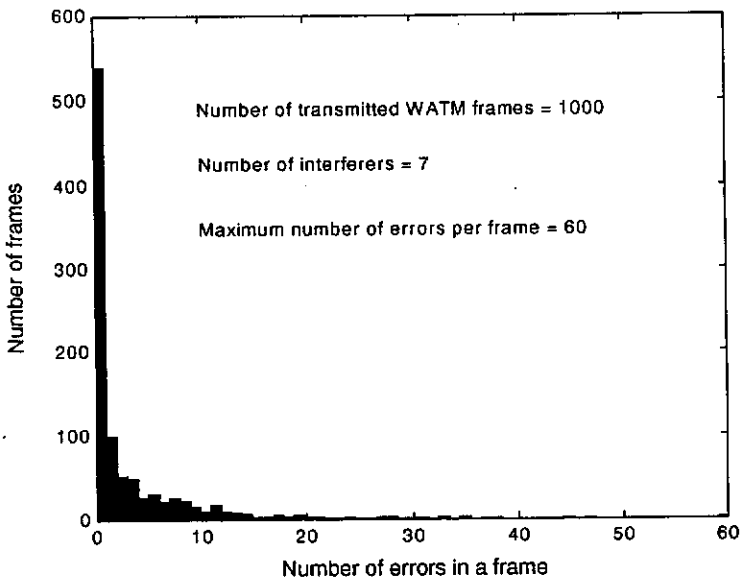

Figure 94: Histogram of the numbers errors during simulated transmission of 1000 WATM frames for 7 interferers, $E_b/N_0 = 20$ dB, in the case of the worst channel.

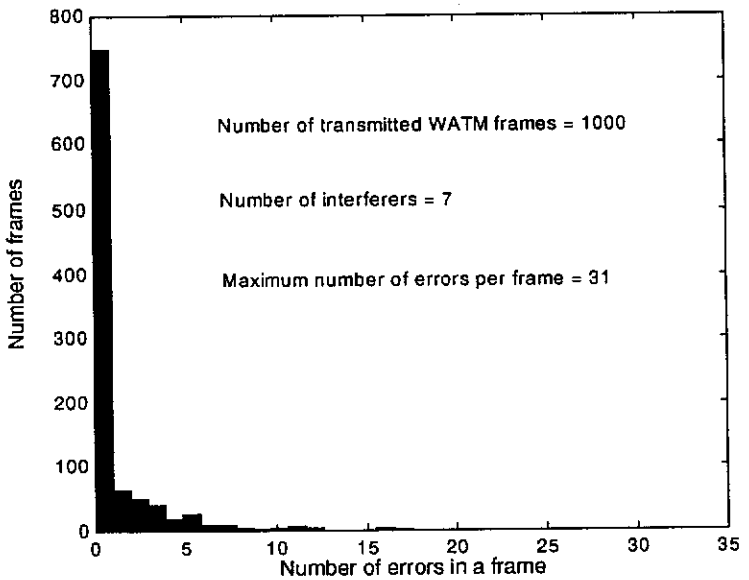

Figure 95: Histogram of the numbers of errors during simulated transmission of 1000 WATM frames for 7 interferers, $E_b/N_0 = 20$ dB, in the case of the best channel.

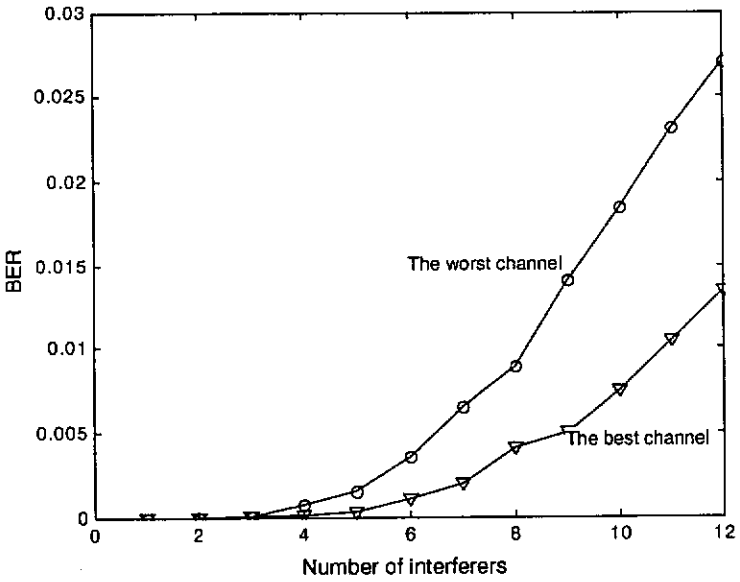

Figure 96: Plots of the BER for a system utilising 16-chip orthogonal Walsh-chirp sequences as functions of the number of interfering channels for the best and the worst channel out of 13 possible channels; $E_b/N_0 = 20$ dB.

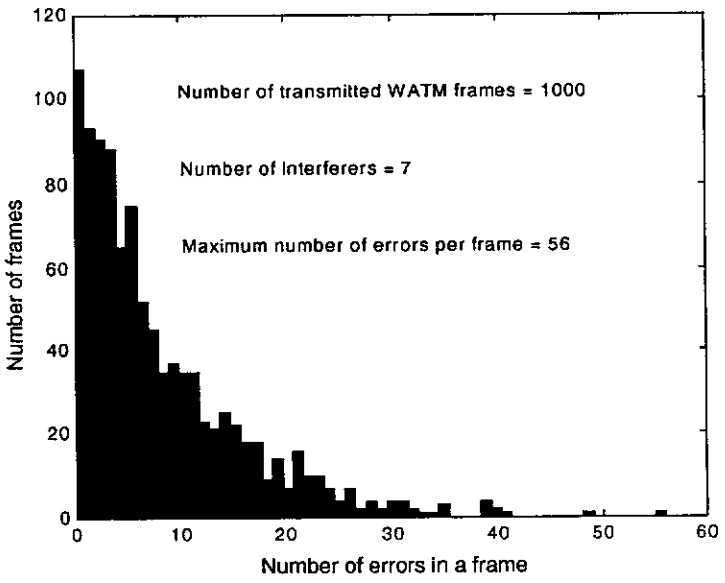

Figure 97: Histogram of the numbers of errors during simulated transmission of 1000 WATM frames for 7 interferers, $E_b/N_0 = 8$ dB, in the case of the worst channel.

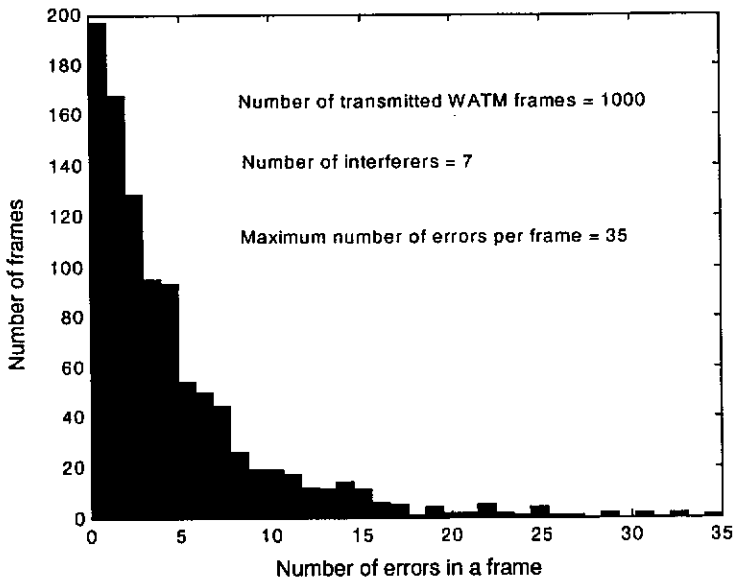

Figure 98: Histogram of the numbers of errors during simulated transmission of 1000 WATM frames for 7 interferers, $E_b/N_0 = 8$ dB, in the case of the best channel.

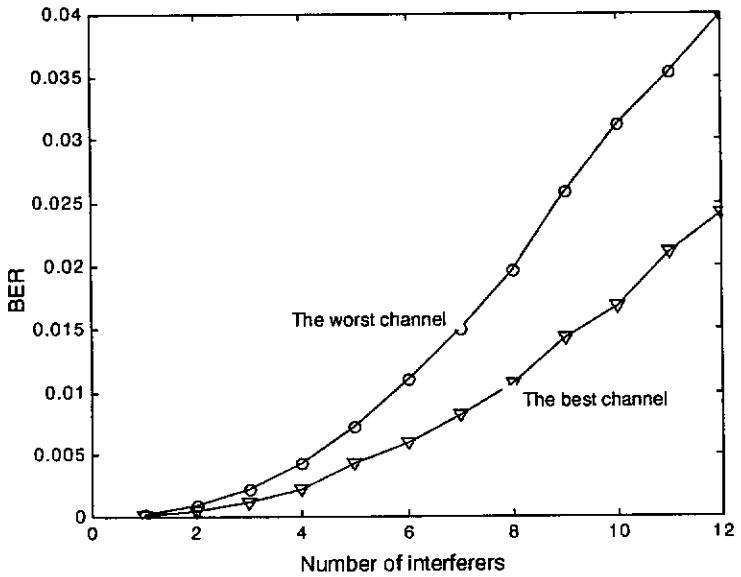

Figure 99: Plots of the BER for a system utilising 16-chip orthogonal Walsh-chirp sequences as functions of the number of interfering channels for the best and the worst channel out of 13 possible channels; $E_b/N_0 = 8$ dB.

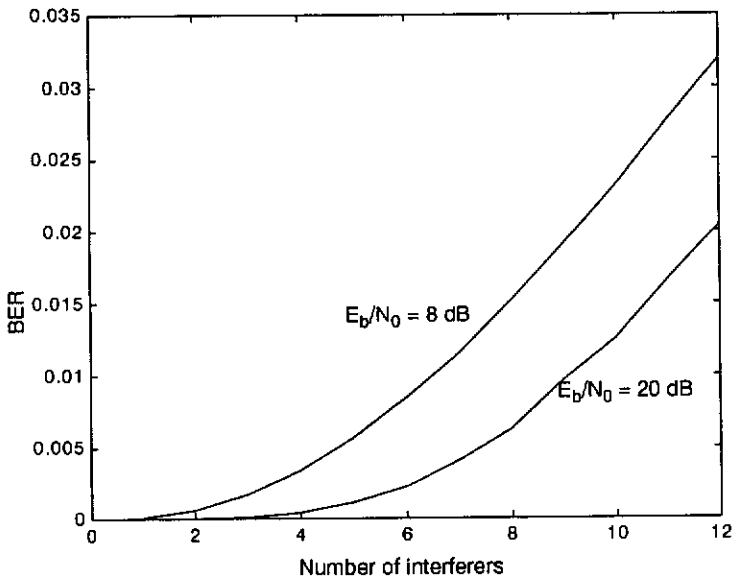

Figure 100: Plots of the BER for a system utilising 16-chip orthogonal Walsh-chirp sequences as functions of the number of interfering channels, averaged over 13 possible channels.

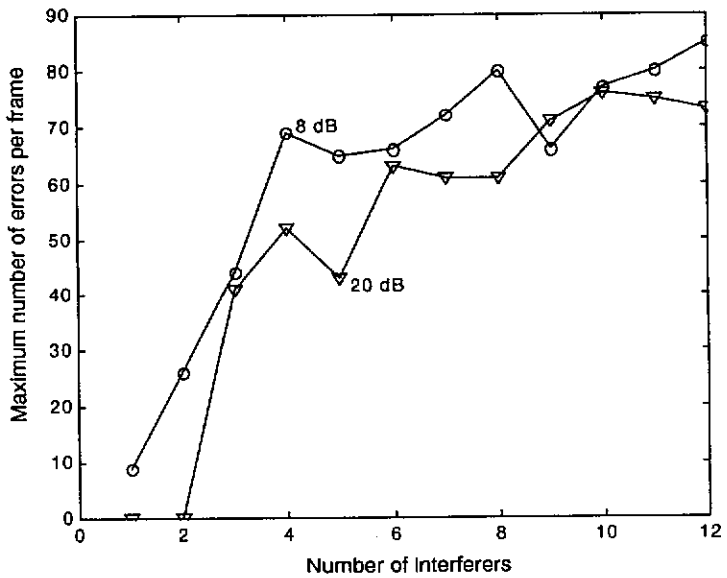

Figure 101: Plots of maximum number of errors per WATM frame for a system utilising 16-chip orthogonal Walsh-chirp sequences as functions of the number of interfering channels.

The simulation results presented in this section show that the properties of the system utilising 16-chip orthogonal Walsh-chirp sequences are significantly better that those of the system utilising 15-chip Gold-like sequences. They are, however, not as good as those of the system utilising 16-chip chirp-double-chirp sequences, as far as

the BER for high number of interferers and the maximum number of errors per WATM frame are concerned. On the other hand, the system capacity measured by the number of simultaneous users for $BER \leq 0.01$ is equal to 7 and 10 for $E_b/N_0 = 8$ dB and $E_b/N_0 = 20$ dB, respectively, which is exactly the same as than in the case of 16-chip chirp-double-chirp sequences.

Additionally, the sequences considered in this section are orthogonal for a perfect synchronisation. Therefore, MAI for a down-link transmission (base station to mobile terminals) can be regarded as negligable.

6.5 System utilising 32-chip non-orthogonal Walsh-chirp sequences

In this section, we consider a system utilising 32-chip non-orthogonal Walsh-chirp sequences developed in Section 5.3.2. Because the length of those sequences is twice the length of considered previously 16-chip sequences and more than twice the length of 15-chip Gold-like sequences, there is no direct way of comparing their performance. However, looking into bandwidth utilisation, we should expect the number of simultaneous users to be more than twice the number achievable for those 16-chip sequences under the same conditions (BER, E_b/N_0).

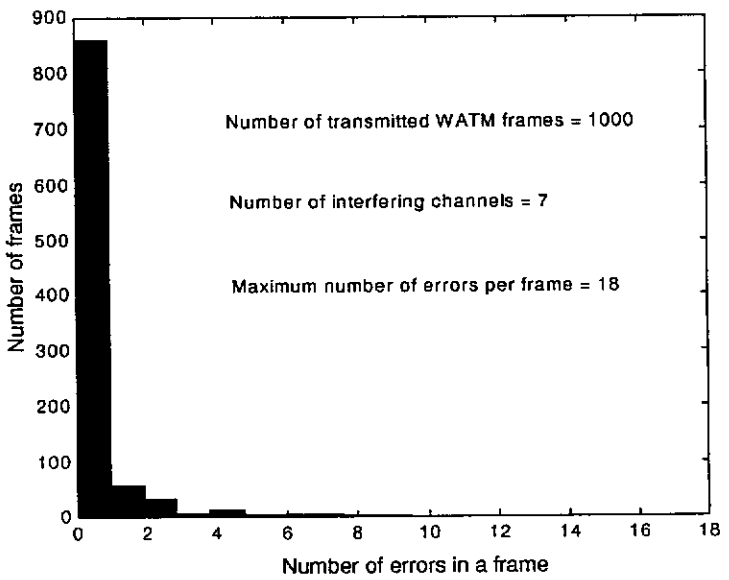

Figure 102: Histogram of the numbers of errors during simulated transmission of 1000 WATM frames for 7 interferers, $E_b/N_0 = 20$ dB, in the case of the worst channel.

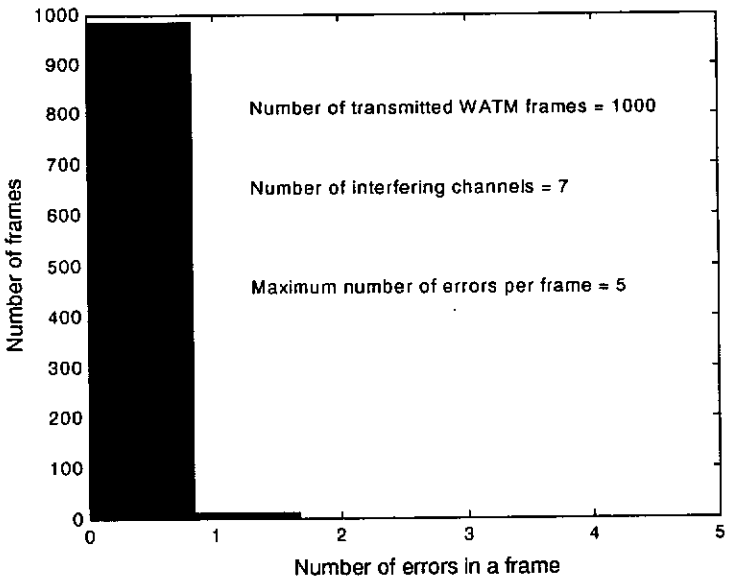

Figure 103: Histogram of the numbers of errors during simulated transmission of 1000 WATM frames for 7 interferers, $E_b/N_0 = 20$ dB, in the case of the best channel.

The set of system simulations, the same as for the system considered in the three previous sections, has been performed and the results are presented in Figure 102 to Figure 109.

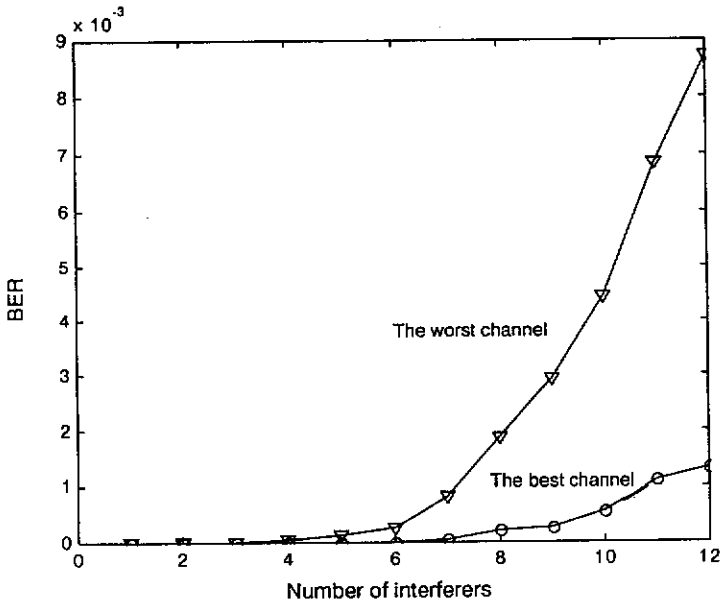

Figure 104: Plots of the BER for a system utilising 32-chip Walsh-chirp sequences as functions of the number of interfering channels for the best and the worst channel out of 13 possible channels; $E_b/N_0 = 20$ dB.

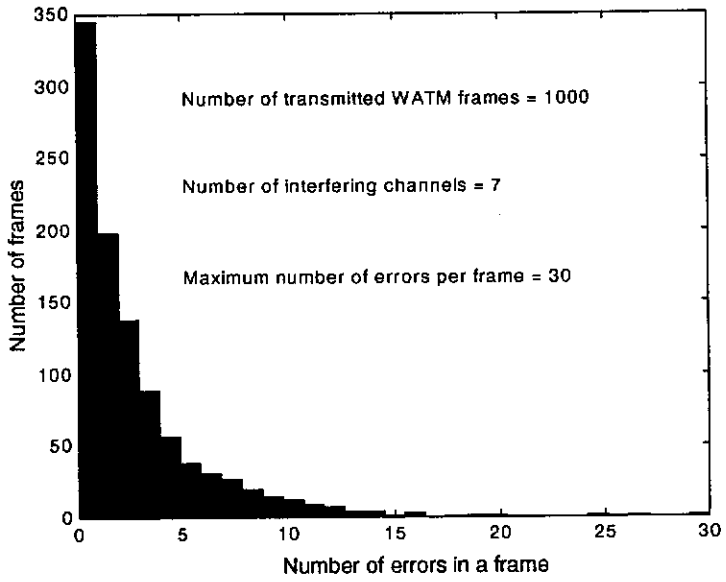

Figure 105: Histogram of the numbers of errors during simulated transmission of 1000 WATM frames for 7 interferers, $E_b/N_0 = 8$ dB, in the case of the worst channel.

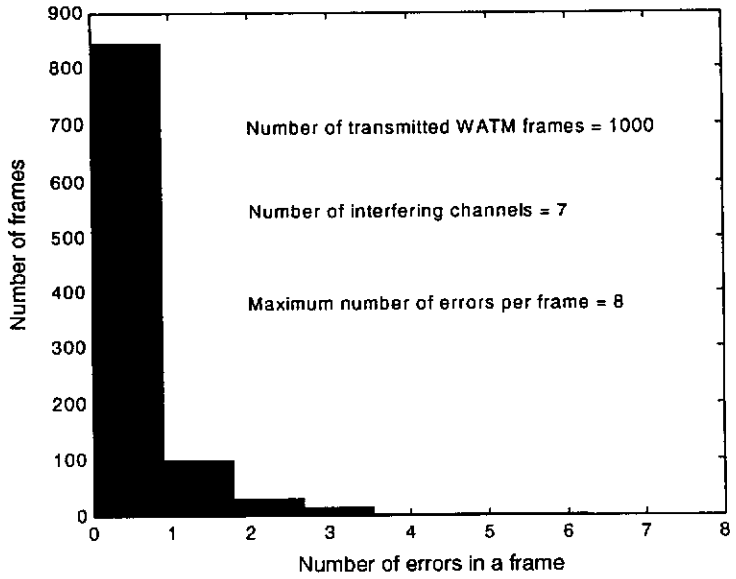

Figure 106: Histogram of the numbers of errors during simulated transmission of 1000 WATM frames for 7 interferers, $E_b/N_0 = 8$ dB, in the case of the best channel.

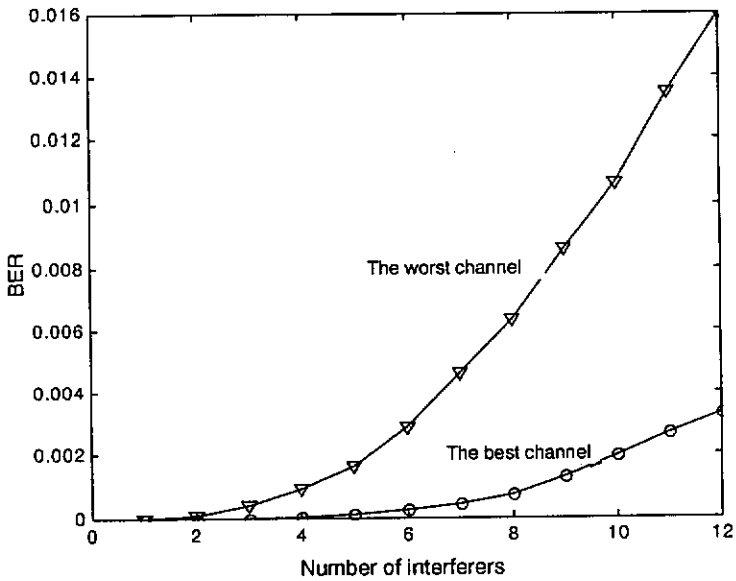

Figure 107: Plots of the BER for a system utilising 32-chip Walsh-chirp sequences as functions of the number of interfering channels for the best and the worst channel out of 13 possible channels; $E_b/N_0 = 8$ dB.

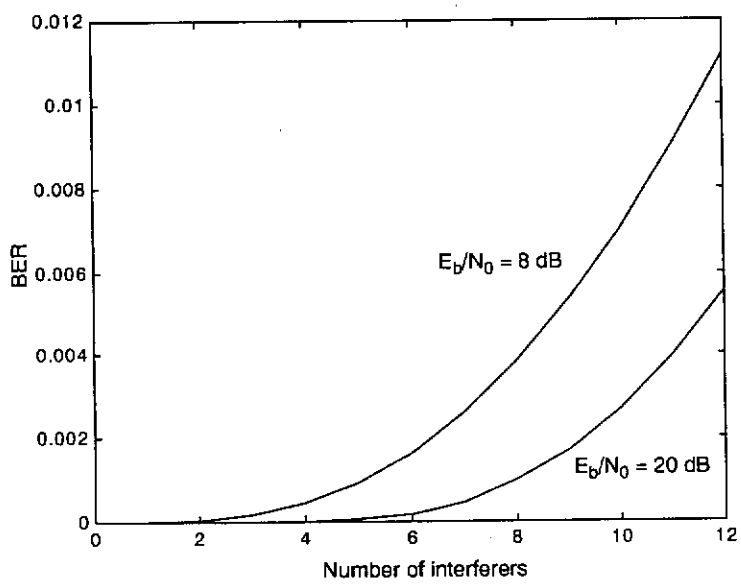

Figure 108: Plots of the BER for a system utilising 32-chip Walsh-chirp sequences as functions of the number of interfering channels, averaged over 13 possible channels.

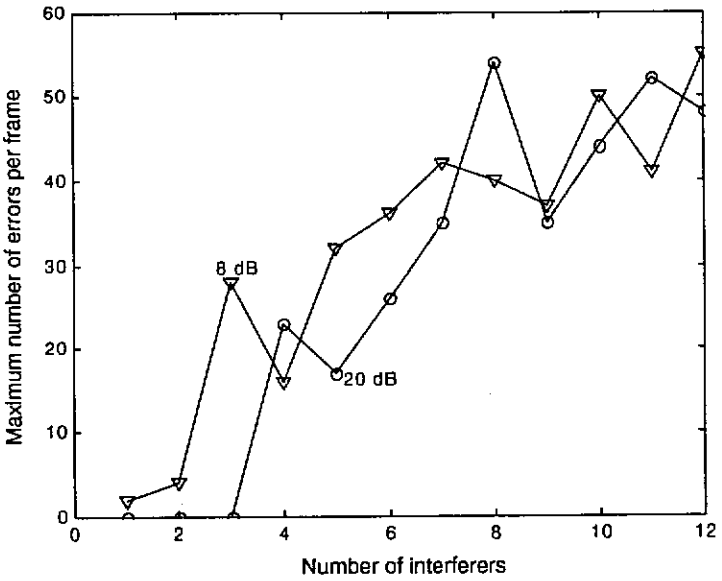

Figure 109: Plots of maximum number of errors per WATM frame for a system utilising 32-chip Walsh-chirp sequences as functions of the number of interfering channels.

It is clearly visible that properties of the system utilising 32-chip non-orthogonal Walsh-chirp sequences are in fact substantially better than properties of any of the systems considered so far in this chapter. However, they lag short of being twice as good as any of the considered systems utilising 16-chip chirp derived sequences, i.e. 16-chip chirp-double-chirp sequences or 16-chip orthogonal Walsh-chirp sequences, if the number of simultaneous users alowed for $BER \leq 0.01$. Therefore, a better badwidth utilisation can be obtained if two such systems utilising 16-chip chirp derived sequences are used with two different carrier frequences instead of a single system utilising 32-chip non-orthogonal Walsh-chirp sequences derived on the basis of 16-chip Walsh functions. Ultimately, one can use the same technique as applied in design of 16-chip orthogonal Walsh-chirp sequences to design 32-chip orthogonal Walsh-chirp sequences based on 32-chip Walsh functions. The resultant set of sequences would have better properties, and, in addition, the set size can be significntly greater.

6.6 Summary

In this chapter we have performed a comparative analysis of four DS CDMA systems. The short comparison of those system performance is given in Table 13 and Table 14. One of the systems has been a system utilising 15-chip Gold-like sequences, to which we have compared characteristics of three other systems utilising the sequence sets

Table 13: Comparison of system performance for E_b/N_0 = 20 dB.

	1	2	3	4
Average (over all channels) *BER* for 7 interferers	0.0084	0.0045	0.0041	4.47e-4
BER for 7 interferers in the worst channel	0.0108	0.0075	0.0065	8.63e-4
BER for 7 interferers in the best channel	0.0052	0.0013	0.0021	4.58e-5
Average number of simultaneous users for $BER \leq 0.01$	8	10	10	13
Maximum number of errors per WATM frame for 8 users	58	57	61	35

1 - Set of 15-chip Gold-like sequences
2 - Set of 16-chip Chirp-Double-Chirp sequences
3 - Set of 16-chip orthogonal Walsh-chirp sequences
4 - Set of 32-chip non-orthogonal Walsh-chirp sequences

Table 14: Comparison of system performance for E_b/N_0 = 8 dB.

	1	2	3	4
Average (over all channels) *BER* for 7 interferers	0.0227	0.0102	0.0115	0.0026
BER for 7 interferers in the worst channel	0.0261	0.0156	0.0150	0.0048
BER for 7 interferers in the best channel	0.0176	0.0066	0.0082	4.77e-4
Average number of simultaneous users for $BER \leq 0.01$	5	7	7	12
Maximum number of errors per WATM frame for 8 users	58	58	72	42

1 - Set of 15-chip Gold-like sequences
2 - Set of 16-chip Chirp-Double-Chirp sequences
3 - Set of 16-chip orthogonal Walsh-chirp sequences
4 - Set of 32-chip non-orthogonal Walsh-chirp sequences

developed in the previous chapter. By doing so we have shown that by using the design methods introduced in the previous chapter, we can produce useful sequence sets for such applications where the short spreading sequences are required.

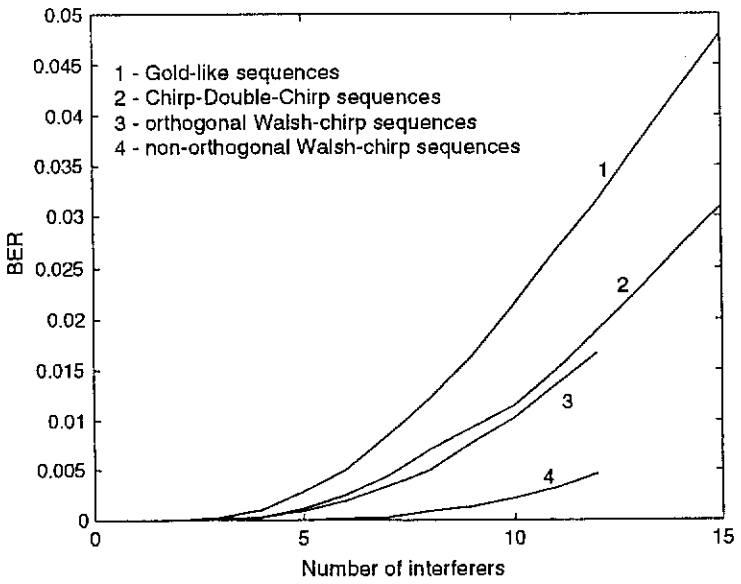

Figure 110: Comparison of the avarage BER as functions of the number of interfering channels for the simulated systems; $E_b/N_0 = 20$ dB .

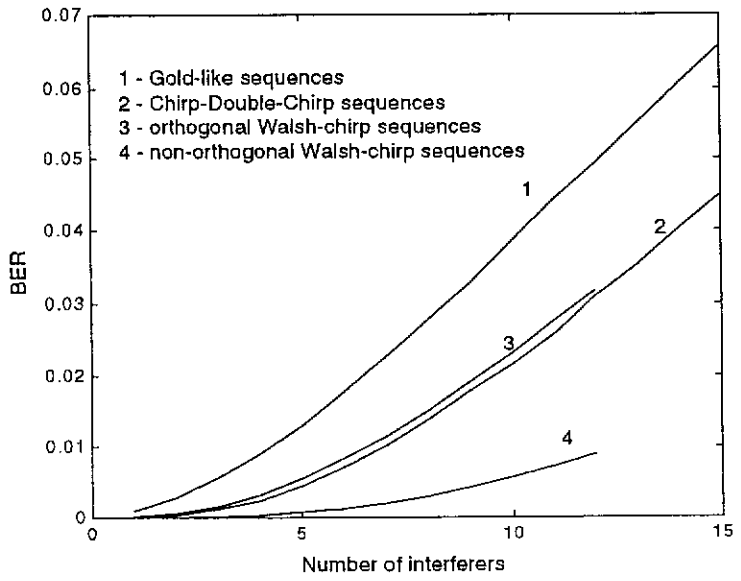

Figure 111: Comparison of the avarage BER as functions of the number of interfering channels for the simulated systems; $E_b/N_0 = 8$ dB .

We have also demonstrated that the performance of systems utilising those sequences can be significantly better than the performance of the system utilising Gold-like sequences of the comparable length. This is clearly visible in Figure 110 and Figure 111, where the average BER characteristics for all of the simulated systems are presented. In addition, it is worth to notice that a system utilising orthogonal Walsh-chirp sequences performed very well even for the simulated up-link transmission. Therefore, we can recommend this for the future applications in wireless data networks.

7. Conclusions

In the thesis we examined several well known families of spreading sequences from the viewpoint of their usefulness for DS CDMA wireless data applications. Therefore, we were particularly interested in the sequences of short lengths (up to 32 chips). Since non of the analysed sequence sets could provide us with the satisfactory characteristics guaranteeing the desired level of system reliability in both synchronous and asynchronous modes of operation, we decided to look into the new ways of designing complex polyphase spreading sequences, which we could optimise to make them suitable for wireless data services.

We proposed four new methods to design sequences for DS CDMA wireless data networks:

i. chirp sequences, (Section 5.1),

ii. sequences being superposition of chirp sequences of different order, (Section 5.2),

iii. modified non-orthogonal Walsh sequences, (Section 5.3),

iv. orthogonal polyphase sequences, (Section 5.4).

Then, we utilised the three most promising sequence sets designed by the use of the introduced methods to simulate the multiuser DS CDMA systems. We compared performance of those simulated systems with the performance of the simulated system utilising 15-chip Gold-like sequences. The comparison results indicate that by using the design methods introduced in the thesis we can produce useful sequence sets for applications where short spreading sequences are required. This is of a special importance in the case of high data rate wireless networks, due to the limited bandwidth available for such services. The presented results also demonstrate that the performance of systems utilising those sequences can be significantly better in terms of the number of simultaneously active users or BER that the performance of the system employing Gold or Gold-like sequences of the similar length.

In addition, a system utilising orthogonal Walsh-chirp sequences performed very well in the simulations, even for the up-link transmission. Therefore, it can be regarded as a good candidate for future high data rates DS CDMA wireless networks.

On the other hand, the two first methods, even though not leading to design of the orthogonal sequences, can be used to design useful sequence sets of any arbitrary chosen length. Hence, they can be very useful in development of systems where variable length sequences are required.

We expect that the application of the sequence design methods developed in the thesis is not limited to the high rate data networks, but they can be also used to improve such parameters of other DS CDMA networks like BER due to MAI, and system capacity measured in the number of active users.

The achieved performance improvement might be not as dramatic as reported in some cases where the sophisticated multiuser detection techniques are applied with Gold or other bipolar sequences employed (e.g. [23]). However, complexity of those multiuser detection techniques, so far, prohibited their use in high data rate systems, while in our case, most of the complexity is removed from the circuitry and passed onto the sequence design. Additionally, the demodulation method employed in the simulated systems was a simple correlational demodulation, which does not require any knowledge neither about spreading sequences of other active users nor about the channel state.

Ultimately, one can always use multiuser detection together with the sequences designed using the methods presented in the thesis. Definitely, the detailed system performance in such a case needs to be carefully assessed, albeit one can expect the overall performance improvement to be even better than when the similar multiuser technique is applied with Gold or other bipolar sequences of the comparable length.

The investigations reported in this thesis inspire the rise of several research questions, which are, in our opinion, worthy of being pursued. Some of such topics complementing our studies are:

i. Research into combination of the multiuser DS CDMA system utilising sequence sets designed by the use of the developed methods with the advanced error control strategies, in order to improve system performance. We have already started research in this direction. Some preliminary results on the use of error and erasure decoding in the case of such a system were reported

in [120].

ii. Investigation into the possible application of the developed sequence design methods to generate low correlation zone (LCZ) sequence sets for use with quasi-synchronous DS CDMA systems like the one proposed by Suehiro in [98].

iii. Analysis of the performance of the system employing the developed sequences in the case of realistic wireless channel models, and with the imperfect power control. We intend to perform simulations of such systems with imperfect power control and under different multipath scenarios, for both, the conventional asynchronous and the quasi-synchronous cases. Firstly we hope to obtain system performance for raw transmission (without any error control involved), and to continue research with advanced error control algorithms.

Appendix 1: MATLAB function '*fmins*'

Matlab function '*fmins*' having a syntax:

$$\mathbf{x} = fmins(\text{'}fun\text{'}, \mathbf{x0}, \mathbf{options});$$

minimizes a function of several variables, '*fun*'. It returns a vector x, which is a local minimizer of *fun*(**x**) near the starting vector **x0**. 'fun' is a string containing the name of the function to be minimized. *fun*(**x**) is a scalar valued function of a vector variable. **options** is a vector containing control parameters. Apparently only four of the 18 components of options are referenced by *fmins*. These four options are:

i. **options**(1) controls the display of the intermediate steps in the solution; if **options**(1) is nonzero, then the itermediate steps are displayed. The default value is **options**(1) = 0.

ii. **options**(2) is the termination tolerance for **x**. The default value is 10^{-4}.

iii. **options**(3) is the termination tolerance for *fun*(**x**). The default value is 10^{-4}.

iv. **options**(14) is the maximum number of steps. The default value is 500.

There are two other, optional parameters of the function *'fmins'*, **grad** and **varargin**, but these are not used in the computations reported in the thesis. We have also not used the extra output value provided by *'fmins'*, which returns a count of the number of the optimization steps.

The function '*fmins*' implements the Nelder-Meade simplex search algorithm. It is a direct search method not requiring gradients or other derivative information. In each step of the search, a new point in or near the current simplex is generated. The function value at this new point is compared with the values at the vertices of the simplex and, one of the vertices is usually replaced by the new point. Thus the new simplex is generated. This step is repeated until the diameter of the simplex is less than the specified tolerance or the maximum number of steps is reached.

The full implementation of the algorithm from the MATLAB 5.2 is shown below.

```
function [x, options] = fmins(funfcn,x,options,grad,varargin)
%FMINS  Minimize function of several variables.
%   X = FMINS('F',X0) attempts to return a vector X which is a local
%   minimizer of F(x) near the starting vector X0.  'F' is a string
%   containing the name of the objective function to be minimized,
%   a string expression representing the objective function, or an
%   inline function object. F(x) should be a scalar valued function
%   of a vector variable.
%
%   X = FMINS('F',X0,OPTIONS) uses a vector of control parameters. If
%   OPTIONS(1) is positive, intermediate steps in the solution are
%   displayed; the default is OPTIONS(1) = 0.  OPTIONS(2) is the
%   termination tolerance for x; the default is 1.e-4.  OPTIONS(3) is
%   the termination tolerance for F(x); the default is 1.e-4.
%   OPTIONS(14) is the maximum number of function evaluations; the
%   default is OPTIONS(14) = 200*length(x). The other components of
%   OPTIONS are not used by FMINS. For more information, see FOPTIONS.
%
%   X = FMINS('F',X0,OPTIONS,[],P1,P2,...) provides for additional
%      arguments which are passed to the objective function,
F(X,P1,P2,...)
%   Pass an empty matrix for OPTIONS to use the default values.
%
%   [X,OPTIONS] = FMINS(...) returns the number of function evaluations
%   in OPTIONS(10).
%
%   FMINS uses the Nelder-Mead simplex (direct search) method.
%
%   See also FMIN, FOPTIONS.
%   Reference: Jeffrey C. Lagarias, James A. Reeds, Margaret H. Wright,
%   Paul E. Wright, "Convergence Properties of the Nelder-Mead Simplex
%   Algorithm in Low Dimensions", May 1, 1997.  To appear in the SIAM
%   Journal of Optimization.
%
%   Copyright (c) 1984-98 by The MathWorks, Inc.
%   $Revision: 5.14 $  $Date: 1997/11/21 23:30:44 $
if nargin<3, options = []; end
options = foptions(options);
prnt = options(1);
tolx = options(2);
tolf = options(3);
% The input argument grad is there for compatability with FMINU in
% the Optimization Toolbox, but is not used by this function.
% Convert to inline function as needed.
funfcn = fcnchk(funfcn,length(varargin));
n = prod(size(x));
if (~options(14))
   options(14) = 200*n;
end
% Initialize parameters
rho = 1; chi = 2; psi = 0.5; sigma = 0.5;
onesn = ones(1,n);
two2npl = 2:n+1;
one2n = 1:n;
% Set up a simplex near the initial guess.
xin = x(:); % Force xin to be a column vector
```

```
v = zeros(n,n+1); fv = zeros(1,n+1);
v = xin;    % Place input guess in the simplex! (credit L.Pfeffer at
Stanford)
x(:) = xin;    % Change x to the form expected by funfcn
fv = feval(funfcn,x,varargin{:});
% Following improvement suggested by L.Pfeffer at Stanford
usual_delta = 0.05;             % 5 percent deltas for non-zero terms
zero_term_delta = 0.00025;      % Even smaller delta for zero elements
of x
for j = 1:n
   y = xin;
   if y(j) ~= 0
      y(j) = (1 + usual_delta)*y(j);
   else
      y(j) = zero_term_delta;
   end
   v(:,j+1) = y;
   x(:) = y; f = feval(funfcn,x,varargin{:});
   fv(1,j+1) = f;
end
% sort so v(1,:) has the lowest function value
[fv,j] = sort(fv);
v = v(:,j);
func_evals = n+1;
if prnt > 0
   clc
   formatsave = get(0,{'format','formatspacing'});
   format compact
   format short e
   disp(' ')
   disp('initial')
   v
   fv
   func_evals
end
% Main algorithm
% Iterate until the diameter of the simplex is less than tolx
%   AND the function values differ from the least by less than tolf,
%   or the max function evaluations are exceeded.
while func_evals < options(14)
   if max(max(abs(v(:,two2np1)-v(:,onesn)))) <= tolx &...
         max(abs(fv(1)-fv(two2np1))) <= tolf
      break
   end
   how = '';

   % Compute the reflection point

   % xbar = average of the n (NOT n+1) best points
   xbar = sum(v(:,one2n), 2)/n;
   xr = (1 + rho)*xbar - rho*v(:,end);
   x(:) = xr; fxr = feval(funfcn,x,varargin{:});
   func_evals = func_evals+1;

   if fxr < fv(:,1)
      % Calculate the expansion point
      xe = (1 + rho*chi)*xbar - rho*chi*v(:,end);
      x(:) = xe; fxe = feval(funfcn,x,varargin{:});
```

```
   func_evals = func_evals+1;
   if fxe < fxr
      v(:,end) = xe;
      fv(:,end) = fxe;
      how = 'expand';
   else
      v(:,end) = xr;
      fv(:,end) = fxr;
      how = 'reflect';
   end
else % fv(:,1) <= fxr
   if fxr < fv(:,n)
      v(:,end) = xr;
      fv(:,end) = fxr;
      how = 'reflect';
   else % fxr >= fv(:,n)
      % Perform contraction
      if fxr < fv(:,end)
         % Perform an outside contraction
         xc = (1 + psi*rho)*xbar - psi*rho*v(:,end);
         x(:) = xc; fxc = feval(funfcn,x,varargin{:});
         func_evals = func_evals+1;

         if fxc <= fxr
            v(:,end) = xc;
            fv(:,end) = fxc;
            how = 'contract outside';
         else
            % perform a shrink
            how = 'shrink';
         end
      else
         % Perform an inside contraction
         xcc = (1-psi)*xbar + psi*v(:,end);
         x(:) = xcc; fxcc = feval(funfcn,x,varargin{:});
         func_evals = func_evals+1;

         if fxcc < fv(:,end)
            v(:,end) = xcc;
            fv(:,end) = fxcc;
            how = 'contract inside';
         else
            % perform a shrink
            how = 'shrink';
         end
      end
      if strcmp(how,'shrink')
         for j=two2np1
            v(:,j)=v(:,1)+sigma*(v(:,j) - v(:,1));
            x(:) = v(:,j); fxcc = feval(funfcn,x,varargin{:});
         end
         func_evals = func_evals + n;
      end
   end
end
[fv,j] = sort(fv);
v = v(:,j);
if prnt > 0
```

```
      disp(' ')
      disp(how)
      v
      fv
      func_evals
   end
end   % while
x(:) = v(:,1);
if prnt > 0,
   % reset format
   set(0,{'format','formatspacing'},formatsave);
end
options(10)=func_evals;
options(8)=min(fv);
if func_evals >= options(14)
   if options(1) >= 0
      disp(' ')
      disp(['Maximum number of function evaluations (', ...
            int2str(options(14)),') has been exceeded']);
      disp( '          (increase OPTIONS(14)).')
   end
end
```

Appendix 2: Optimisation of coefficients for Example 5.2.2

The set of coefficients $h_1^{(r)}$ and $h_2^{(r)}$ in Example 5.2.2 are optimised to achieve minimum of R_{CC}. To do that we used the MATLAB function '*fmins*', described in Appendix 1 in the following way:

H_opt = *fmins*('*dchopt*', **H0**, [0, 1.e-3, 1.e-3, 0,0,0,0,0,0,0,0,0,0, 10000]);

where **H0** denotes the matrix containing the coefficients $h_1^{(r)}$ and $h_2^{(r)}$ given in Table 10, **H_opt** is the matrix containing the optimised coefficients (given later in Table 11), and '*dchopt*' is the name of the function *dchopt*(**H**) returning the value of R_{CC} for the set of 16 chip chirp-double chirp sequences defined by equation (144) with the coefficients $h_1^{(r)}$ and $h_2^{(r)}$ contained in the matrix **H**.

The listing of the function *dchopt*(**H**) is given below.

```
function csm = dchopt(H);
%
% Function returning the value of mean square aperiodic
% crosscorrelation R_cc for the set of 16-chip chirp-double chirp
% sequences generated by the function d_chirp_16(H).
% H is the matrix containing the coefficients h_1(r) and h_2(r),
% where r is the number of the sequence; r = 1, 2, ..., 16.
%
% Author: Beata Wysocki            Date:12/11/98
% ____________________________________________________________

S = d_chirp_16(H);                 % Generation of the sequence set
S.

csm = cormeas(S);                  % Calculation of R_cc
```

The function *d_chirp_16*(**H**) generates the set of 16 sequences using equation (144), while the function *cormeas*(**S**) computes the value of R_{CC} for the set of sequences contained within the matrix **S**.

Appendix 3: Optimisation of coefficients for Example 5.3.2

The values of the coefficients $\alpha^{(i)}$, $\beta^{(i)}$, $\gamma^{(i)}$, $i = 1, \ldots, 13$ are optimised in Example 5.3.2 to find the values minimising $R_{CC}(A)$:

$$A = \begin{bmatrix} \alpha^{(1)} & \ldots & \alpha^{(13)} \\ \beta^{(1)} & \ldots & \beta^{(13)} \\ \gamma^{(1)} & \ldots & \gamma^{(13)} \end{bmatrix}. \qquad \text{(Ap:1)}$$

To do that we used the MATLAB function '*fmins*', described in Appendix 1 in the following way:

A_opt = *fmins*('*wal_mod_opt*', **A0**, [0, 1.e-3, 1.e-3, 0,0,0,0,0,0,0,0,0,0, 10000]);

where

$$\mathbf{A0} = \begin{bmatrix} \alpha^{*} \\ \beta^{*} \\ \gamma^{*} \end{bmatrix} \otimes \begin{bmatrix} 1 & 1 & 1 & 1 & 1 & 1 & 1 & 1 & 1 & 1 & 1 & 1 & 1 \end{bmatrix}. \qquad \text{(Ap:2)}$$

The α^{*}, β^{*}, and γ^{*} are the values of α, β, and γ, respectively, for which $R_{CC}(A)$ reaches the minimum when the triple (α, β, γ) is the same for all 13 sequences and the values of $R_{CC}(A)$ are calculated for all $-20 \le \alpha, \beta, \gamma \le 20$ with grid step being equal to 0.2 for each of the parameters α, β, and γ. The function *wal_mod_opt*(**A**) returns the value of R_{CC} for the set of sequences from Example 5.3.2 for the given matrix of coefficients **A**.

The listing of the function *wal_mod_opt*(**A**) is given below.

```
function csm = wal_mod_opt(A);
%
% Function returning the value of mean square aperiodic
% crosscorrelation R_cc for the set of 13 nonorthogonal Walsh-chirp
% sequences generated by the function wal_chirp_non(A).
% A is the matrix containing the coefficients alfa, beta, and gamma
% being, in general, different for different sequences.
```

```
%
% Author: Beata Wysocki                Date:17/02/98
% ____________________________________________________________

S = wal_chirp_non(A);                  % Generation of the sequence set
S.

csm = cormeas(S);                      % Calculation of R_cc
```

The function *wal_chirp_non*(**A**) generates the set of 13 sequences from the Example 5.3.2, while the function *cormeas*(**S**) computes the value of R_{CC} for the set of sequences contained within the matrix **S**.

References

[1] M.H. Ackroyd: "Huffman sequences with approximately uniform envelopes or cross-correlation functions", IEEE Trans. Info. Theory, vol.It-23, pp.620-623, 1977.

[2] P.D.Alexander, A.J.Grant, M.J.Miller, L.K.Rasmussen and P.Whiting: "Multi-user Mobile Communications," Invited Paper, presented at ISITA'94, Sydney, Nov. 1994.

[3] S. Allpress et al.: "An investigation of RAKE receiver operation in an urban environment for various spreading bandwidth allocations," Proc. 1992 IEEE Veh. Technol. Conf., VTC'92, Denver, CO, May 1992, pp.506-510.

[4] W.O. Alltop: "Complex sequences with low periodic correlations", IEEE Trans. on Info. Theory, vol.IT-26, pp.350-354, 1980.

[5] D.R. Anderson and P.A. Wintz: "Analysis of a spread-spectrum multiple-access system with a hard limiter", IEEE Trans. on Commun. Techn., vol. COM-17, pp. 285-290, 1969.

[6] M.Antweiler and L.Boemer: "Complex sequences over $gf(p^m)$ with a two-level autocorrelation function and a large linear span", IEEE Trans. on Info. Theory, vol.IT-38, pp.120-130, 1992.

[7] R.H. Barker: "Group synchronising of binary systems," in "Communication Theory," W.Jackson, Ed., Butterworths, London 1953, pp.273-287.

[8] G.W.Barnes, D.Hirst, and D.J.James: "Chirp modulation system in aeronautical satellites," AGARD Conf. Proc. 87 on Avionics in Spacecraft, NATO, vol.30, pp.1-10, 1971.

[9] K.G. Beauchamp: "Walsh Functions and their applications", Academic Press, London, 1975.

[10] G.F.M. Beenker: T.A.C.M. Claasen, and P.W.C. Hermens: "Binary sequences with a maximally flat amplitude spectrum", Phillips J. Res., vol. 40, pp. 289-304, 1985.

[11] I.F. Blake and J.W. Mark: "A note on complex sequences with low correlations", IEEE Trans. on Info. Theory, vol. IT-28, pp.814-816, 1982.

[12] R.B. Blackman and J.W. Tukey: "The measurement of power spectra," Dover Pub., New York, 1958.

[13] J.A. Cadzow: "Spectral estimation: an overdetermined rational model equation approach," Proc. of IEEE, vol.PROC-70, pp.907-938, 1982.

[14] M.H. Callendar, Ed.: "Special Issue on IMT-2000 Standards Efforts of the ITU," IEEE Personal Communications, vol. 4, No. 4, 1997.

[15] J.A. Chang: "Generation of 5-level maximal-length sequences," Electron. Letters, p.258, 1966.

[16] K. Cheun: "Performance of direct-sequence spread spectrum RAKE receivers with random spreading sequences," IEEE Trans. on Commun., vol. COM-45, pp.1130-1143, 1997.

[17] D.C. Chu: "Polyphase codes with good periodic correlation properties", IEEE Trans. on Info. Theory, vol. IT-18, pp.531-533, 1972.

[18] C.E.Cook: "Pulse compression - key to more efficient radar transmission," Proc. of IRE, vol.48, pp.310-316, 1960.

[19] C.E.Cook and M.Bernfeld: "Radar Signals: An introduction to theory and application," Academic, New York, 1967.

[20] L. Dellaverson (Editor), "Proposed Charter, Work Plan and Schedule for a Wireless ATM Working Group," *ATM Forum / 96-0712*, June 1996.

[21] R.C. Dixon: "Spread Spectrum Systems", John-Wiley & Sons, New York, 1984.

[22] T.A. Dowing and R.J. McEliece: "Cross-correlation of reverse maximal-length shift register sequences," Technical Report vol.3, JPL Space Programs Summary 37-53, pp.192-193, 1968.

[23] A.Duel-Hallen: "On suboptimal detection for asynchronous code-division multiple access channels," Proc. of the 26th Annual Conf. on Information Sciences and Systems, Princeton University, Princeton, NJ, pp.838-843, March 1992.

[24] A.Duel-Hallen: "Decorrelating decission-feedback multiuser detector for synchronous code-division multiple access channel," IEEE Trans. on Commun., vol.COM-41, pp.285-290, 1993.

[25] A.Duel-Hallen: "A family of multiuser decision-feedback detectors for asynchronous code-division multiple access channels," IEEE Trans. on Commun.,

vol.COM-43, 1995.

[26] A.Duel-Hallen, J.Holtzman and Z.Zvonar: "Multiuser Detection for CDMA Systems," IEEE Personal Communications, April 1995, pp.46-58.

[27] M.L. Dukic and Dobrosavljevic: "A method of spread-spectrum radar polyphase code design", IEEE Journal on Selected Areas in Communications, vol. JSAC-8, pp.743-749, 1990.

[28] A.K.Elhakeem and A.Targi: "Performance of hybrid chirp/DS signals under Doppler and pulsed jamming," Proc. of GLOBECOM'89, vol.3, pp.1618-1623, 1989.

[29] P. Fan and M. Darnell: "Sequence Design for Communications Applications", John Wiley & Sons, New York, 1996.

[30] S.G.Fischer, T.A.Wysocki, and H.-J.Zepernick: "MAC Protocol for a CDMA Based Wireless ATM LAN", ICC'97, pp.1202-1206, Montreal 1997.

[31] R.L. Frank: "Polyphase codes with good nonperiodic correlation properties", IEEE Trans. on Info. Theory, vol. IT-9, pp.43-45, 1963.

[32] R.L. Frank and S.A. Zadoff: "Phase shift pulse codes with good periodic correlation properties", IRE Trans. on Info. Theory, vol. IT-8, pp.381-382, 1962.

[33] B. Friedlander: "Lattice methods for spectral estimation," Proc. of IEEE, vol. PROC-70, pp.990-1017, 1982.

[34] H. Fukumasa, R. Kohno, and H. Imai: "Design of pseudonoise sequences with good odd and even correlation properties for DS/CDMA", IEEE Journ. on Selected Areas in Communications, vol. JSAC-12, pp.828-836, 1994.

[35] T.R.Giallorenzi and S.G.Wilson: "Decision feedback multiuser receivers for asynchronous CDMA systems," Proc. of GLOBECOM'93, Houston, TX, Nov.-Dec. 1993, pp.1677-1681.

[36] K.R. Godfrey: "Three-level m sequences," Electron. Letters, pp.241-243, July 1966.

[37] D. Goeckel and W. Stark: "Performance of coded direct-sequence system with RAKE reception," European Trans. on Telecommun., vol.6., pp. 41-51, Jan./ Feb. 1995.

[38] M.J.E. Golay: "The merit factor of long low autocorrelation binary sequences",

IEEE Trans. on Inf. Theory, vol. IT-28, pp.543-549, 1982.

[39] R. Gold: "Optimal binary sequences for spread spectrum multiplexing," IEEE Trans. on Inf. Theory, vol. IT-13, pp.619-621, 1967.

[40] R. Gold: "Maximal recursive sequences with 3-valued recursive crosscorrelation functions," IEEE Trans. on Inf. Theory, vol. IT-14, pp.154-156, 1968.

[41] S.W. Golomb and R.A. Scholtz: "Gneralized Barker sequences", IEEE Trans. on Info. Theory, vol. IT-11, pp.533-537, 1965.

[42] S.W. Golomb and M.Z. Win: "Recent results on polyphase sequences", IEEE Trans. on Info. Theory, vol. IT-44, pp.817-824, 1998.

[43] D. Grillo, S.T.S. Chia, and N. Rouelle, Eds.: "Special Issue on The European Path Towards Advanced Mobile Systems," IEEE Personal Communications, vol. 2, No.1, 1995.

[44] H.F. Harmuth: "Transmission of Information by Orthogonal Functions", Springer-Verlag, Berlin, 1970.

[45] T. Helleseth: "Some results about the cross-correlation function between two maximal linear sequences", Discrete Math., vol.16, pp.209-232, 1976.

[46] M.Holtzman: "DS/CDMA successive interference cancellation," Proc. of ISSSTA'94, Oulu, Finland, pp.69-78, July 1994.

[47] E.C. Ifeachor and B.W. Jervis: "Digital signal processing: A practical approach," Addison-Wesley, New York, 1993.

[48] V.P. Ipatov: "Ternary sequences with ideal autocorrelation properties," Radio Eng. Electron. Phys., vol.24, pp.75-79, 1979.

[49] V.P. Ipatov: "Contribution to the theory of sequences with perfect periodic autocorrelation properties," Radio Eng. Electron. Phys., vol.25, pp.31-34, 1980.

[50] W.C.Jakes; "Microwave Mobile Communications", IEEE Press, Piscataway, 1994.

[51] N. Kalouptsidis and S. Theodoridis: "Fast adaptive least-square algorithms for power spectral estimation," IEEE Trans. on Acoustics, Speech and Signal Processing, vol. 35, pp.661-670, 1987.

[52] K.H. Kärkkäinen: "Mean-square cross-correlation as a performance measure for spreading code families", Proc. IEEE 2nd Int. Symp. on Spread Spectrum Tech-

niques and Applications (ISSSTA'92), pp. 147-150.

[53] T.Kasami: "Combinatorial Mathematics and its Applications," chapter on Weight distribution of Bose-Chaudhuri-Hocquenghem codes, Univ. of North Carolina Press, Chapel Hill, 1969.

[54] S.M. Kay: "A new ARMA spectral estimator", IEEE Trans. on Acoustics, Speech and Signal Processing, vol. 28, pp.585-588, 1980.

[55] A.M. Kerdock, F.J. MacWilliams and A.M. Odlyzko: "A new theorem about the Mattson-Solomon polynomial and some applications," IEEE Trans. on Inf. Theory, vol. IT-20, pp.85-89, 1974.

[56] M.Kowatsch and J.T.Lafferl: "A spread-spectrum concept combining chirp modulation and pseudonoise coding," IEEE Trans. on Commun. vol. COM-31, 1133-1142, 1983.

[57] P.V. Kumar and O. Moreno: "Polyphase sequences with periodic correlation properties better than binary sequences", IEEE Trans. on Info. Theory, vol. IT-37, 1991.

[58] A.W. Lam and S. Tantaratana: "Theory and applications of spread-spectrum systems", IEEE/EAB Self-Study Course, IEEE Inc., Piscatawy, 1994.

[59] S.C. Liu and J.J. Komo: "Nonbinary Kasami sequences", Proc. of IEEE Int. Symp. on Info. Theory, ISIT'91, Budapest, Hungary , June 24-28, p. 387, 1991.

[60] H.D. Lueke: "Families of polyphase sequences with near-optimal two-valued auto- and crosscorrelation functions", IEE Electronics Letters, vol. 28, pp.1-2, 1992.

[61] H.D. Lueke, "Large family of cubic phase sequences with low correlation", IEE Electronics Letters, vol.31, pp.163, 1995.

[62] R.Lupas and S.Verdu: "Linear multiuser detectors for synchronous code-division multiple access channels," IEEE Trans. on Info. Theory, vol. IT-35, pp.123-136, 1989.

[63] R.Lupas and S.Verdu: "Near-far resistance of multiuser detectors in asynchronous channels," IEEE Trans. on Commun., vol. COM-38, pp. 496-508, 1990.

[64] F.J. MacWilliams and N.J. Sloane: "The theory of error-correcting codes," North-Holland, New York, 1977.

[65] F.J. MacWilliams and N.J. Sloane: "Pseudo-random sequences and arrays," Proc. IEEE, vol.64, pp.1715-1729, 1976.

[66] S.L. Marple: "A new autoregresive spectrum analysis algorithm," IEEE Trans. on Acoustics, Speech and Signal Processing, vol. 28, pp.441-454, 1980.

[67] J.L. Massey and J.J. Uhran: "Sub-baud coding", Proc. of the Thirteenth Annual Allerton Conference on Circuit and System Theory, pp. 539-547, October 1975.

[68] MATLAB: "Reference guide," The Math Works, 1992.

[69] MATLAB: "Signal processing toolbox: user's guide," The Math Works, 1996.

[70] S.Matsufuji and K.Imamura: "P-ary sequences whose periodic correlations have only two values", Proc. of IEEE Int. Symp. on Info. Theory, ISIT'91, Budapest, Hungary , June 24-28, p. 279, 1991.

[71] A.Milewski: "Periodic sequences with optimal properties for channel estimation and fast start-up equalization", IBM Journal on Res. and Develop., vol. 27, pp.426-431, 1983.

[72] P.S. Moharir: "Generalized PN sequences," IEEE Trans. on Info. Theory, vol. IT-23, pp.782-784, 1977.

[73] T. Moriuchi and K. Imamura: "Balanced polyphase sequences with good periodic correlation properties obtained from modified Kumar-Moreno", Proc. of IEEE Int. Symp. on Info. Theory, ISIT'91, Budapest, Hungary , June 24-28, p. 382, 1991.

[74] W.H. Mow: "Best quadriphase codes up to length 24", IEE Electronics Letters, vol.29, pp.923-925, 1993.

[75] W.H. Mow: "A general construction of cubic phase sequences", Proc. of 3rd Int. Symposium on Communication Theory and Applications, Ambleside, U.K., pp.318-322, July 10-14, 1995.

[76] J.A.Nelder and R.Mead: "A Simplex Method for Function Minimization," Computer Journal, Vol.7, pp.308-313.

[77] Y.Niho: "Multi-valued cross-correlation functions between two maximal linear recursive sequences," PhD thesis, Dept. of Electr. Eng., University of Southern California, Los Angeles, 1972.

[78] E. Nikula, A.Toskala, E. Dahlman, L. Girard, and A. Klein: "FRAMES multiple

access for UMTS and IMT-2000," IEEE Personal Communications, vol. 5, No. 2, pp. 16-24, 1998.

[79] I. Oppermann and B.S. Vucetic: "Complex spreading sequences with a wide range of Correlation Properties", IEEE Trans. on Commun., vol. COM-45, pp. 365-375, 1997.

[80] I. Oppermann, P. Rapajic, and B.S. Vucetic: "Complex valued spreading sequences with good cross-correlation properties", Proc. Int. Symp. on Spread Spectrum Techniques and Applications (ISSTA'94), Oulu, Finland, July 1994, pp. 500-504.

[81] P.Patel and J.Holtzman: "Performance comparison of a DS/CDMA system using a successive interference cancellation (IC) scheme and a parallel IC scheme under fading," Proc. of ICC'94, New Orleans, LA, May 1994, pp.510-515.

[82] W.W. Peterson: "Error-Correcting Codes", J. Wiley & Sons, New York, 1961.

[83] B.M. Popovic: "GCL polyphase sequences with minimum alphabets", IEE Electronics Letters, vol. 30, pp.106-107, 1994.

[84] J.G. Proakis: "Digital Communications", 3rd ed., McGraw-Hill, New-York, 1995.

[85] M.B. Pursley: "Performance Evaluation for Phase-Coded Spread-Spectrum Multiple-Access Communication - Part I: System Analysis", IEEE Trans. on Commun., vol. COM-25, pp. 795-799, 1977.

[86] D.Radford: "Spread-spectrum data leap through ac power wiring," IEEE Spectrum, Nov. 1996.

[87] T.S. Rappaport: "Wireless Communications", IEEE Press, New York, Prentice Hall PTR, Upper Saddle River, 1996.

[88] D.V. Sarwate: " An upper bound on the aperiodic autocorrelation function for a maximal-length sequence", IEEE Trans. on Inf. Theory, vol. IT-30, pp. 685-687, 1984.

[89] D.V. Sarwate: "Bounds on crosscorrelation and autocorrelation of sequences", IEEE Trans. on Inf. Theory, vol. IT-25, pp.720-724, 1979.

[90] D.V. Sarwate and M.B. Pursley: "Crosscorrelation properties of pseudorandom and related sequences," Proc. of IEEE, vol. 68, pp.593-620, 1980.

[91] R. Scholtz: "The origin of spread spectrum communications", IEEE Trans. on Commun., vol. COM-31, pp.822-854, 1982.

[92] R.A. Scholtz and L.R. Welch: "Group characters: sequences with good correlation properties", IEEE Trans. on Info. Theory, vol.IT-24, pp.537-545, 1978.

[93] J. Seidler: "Nauka o Informacji", vol. II, WNT, Warszawa, 1983.

[94] D.A. Shedd and D.V. Sarwate: "Construction of sequences with good correlation properties," IEEE Trans. on Info. Theory, vol. IT-25, pp.94-97, 1979.

[95] V.M. Sidelnikov: "On mutual correlation of sequences", Soviet Math Doklady, vol.12, pp.197-201, 1971.

[96] B.Sklar; "Digital Communications; Fundamentals and Applications", Prentice Hall, Englewood Cliffs, New Jersey 07632, 1988.

[97] W. Stahnke: "Primitive binary polynomials," Math. Comput., vol. 27, pp.977-980, 1973.

[98] N.Suehiro: "A signal design without co-channel interference for approximately synchronized CDMA systems," IEEE Journal on Selected Areas in Commun., vol. JSAC-12, pp.111-117, 1997.

[99] N.Suehiro and M. Hatori: "Modulatable orthogonal sequences and their application to SSMA systems", IEEE Trans. on Info. Theory, vol.IT-34, pp.93-100, 1988.

[100] J. Szabatin: "Podstawy Teorii Sygnalow", WKiL, Warszawa, 1982.

[101] H.Takai, Y.Urabe, and H.Yamasaki: "Anti-multipath and anti-jamming modulation/demodulation scheme SR-chirp PSK for high-speed data transmission in dispersive fading channel with interference," Proc. VTC'94, vol.2, pp.1355-1359, 1994.

[102] R.J. Turyn and J. Storer: "On binary sequences", Proc. of Amer. Math. Soc., vol. 12, pp.524-525, July 1967.

[103] UMTS Forum: "A regulatory framework for UMTS," Rep. no. 1, 25 June 1997.

[104] P. Van Rooyen et al.: "Performance of coded SSMA system and RAKE reception on a Nakagami fading environment," Proc. Int. Symp. on Inform. Theory and Applications, ISITA'94, Sydney, Nov. 1994, pp.121-125.

[105] M.K.Varanasi and B.Aazhang: "Multistage detection in asynchronous code di-

vision multiple-access communications," IEEE Trans. on Commun., vol.COM-38, pp.509-519, 1990.

[106] M.K.Varanasi and B.Aazhang: "Near-optimum detection in synchronous code division multiple-access systems," IEEE Trans. on Commun., vol.COM-39, pp.725-736.

[107] S.Verdu: "Minimum probability of error for asynchronous gaussian multiple access channels," IEEE Trans. on Info. Theory, vol.IT-32, pp.85-96, 1986.

[108] S.Verdu: "Optimum multiuser asymptotic efficiency," IEEE Trans. on Commun., vol. COM-34, pp. 890-897, 1986.

[109] I.M.Vinogradov: "An Introduction to the Theory of Numbers," Pergamon Press, London, New York, 1955.

[110] A.Weil: "Number Theory - An approach through history," Birkhaeuser Inc., Boston, 1984

[111] L.R. Welch: "Lower bounds on the maximum cross correlation of signals", IEEE Trans. on Info. Theory, vol. IT-20, pp. 397-399, 1974.

[112] P.D. Welch: "The use of fast Fourier transform for estimation of power spectra," IEEE Trans. on Audio and Electroacoustics, vol. 15, pp.70-73, 1967.

[113] A. Wojnar: "Teoria Sygnalow", WNT, Warszawa, 1980.

[114] B.Wysocki, T.Wysocki; "A Method to Partially Suppress ISI and MAI for DS SS CDMA Wireless Networks", Proc. of ICC'97, pp.899-903, Montreal 1997.

[115] B.J.Wysocki, H.-J.Zepernick, T.A.Wysocki: "DS CDMA Scheme for WATM LAN with Error Control", Proc. of IEEE GLOBECOM'98, Sydney 8-12 Nov. 1998, pp.1919-1923.

[116] B.Wysocki, T.Wysocki; "DS-CDMA System for Wireless Digital Communication Channels", Provisional Patent - Lodged June 1995.

[117] B.J. Wysocki, T. Wysocki; "DS-CDMA Scheme with Reduced ISI and MAI", Australian Telecommunications Research Institute, Design Note, RSL-DN-002.

[118] B.J.Wysocki, T.A.Wysocki, and H.-J. Zepernick; "Error Performance of the 13-Channel DS CDMA WATM LAN", Proc. of ICUPC'98, pp. Florence 1998.

[119] B.J. Wysocki, T.A.Wysocki; " Optimization of Signature Sets for DS-SS CDMA Wireless LANs" - Proc. of Int. Symp. on Communication Theory and Applica-

tions, Ambleside, U.K., July 1997.

[120] B.J. Wysocki, H.-J.Zepernick, and T.A. Wysocki: "DS CDMA scheme for WATM with errors and erasures decoding," accepted for IEEE Wireless Communications and Networking Conference, WCNC'99, New Orleans, 21-24 Sept. 1999.

[121] T.Wysocki, "Chirp Modulation". In J.G.Webster, ed. "Encyclopedia of Electrical and Electronics Engineering" - John Wiley & Sons, Inc., New York, Brisbane, Toronto, Singapore, vol.3, 1999.

[122] N. Zierler and J. Brillhart: "On primitive trinomials (mod 2)," Inform. Cont., vol. 13, pp.541-554, 1968, and vol. 14, pp.566-569, 1969.